# CLASSIFICATION OF LABOUR PAIN USING ELECTROENCEPHALOGRAM SIGNAL BASED ON WAVELET METHOD

SAI CHONG YEH

DEPARTMENT OF ELECTRICAL ENGINEERING
FACULTY OF ENGINEERING
UNIVERSITY OF MALAYA
KUALA LUMPUR

2020

# CLASSIFICATION OF LABOUR PAIN USING ELECTROENCEPHALOGRAM SIGNAL BASED ON WAVELET METHOD

**SAI CHONG YEH**

**THESIS SUBMITTED IN FULFILMENT OF THE REQUIREMENTS FOR THE DEGREE OF DOCTOR OF PHILOSOPHY**

**DEPARTMENT OF ELECTRICAL ENGINEERING**
**FACULTY OF ENGINEERING**
**UNIVERSITY OF MALAYA**
**KUALA LUMPUR**

**2020**

**UNIVERSITY OF MALAYA**

**ORIGINAL LITERARY WORK DECLARATION**

Name of Candidate: Sai Chong Yeh

Matric No: KHA140073

Name of Degree: Doctor of Philosophy

Title of Project Paper/Research Report/Dissertation/Thesis ("this Work"):

CLASSIFICATION OF LABOUR PAIN USING ELECTROENCEPHALOGRAM SIGNAL BASED ON WAVELET METHOD

Field of Study: Signal Processing

I do solemnly and sincerely declare that:

(1) I am the sole author/writer of this Work;
(2) This Work is original;
(3) Any use of any work in which copyright exists was done by way of fair dealing and for permitted purposes and any excerpt or extract from, or reference to or reproduction of any copyright work has been disclosed expressly and sufficiently and the title of the Work and its authorship have been acknowledged in this Work;
(4) I do not have any actual knowledge nor do I ought reasonably to know that the making of this work constitutes an infringement of any copyright work;
(5) I hereby assign all and every rights in the copyright to this Work to the University of Malaya ("UM"), who henceforth shall be owner of the copyright in this Work and that any reproduction or use in any form or by any means whatsoever is prohibited without the written consent of UM having been first had and obtained;
(6) I am fully aware that if in the course of making this Work I have infringed any copyright whether intentionally or otherwise, I may be subject to legal action or any other action as may be determined by UM.

Candidate's Signature Date:

Subscribed and solemnly declared before,

Witness's Signature Date:

Name:

Designation:

**CLASSIFICATION OF LABOUR PAIN USING**

**ELECTROENCEPHALOGRAM SIGNAL BASED ON WAVELET METHOD**

## ABSTRACT

Electroencephalogram (EEG) is the recording of electrical activity of the cerebral cortex through electrodes placed on the scalp. EEG is used to acquire neurophysiological signals for application in clinical diagnosis and brain computer interface (BCI). However, in practical settings the EEG signals are often contaminated by signal artifacts known as the biological and environmental artifacts. These artifacts degrade EEG signals, thereby obstructing clinical diagnosis or BCI applications by distorting the observed power spectrum. Procedures for automated removal of EEG artifacts are frequently sought after in pre-processing and filtering of the EEG signals.

In recent years, a combination of independent component analysis (ICA) and discrete wavelet transform (DWT) has been introduced as standard technique for EEG artifact removal. However, in performing the wavelet-ICA procedure, visual inspection or arbitrary thresholding may be required to identify the artifactual components in the EEG signal. This study proposed an integrated system for EEG signals pre-processing by using machine learning algorithms in the identification of artifactual components during the process of Wavelet-ICA. Supervised and unsupervised machine learning algorithms particularly the Support Vector Machine (SVM) and Density Based Spatial Clustering of Application with Noise (DBSCAN) are used in this study. These methods present a robust system that enables fully automated identification and removal of artifacts from EEG signals, without the need of visual inspection or arbitrary thresholding. The training and parameters selection of the machine learning algorithms are conducted using EEG data collected from ten subjects in the laboratory. Using test data contaminated by eye blink artifacts and public dataset from EEGLAB, it was shown that these methods performed

better in identifying artifactual components than did existing thresholding methods. Furthermore, wavelet-ICA in conjunction with machine learning algorithm successfully removed target artifacts, while largely retaining the EEG source signals of interest. This method is also extendable to accommodate multiple types of artifacts present in multichannel EEG.

As a practical application of this study, the developed system is used in an application to monitor pain response due to uterine contractions during labour. This part of the study aimed to assess the utility of EEG as an objective marker of pain during the first stage of labour. We obtained EEG and cardiotocography (CTG) data in ten parturient women during their first stage of labour. The study subjects reported the extent of their pain experienced due to uterine contractions, which were recorded by the CTG tracing. Simultaneous 16-channels EEG traces were obtained for spectral analysis and a subsequent classification using SVM aiming to predict the pain experienced in relation to uterine contractions. It was found that pain due to uterine contraction correlated positively with relative delta and beta band activities and negatively with relative theta and alpha band activities of the EEG signals. SVM using the spectral activities, statistical and non-linear features classified the state of pain with an accuracy of 83% using a classification model generalizable across subjects. Furthermore, dimension reduction using principal component analysis (PCA) successfully reduced the number of features used in the classification while achieving a maximum classification accuracy of 84%. The results shown that continuous EEG affords the means to assess objectively maternal pain experienced.

All in all, this study aims to design, develop, optimize and test the method of pain assessment using the EEG signal during the active contraction phase of the first stage of

labour. Future studies are envisioned to investigate EEG markers of pain in other clinical states, aiming to generalize the use of EEG as an objective method of pain assessment.

Keywords: Electroencephalogram, Machine Learning, Pain Assessment, Wavelet-ICA, Support Vector Machine (SVM)

**KLASIFIKASI KESAKITAN PERSALINAN MENGGUNAKAN ISYARAT ELECTROENCEPHALOGRAM BERDASARKAN KAEDAH WAVELET**

## ABSTRAK

Electroencephalogram (EEG) merupakan rakaman aktiviti elektrik di korteks serebrum melalui elektrod yang diletakkan pada kulit kepala. EEG digunakan untuk mengumpul isyarat neurofisiologi bagi aplikasi di peringkat diagnosis klinikal dan antara muka komputer otak (BCI). Namun, penggunaan isyarat EEG secara praktikal sering menghadapi cabaran di mana isyarat EEG mudah dikontaminasi oleh isyarat artifak terutamanya artifak biologi dan persekitaran. Artifak-artifak ini memudaratkan isyarat EEG dan mengganggu diagnosis klinikal atau aplikasi BCI melalui hingar kepada spektrum kuasa EEG. Justera, prosedur pemprosesan isyarat EEG amat penting untuk mengalihkan isyarat artifak secara automatik sebelum digunakan untuk sebarang aplikasi.

Dalam kebelakangan ini, gabungan antara analisis komponen bebas (ICA) dan transformasi gelombang kecil diskrit (DWT) telah diperkenalkan sebagai teknik yang berkesan untuk pengalihan isyarat artifak. Walau bagaimanapun, komponen artifak dalam isyarat EEG perlu dikenal pasti terlebih dahulu dengan menggunakan kaedah pemerhatian atau ambang sebarangan dalam prosedur Wavelet-ICA. Kajian ini mencadangkan satu sistem bersepadu bagi pra-pemprosesan isyarat EEG dengan menggunakan algorithma pembelajaran mesin untuk mengenal pasti komponen artifak dalam proses Wavelet-ICA. Algorithma pembelajaran mesin berselia yang digunakan dalam kajian ini adalah Mesin Vektor Sokongan (SVM), manakala algorithma pembelajaran mesin tidak berselia yang digunakan adalah Pengelompakan Ruang bagi Aplikasi dengan Hingar Berdasarkan Ketumpatan (DBSCAN). Sistem yang dibangunkan ini boleh digunakan untuk mengenalpasti dan mengalih isyarat artifak dari isyarat EEG secara automatik, tanpa perlu kaedah pemerhatian atau ambang sebarangan. Pembelajaran dan pemilihan parameter

bagi algorithma tersebut dijalankan dengan menggunakan data EEG yang dikumpul dari sepuluh subjek di makmal. Dengan menggunakan data kajian yang dikontaminasi oleh artifak kelip mata dan data awam dari EEGLAB, sistem ini berjaya mengenal pasti komponen artifak dengan lebih berkesan berbanding dengan kaedah ambangan sebarangan yang sedia ada. Tambahan pula, kaedah Wavelet-ICA dengan algorithma pembelajaran mesin juga berjaya mengalihkan artifak sasaran tanpa menjejaskan isyarat dari sumber EEG. Kaedah ini juga boleh dibangunkan untuk menampung pelbagai jenis artifak lain yang boleh didapati di rakaman EEG berbilang saluran.

Sebagai aplikasi yang praktikal, sistem yang dibangunkan ini telah digunakan dalam aplikasi pemantauan klinikal untuk memantau kesakitan akibat kontraksi semasa persalinan. Kajian ini bertujuan untuk menilai kegunaan isyarat EEG sebagai penanda kesakitan secara objektif semasa peringkat pertama persalinan. Data isyarat EEG dan cardiotocogram (CTG) telah diperoleh dari sepuluh wanita semasa peringkat pertama persalinan. Subjek kajian melaporkan tahap kesakitan yang mereka alami akibat daripada kontraksi yang dicatatkan oleh CTG. Isyarat EEG sebanyak 16 saluran telah diperoleh untuk analisis spektrum dan klasifikasi menggunakan SVM bertujuan untuk menilai kesakitan yang dialami. Kesakitan akibat daripada kontraksi berkorelasi secara positif dengan aktiviti relatif delta dan beta tetapi secara negatif dengan aktiviti relatif theta dan alfa dalam isyarat EEG. SVM menggunakan aktiviti spektrum, ciri-ciri statistik dan bukan linear berjaya mengklasifikasi tanda kesakitan dengan ketepatan setinggi 83% berdasarkan model klasifikasi secara umum. Selain itu, pengurangan dimensi menggunakan analisis komponen prinsip (PCA) telah berjaya mengurangkan bilangan ciri-ciri yang digunakan dalam klasifikasi SVM disamping mencapai ketepatan klasifikasi maksimum sebanyak 84%. Keputusan kajian menunjukkan bahawa

pemantauan EEG secara berterusan boleh digunakan sebagai cara untuk menilai kesakitan yang dialami akibat daripada kontraksi semasa peringkat pertama persalinan.

Secara keseluruhannya, kajian ini bertujuan untuk merekabentuk, membangunkan, mengoptimumkan dan menguji kaedah penilaian kesakitan dengan menggunakan isyarat EEG semasa peringkat pertama persalinan. Lebih kajian perlu dijalankan pada masa depan untuk mengkaji kegunaan isyarat EEG sebagai penanda kesakitan dalam keadaan klinikal yang lain, dengan tujuan untuk mempertingkatkan penggunaan EEG sebagai kaedah penilaian kesakitan secara objektif.

Kata kunci: Electroencephalogram, Pembelajaran Mesin, Penilaian Kesakitan, Wavelet-ICA, Mesin Vektor Sokongan (SVM)

## ACKNOWLEDGEMENTS

I would like to express my deepest appreciation to my supervisors, Dr. Norrima Mokhtar and Prof. Dr. Hamzah Arof, both from the Department of Electrical Engineering, Faculty of Engineering, University of Malaya, without whom none of this work would have been possible.

I also want to thank the team involved in the research and publication of the study, in no particular order Prof. Dr. Masahiro Iwahashi from Image and Signal Processing Laboratory, Nagaoka University of Technology, who has provided valuable insights during my 3 months affiliation with his laboratory, Prof. Dr. Paul Cumming from School of Psychology and Counselling, Queensland University of Technolgy / QIMR Berghofer Institute, who has provided equally important insights and advices to the study, Dr. Yip Hing Wa and Dr. Mohd Shahnaz Hasan from Department of Anesthesiology, Faculty of Medicine / University Malaya Medical Centre, who have assisted and advised on the ethics approval and data collection of the study, Dr. Lindy Bak Li Mei and also Prof. Dr. Noor Azmi Mat Adenan from Department of Obstetrics and Gynaecology, Faculty of Medicine / University Malaya Medical Centre, who have given tremendous helps and advices on their expertise over the course of the study.

There are many more individuals who have contributed directly or indirectly to the outcome of the study that are not named but deserved to be mentioned including the participants of the study, the technicians and administrative staffs of the Faculty of Engineering, University of Malaya, and not to forget my colleagues and friends from the university who have assisted and given their valuable suggestions during the meetings, seminars and discussions that was held.

I would also like to acknowledge the Malaysia Ministry of Higher Education for High Impact Research (HIR) grant (UM.C/HIR/MOHE/ENG/16 Account Code: D000016-16001) and also the Institute of Graduate Studies for Postgraduate Research (PPP) grant

(PG260-2015B) provided over the course of the study. Moreover, I would like to express my humble gratitude to the Conference of Rulers (Majlis Raja-Raja) and Public Service Department (JPA) of Malaysia as recipient of King's Scholarship (Biasiswa Yang Di-Pertuan Agong) 2015/2016.

Last but not least, I would also like to thank my family and friends who have given their support over the course of my PhD study.

## TABLE OF CONTENTS

## LIST OF FIGURES

## LIST OF TABLES

## LIST OF SYMBOLS AND ABBREVIATIONS

| | | |
|---|---|---|
| 3D | : | Three-Dimensional |
| **A** | : | Mixing Matrix |
| $A_n(t)$ | : | Mother Wavelet of Level *n* in Time Domain |
| ACC | : | Anterior Cingulate Cortex |
| AD | : | Alzheimer's Disease |
| ADD | : | Attention Deficit Disorder |
| ADHD | : | Attention Deficit Hyperactive Disorder |
| AI | : | Artificial Intelligence |
| ALS | : | Amyotrophic Lateral Sclerosis |
| ANN | : | Artificial Neural Network |
| AR | : | Autoregressive modelling |
| b | : | Intercept Term |
| BCI | : | Brain Computer Interface |
| BMI | : | Brain Machine Interface |
| BP | : | Band Pass |
| BSS | : | Blind Source Separation |
| c | : | Soft Margin Constant |
| CC | : | Correlation Coefficient |
| $\mathrm{cov}(X, Y)$ | : | Covariance of Variables X and Y |
| CTG | : | Cardiotocography |
| $D_n(t)$ | : | Wavelet Details of Level *n* in Time Domain |
| DBSCAN | : | Density Based Spatial Clustering of Application with Noise |
| DLN | : | Deep Learning Network |
| DWT | : | Discrete Wavelet Transform |

| | | |
|---|---|---|
| ECG | : | Electrocardiography |
| ECoG | : | Electrocorticogram |
| EEG | : | Electroencephalography |
| EMG | : | Electromyography |
| EOG | : | Electrooculogram |
| EP | : | Evoked Potential |
| ERD | : | Event Related Desynchronization |
| ERP | : | Event Related Potential |
| ERS | : | Event Related Synchronization |
| $f_s$ | : | Sampling Frequency |
| FFT | : | Fast Fourier Transform |
| FLM | : | Firefly + Levenberg Marquardt |
| fMRI | : | Functional Magnetic Resonance Imaging |
| FN | : | False Negative |
| FP | : | False Positive |
| g | : | Gamma; Parameter of Gaussian Radial Basis Function |
| HCI | : | Human Computer Interface |
| HMI | : | Human Machine Interface |
| HOS | : | Higher Order Statistics |
| HP | : | High Pass |
| Hz | : | Hertz; cycles per second |
| IC | : | Independent Component |
| ICA | : | Independent Component Analysis |
| $k(x, y)$ | : | Kernel Function |
| LDA | : | Linear Discriminant Analysis |

| | | |
|---|---|---|
| LP | : | Low Pass |
| LPM | : | Linear Programming Machine |
| MEG | : | Magnetoencephalogram |
| MEMD | : | Multivariate Empirical Mode Decomposition |
| MI | : | Mutual Information |
| *MinPts* | : | Minimum Number of Points |
| ML | : | Machine Learning |
| MRI | : | Magnetic Resonance Imaging |
| MSE | : | Mean Squared Error |
| NN | : | Neural Network |
| NRS | : | Numerical Rating Scale |
| OA | : | Ocular Artifact |
| PAF | : | Peak Alpha Frequency |
| PC | : | Principal Component |
| PCA | : | Principal Component Analysis |
| PDF | : | Probability Density Function |
| PET | : | Positron Emission Tomography |
| PFC | : | Prefrontal Cortex |
| REG | : | Regression Analysis |
| RBF | : | Radial Basis Function |
| RM | : | Regression Model |
| **s** | : | Source Component |
| SI | : | Primary Somatosensory Cortex |
| SII | : | Secondary Somatosensory Cortex |
| SNR | : | Signal to Noise Ratio |

| | | |
|---|---|---|
| SuBAR | : | Surrogate-Based Artifact Removal |
| Th | : | Thalamus |
| TN | : | True Negative |
| TP | : | True Positive |
| SVM | : | Support Vector Machine |
| V | : | Volt, Difference in Electric Potential |
| VAS | : | Visual Analogue Scale |
| VEP | : | Visual Evoked Potential |
| $\mathbf{w}$ | : | Weight Vector |
| $\mathbf{W}$ | : | Un-mixing Matrix |
| $W(j,k)$ | : | Wavelet Coefficient |
| WMA | : | Wavelet Multiresolution Analysis |
| WT | : | Wavelet Transform |
| $\alpha$ | : | Alpha Brain Rhythm |
| $\beta$ | : | Beta Brain Rhythm |
| $\gamma$ | : | Gamma Brain Rhythm |
| $\delta$ | : | Delta Brain Rhythm |
| $\varepsilon$ | : | Epsilon; Radius of Circle |
| $\theta$ | : | Theta Brain Rhythm |
| $\lambda$ | : | Eigenvalue |
| $\mu$V | : | Microvolts |
| $\sigma$ | : | Standard Deviation |
| Ω | : | Ohm, Unit of Resistance / Impedance |
| $\lvert . \rvert$ | : | Absolute Value |

# CHAPTER 1: INTRODUCTION

The study of human brain has always been a fascinating subject since the beginning of human civilization. It is believed that the electrical signals generated by the human brain represent not only the brain function but also the status of the whole body (Sanei & Chambers, 2007). In the early 20th century, physiologist Hans Berger in search for the physical being of mind has discovered a way of recording the electrical activities of human brain by placing electrodes on the scalp. This approach is later known as the electroencephalography (EEG). The first recording of EEG on human brain is thus credited to Hans Berger in the late 1920s (La Vaque, 1999). In his reports following the discovery, Berger demonstrated the alpha and beta rhythms of human EEG and also the effect of several brain disorders on the EEG signals (Haas, 2003). Since then, many researches have been conducted to study the effect on EEG due to other diseases such as Alzheimer's disease (Yagneswaran et al., 2002), epilepsy (Kannathal et al., 2005), Attention Deficit Disorder (ADD) and Attention Deficit Hyperactive Disorder (ADHD) (Arns et al., 2013; Loo & Smalley, 2008).

Together with the development of modern computer and advances in computer science, particularly in the field of machine learning and artificial intelligence (AI), EEG has seen unprecedented use cases in the field of Brain Computer Interface (BCI) (Hong & Khan, 2017; Wolpaw et al., 2000). For example, the EEG can be used as control input of robotics arm for patients who suffered from Amyotrophic Lateral Sclerosis (ALS) (Gu et al., 2009) or for use in rehabilitation of stroke patients (Ang et al., 2015). Processing of EEG data using machine learning algorithm such as Artificial Neural Network (ANN) can also be used to detect the sign of epileptic seizure (Srinivasan et al., 2007). The need for technical methods to process the EEG signals is becoming more important as the use

cases and the databases of EEG continue to expand. The following chapters explore the background, basic tools and the objectives of this study.

## 1.1 Electroencephalogram

EEG is the recording of electrical activities of the cerebral cortex through electrodes, which are usually placed on the scalp. EEG has great advantages of being non-invasive, has excellent time resolution and allow repeat testing on a subject (André-Obadia et al., 2015). EEG recording is also relatively inexpensive and enable close patient monitoring as there are no known medical contraindications or adverse effects limiting its uses. The EEG technique is widely used for the clinical diagnosis of epilepsy and sleep disorders, and is finding increasing applications for research in the field of BCI (Hong et al., 2018).

In taking EEG recording of an adult in a laboratory or patient's bedside, it is recommended that the recording take place in a quiet, dimly lit room with a moderate temperature to allow the subject to be completely relaxed. Electrodes are placed in accordance to the international 10-20 system as illustrated in Figure 1.1 (Oostenveld & Praamstra, 2001). The recording is recommended to be performed at a sampling rate of 256 or 128 Hz, with reference to linked ear lobe (A1 or A2) and forehead (FPz) acting as ground (André-Obadia et al., 2015). The scalp impedance is recommended to be below 5 kΩ for the duration of the recording (Teplan, 2002). Band pass filter of 0.5 – 100 Hz is applied to remove high frequency noise and linear trend movement at extremely low frequency during the recording. The EEG signals are conventionally described in frequency bands of delta (0.5 to 4 Hz), theta (4 to 8 Hz), alpha (8 to 12 Hz) and beta (12 to 32 Hz) shown in Figure 1.2, each of which is attributable to different aspects of brain activity (Sanei & Chambers, 2007).

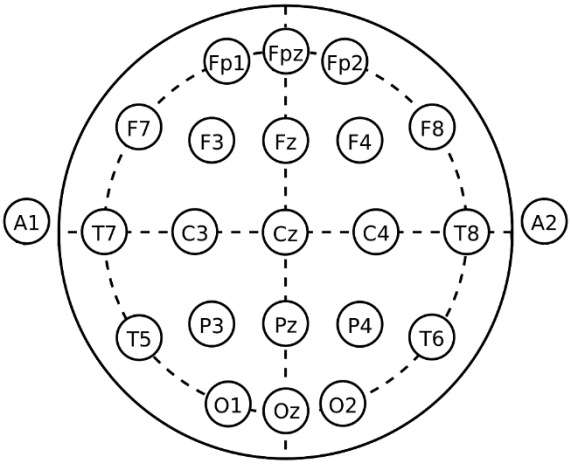


**Figure 1.1: The electrodes position and corresponding labels of the 10-20 system (Oostenveld & Praamstra, 2001).**

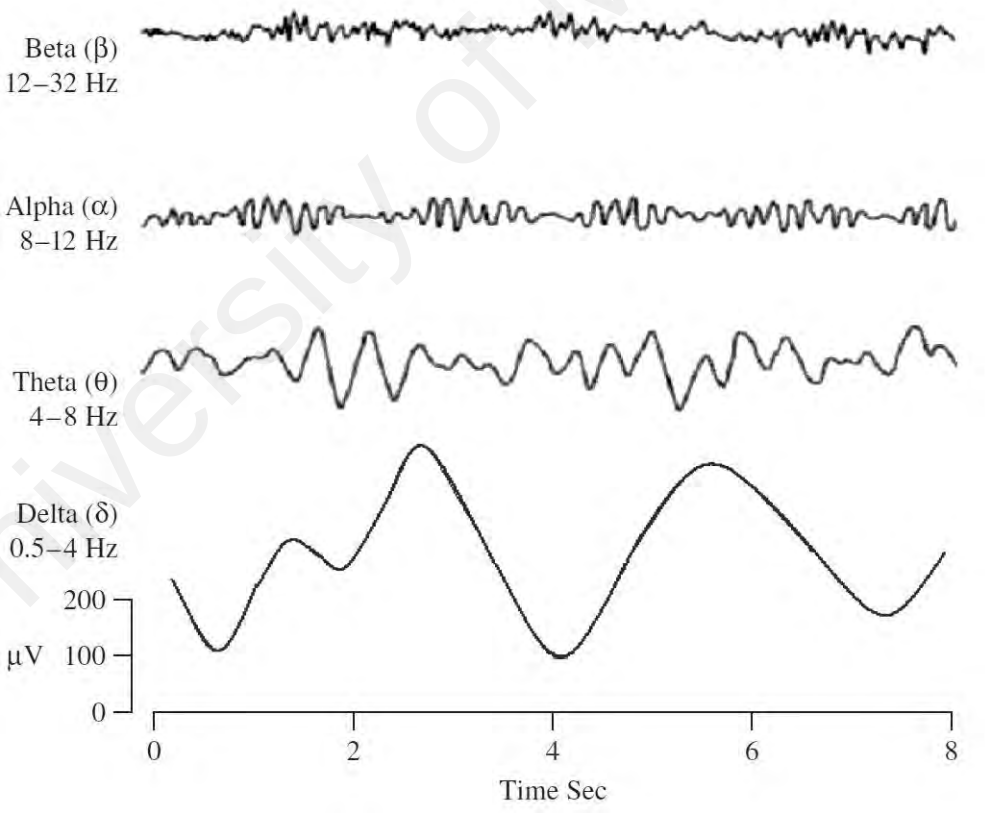


**Figure 1.2: The dominant brain rhythms of the EEG signal consisting of delta (0.5 to 4 Hz), theta (4 to 8 Hz), alpha (8 to 12 Hz) and beta (12 to 32 Hz) frequency bands (Sanei & Chambers, 2007).**

## 1.2 EEG Artifacts

In practical settings, the EEG signals are often contaminated by both biological and environmental artifacts (Hamaneh et al., 2014; Jung et al., 2000). Examples of biological and environmental artifacts that contaminate the EEG signals are shown in Figure 1.3 (Marella, 2015). Biological artifacts are signals arising from non-cerebral sources in the human body, such as cardiac, ocular or muscles activity. On the other hand, environmental artifacts originate from outside of the human body, due to electrode movement or interference from external devices such as power line or electric motor. Together, biological and environmental artifacts degrade EEG signals, thereby obstructing clinical diagnosis or BCI applications by distorting the observed power spectrum. A pre-processing or filtering step is often required to suppress the effect of artifacts on the EEG signal.

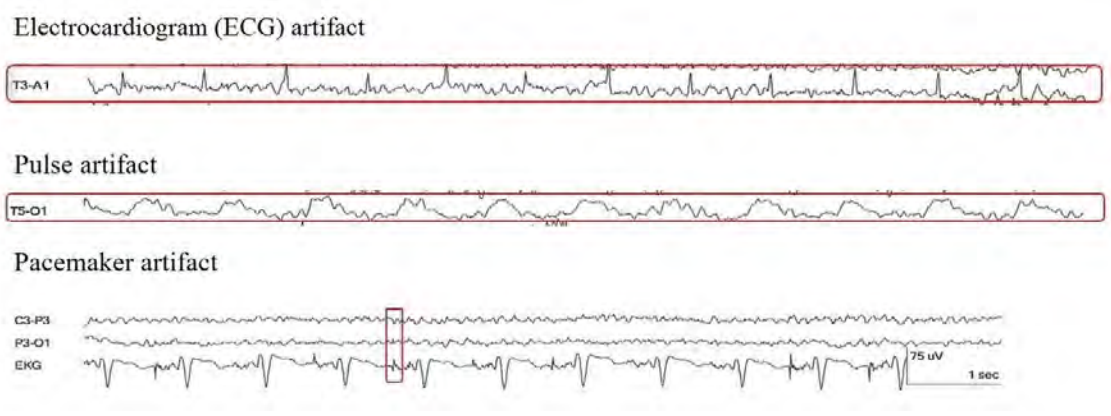


(a) Cardiac Artifacts

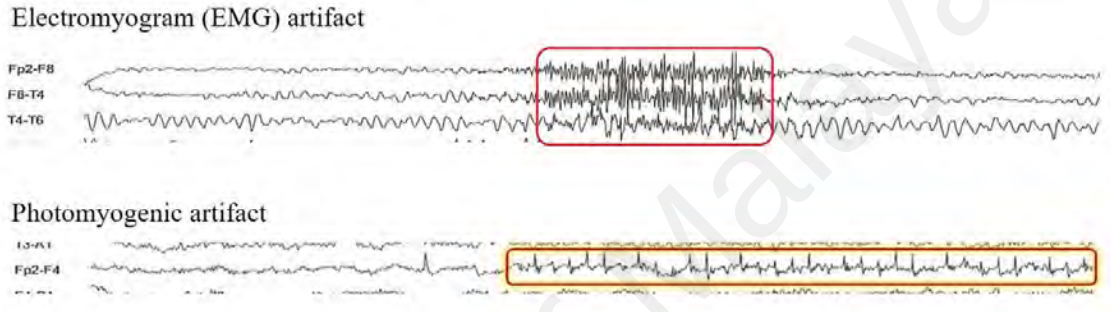


(b) Muscle Artifacts

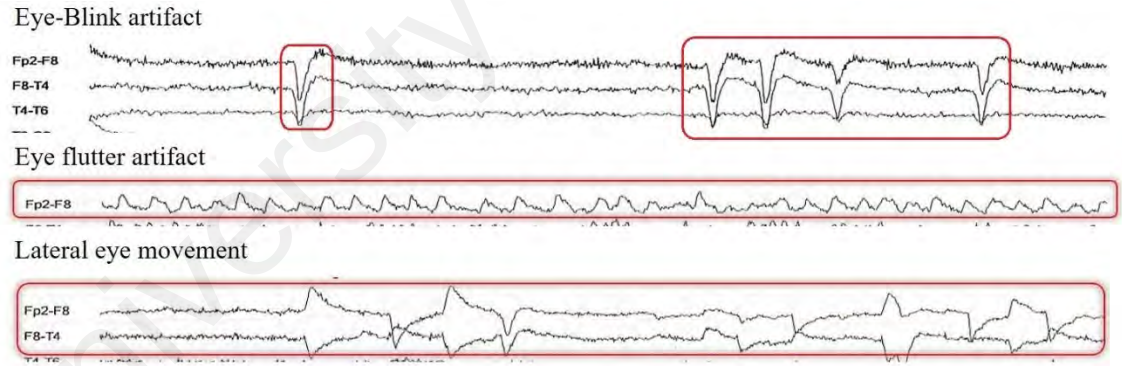


(c) Ocular Artifacts

**Figure 1.3: Examples of EEG signals contaminated by biological and environmental artifacts. Artifacts shown included (a) Cardiac, (b) Muscles, (c) Ocular, (d) Electrodes and (e) Artifacts due to External Devices.**

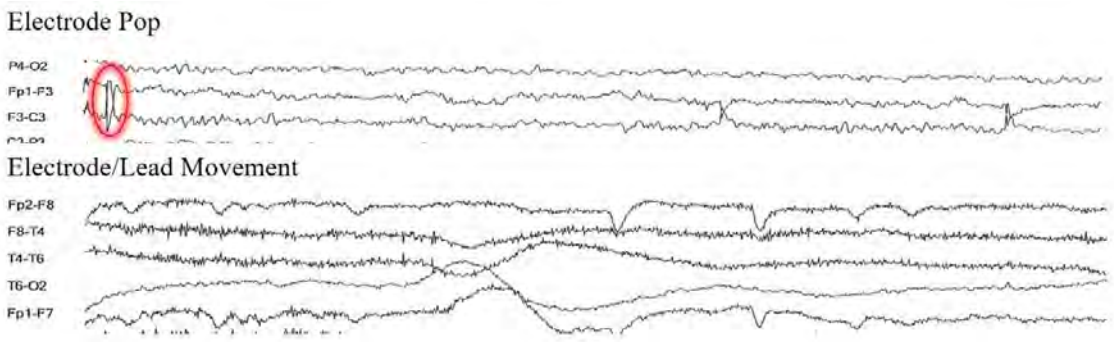


(d) Electrode Artifacts

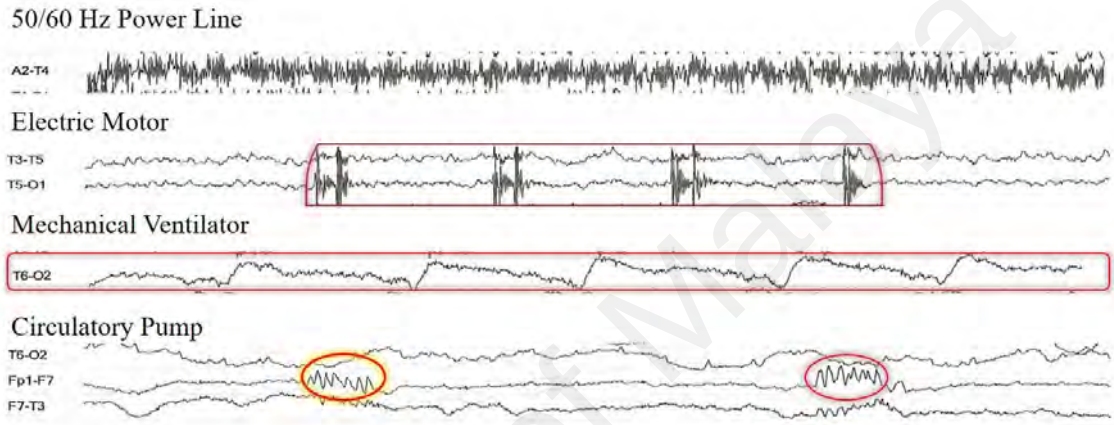


(e) Artifacts due to External Devices

**Figure 1.3, continued.**

## 1.3 Cardiotocogram

Cardiotocogram (CTG) is the recording of fetal heartbeat and the abdominal muscles contraction during labour. CTG monitoring is generally used to assess the fetal wellbeing (Alfirevic et al., 2006). The fetal heart rate and the activity of the abdominal muscles are detected by placing two transducers on the subject's abdomen. CTG can also be used to assess the frequency and intensity of uterine contractions during the first stage of labour, which presumably caused pain to the subject. An example of CTG that measured fetal heart rate and uterine contraction is showed in Figure 1.4.

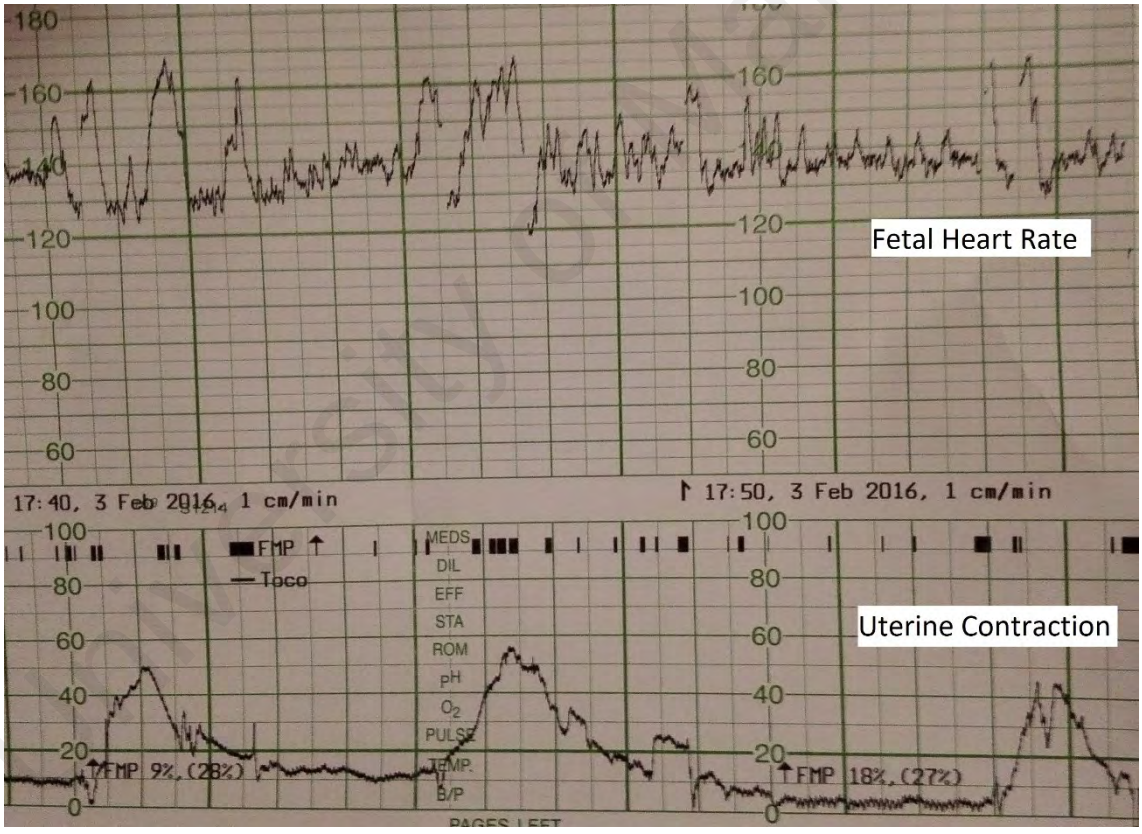


**Figure 1.4: Example of CTG recording measuring the fetal heart rate and the intensity of uterine contractions.**

## 1.4 Perception of Pain

Pain is a protective somatic sensation which acts as a warning of potential injury. When a stimulus is applied at adequate intensity, first pain and second pain are elicited by A$\delta$-fibers and C-fibers respectively (Bromm & Lorenz, 1998). The nociceptors terminate in the superficial layers of the dorsal horn as the first order neurons. The dorsal horn neurons send their axons directly to the thalamus in second order neurons. Then, in the thalamus, third order neurons send axons to the primary somatosensory cortex (SI) which interact with the secondary somatosensory cortex (SII) and other subcortical structures resulting in the feeling of pain (Egsgaard, L. L., 2009).

The subjective perception of pain is a multi-dimensional experience that can be divided into sensory, cognitive and affective components (Peng et al., 2015). The sensory component involves sensations with qualities such as stinging, burning or arching in identifiable location and duration. On the other hand, the cognitive component is associated with the attention modulation of an individual toward the pain perception. Lastly, the affective component involves the emotional unpleasantness due to pain experienced by an individual. All of the three components of pain combined results in the changes of human brain activity observable by brain imaging techniques available today (Bromm & Lorenz, 1998; Peng et al., 2015).

Physicians sometimes encounter difficulties in making important clinical decisions due to difficulties in the assessment of the extent of pain experienced by their patients. Indeed, the perception of pain is by nature highly subjective, and there are no reliable markers of the individual's internal state. Current methods used by physicians to quantify pain intensity generally rely on the patient's subjective rating according to a Numerical Rating Scale (NRS) or a Visual Analogue Scale (VAS) (Bijur et al., 2003). An example of an NRS and Wong-Baker FACES Pain Rating Scale used to describe the intensity of

pain is shown in Figure 1.5 (Wong & Baker, 1988). Here, the patient is asked to assign a value for their experience on a rating scale from 0 to 10, where 0 indicates no pain, and 10 represents the worst imaginable pain. However, these tests are often scored retrospectively, and are inherently subjective, being based on each individual patient's report, and the health staff interpretation of that report (Kumar, S. et al., 2015).

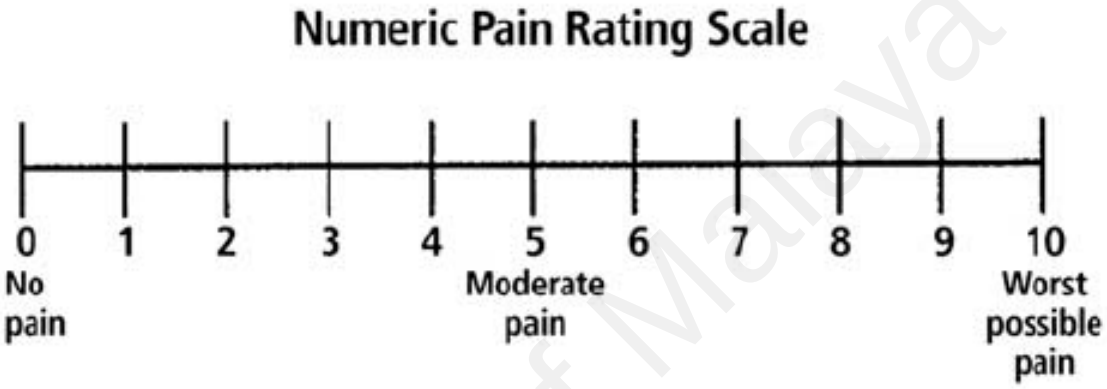


(a)


(b)

**Figure 1.5: Example of tools used to describe the intensity of pain using (a) Numeric Pain Rating Scale and (b) Wong-Baker FACES Pain Rating Scale (Wong & Baker, 1988).**

## 1.5 Objectives

This study aims to propose an integrated system for EEG signals processing in an application to monitor the pain response during a clinical state. The proposed system is applied to monitor and predict the pain response due to uterine contractions during the first stage of labour.

This study aims to achieve the following objectives:

- To enable EEG signals as a tool for clinical monitoring and BCI application by utilizing signal processing and machine learning algorithms.
- To investigate the neurophysiological changes of human brain in response to pain due to uterine contraction during the first stage of labour.
- To design and develop an objective method of pain assessment using the EEG signals.
- To optimize and test the developed system of pain assessment using the EEG signals.

# CHAPTER 2: LITERATURE REVIEW

In the last decades, various researches have been conducted to explore the use of EEG in clinical monitoring and BCI application. However, EEG signals are vulnerable to signal artifacts and often produce inconsistent results due to the occurrence of signal artifacts. Artifacts removal process is therefore essential in order to obtain reliable result from filtered clean EEG signals before utilizing the EEG signals in the application of clinical monitoring or BCI. This chapter will discuss several methods used to remove EEG signal artifacts and the neurophysiological interpretation of pain and its correlation to EEG.

## 2.1 Artifacts Removal and Pre-Processing of EEG signals

Conventional methods to remove EEG artifacts employ linear filters or regression, in relation to the time of occurrence or the frequency range of the target artifacts (Gotman et al., 1973; Woestenburg et al., 1983). However, filtering in either the time or frequency domain incurs substantial loss of observed cerebral activity because of the inherent spectral overlap between neurological activity and signal artifacts (De Beer et al., 1995). Wavelet based multiresolution analysis using a discrete wavelet transform (DWT) is shown to be more effective in removing target artifacts, while better preserving the structure of the true EEG signal in both time and frequency domains (Mamun et al., 2013; Zhang et al., 2004). On the other hand, independent component analysis (ICA) is proven useful to isolate target artifacts into a separated independent component (IC) using blind source separation (BSS) (Hamaneh et al., 2014; Jung et al., 2000). In recent years, artifact removal using a combination of wavelet and ICA methods have shown promising results

in practical applications and is further explored in this study (Mahajan & Morshed, 2015; Mammone et al., 2012).

Other methods incorporating ICA in the artifacts removal process of EEG signals have also been presented. In a recent study, the authors presented a method to remove ocular artifacts (EOG) in EEG signals using ICA and deep learning network (DLN) (Yang et al., 2018). Meanwhile, another method to remove EOG artifacts using ICA and Multivariate Empirical Mode Decomposition (MEMD) is also presented (Wang et al., 2016). In another study, a linear classifier based on optimized feature subset determined by Linear Programming Machine (LPM) is used to identify artifactual ICs for artifacts removal in EEG signals (Winkler et al., 2011). However, similar to an earlier study using the BSS-SVM method, these methods did not consider the use of wavelet transform and introduced unnecessary removal of cerebral activities observed in the EEG signals (Shoker et al., 2005).

Several methods of artifacts removal for single-channel EEG are also presented in the literature. One study presented a method that effectively utilized wavelet transform to remove ocular artifacts for single-channel EEG data (Khatun et al., 2016). Meanwhile in another study, a novel method using surrogate-based artifact removal (SuBAR) by means of time-frequency analysis of surrogate data to identify ocular and muscular artifacts embedded in single-channel EEG are presented (Chavez et al., 2018). A group of authors also presented a novel method to remove EOG artifacts from single-channel EEG using combined singular spectrum analysis and adaptive noise canceler (Maddirala & Shaik, 2016). In another study, the authors explored several features to be used in the classification using linear discriminant analysis (LDA) to detect ocular artifacts in single-channel EEG (Li et al., 2017). However, these methods are based on single-channel EEG and therefore not applicable in the present study that require the use of multichannel EEG.

Other approach of artifacts removal are also presented such as the Firefly + Levenberg Marquardt (FLM) optimization based learning algorithm for neural network (NN) enhanced active filtering (Quazi & Kahalekar, 2017). In this study, the weights for the training of NN were optimally selected by using the FLM algorithm. Other solution to remove artifacts from EEG signals have also been proposed by using blind source separation and regression analysis (BSS-REG), a method that relies on the availability of a calibration dataset to initialize the spatial filter (Guarnieri et al., 2018). Of late, method that completely sidestep the conventional wavelet transform and ICA methods have also been proposed, such as sparsity based technique and dictionary learning algorithm (Sreeja et al., 2018). A recent review of the methods for artifacts detection and removal of the EEG signals are summarized (Islam et al., 2016). It can be concluded that there are increasingly varying methods that are introduced to remove artifactual components in the EEG signals, and more are expected to be generated for the time to come. The following chapters explore the fundamental methods that are combined in several manners to form the complete solution for artifacts removal in the EEG signals applied in this study.

### 2.1.1 Discrete Wavelet Transform

Wavelet Multiresolution Analysis (WMA) incorporates the steps of DWT and inverse DWT. The initial DWT consists of sequential applications of low- and high-pass filters to decompose a discrete signal into multiple wavelet components, as shown in Figure 2.1(a). Here, x[n] represents a channel of discrete EEG signal passed through a low pass filter, g[n] and a high pass filter, h[n] simultaneously. This process is repeated until each channel of the EEG signal is decomposed into $n$ levels of wavelet details, i.e. $D_1(t), D_2(t), \cdots, D_n(t)$ and a mother wavelet $A_n(t)$. The mother wavelet and wavelet details are obtained using the formula as follow

$$A_n = \sum_{k=-\infty}^{\infty} x[k]g[2n-k] \tag{2.1}$$

$$D_n = \sum_{k=-\infty}^{\infty} x[k]h[2n-k] \tag{2.2}$$

Inverse DWT is applied in a similar but reversed sequence by recombining the wavelet details and the mother wavelet into a single channel, x'[n] as shown in Figure 2.1(b). In practical use of WMA, only the wavelet details and mother wavelet corresponding to the frequency range of interest are retained.

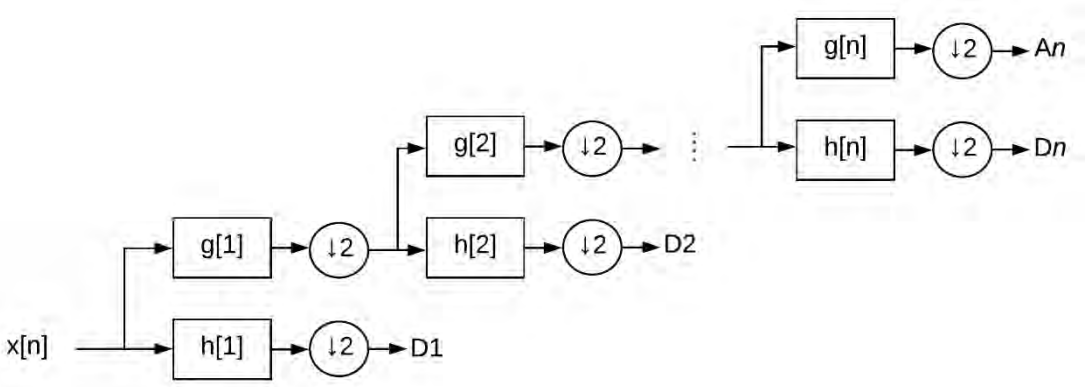


(a) Discrete Wavelet Transform

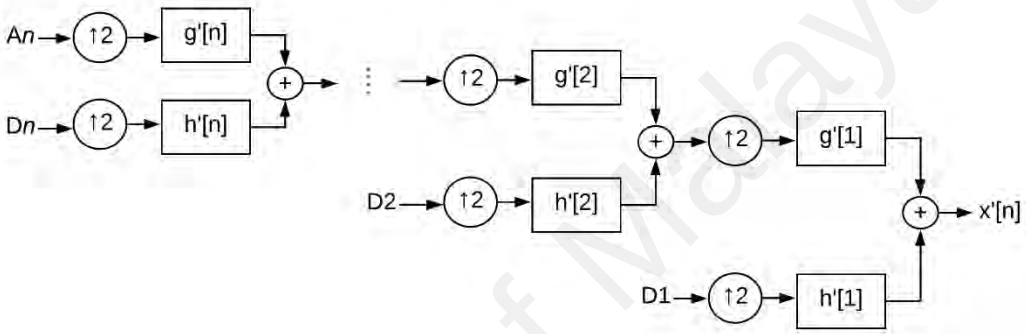


(b) Inverse Discrete Wavelet Transform

**Figure 2.1: Block diagram of (a) DWT and (b) inverse DWT of a signal, x[n] and its reconstructed equivalent, x'[n]. The annotation ↓2 denotes reduction of the signal by a factor of 2, i.e. two-fold down-sampling and ↑2 denotes two-fold up-sampling.**

### 2.1.2 Independent Component Analysis

ICA model describes multivariate signals in terms of a mixing of source components (Hyvarinen & Oja, 2000), by making the general assumption that multivariate signals, **x** are separable into their statistically independent and non-Gaussian source components, **s**. This approach has been widely applied in EEG signal processing to separate EEG artifacts (Castellanos & Makarov, 2006; Jung et al., 2000), with the requirement that several assumptions are met:

- The multivariate signals consist of cerebral and artifactual sources that are linearly mixed and statistically independent.
- Number of observed signals is greater than or equal to the number of source components.
- At most one source component is Gaussian.
- The propagation delay of artifactual sources through the scalp is negligible.

The source components are synonymous with independent components (ICs). The relationship between a recorded signal and its source components is described by the equation

$$\mathbf{x} = \mathbf{A}\mathbf{s} \tag{2.3}$$

In equation (2.3), **A** is the unknown mixing matrix, which is to be estimated by using the ICA algorithms (Chunqi et al., 2000; Hyvarinen, 1999; Hyvarinen & Oja, 2000; Lee et al., 1999). Then, the inverse of matrix **A** can be computed as the estimated un-mixing matrix, **W**. Finally, the source components, **s** are revealed by using the equation

$$\mathbf{s} = \mathbf{W}\mathbf{x}. \tag{2.4}$$

The source components can be reconstructed into multivariate signals by inverse ICA, which is accomplished by multiplying the inverse of the estimated mixing matrix, $\mathbf{W}^{-1}$ with the source components, **s**.

### 2.1.3 Principal Component Analysis

Principal Component Analysis (PCA) is a multivariate method that transform multiple variables to a new set of linearly uncorrelated variables known as the principal components (PCs) (Abdi & Williams, 2010). PCA reduces the dimension of data by projecting the data onto a lower dimension, with the goal of finding the best summary of the data using a limited number of PCs (Lever et al., 2017). The first principal component accounts for the maximum variance of the variables, and each subsequent principal component accounts for as much of the remaining variability as possible, with the additional requirement of being uncorrelated with all previous PCs. The PCs are also the eigenvectors of the covariance matrix of the original dataset. Whereas the covariance matrix of two variables X and Y is obtained by using the formula as shown in equation (2.5).

$$\mathrm{cov}(\mathrm{X},\mathrm{Y}) = \frac{1}{\mathrm{n}-1}\sum_{\mathrm{i}=1}^{\mathrm{n}}(\mathrm{X_i}-\bar{\mathrm{x}})\,(\mathrm{Y_i}-\bar{\mathrm{y}}) \tag{2.5}$$

The objectives of PCA as a method of dimensionality reduction or data compression is to extract important information from possibly correlated variables and to represent it as orthogonal variables.

#### 2.1.3.1 Eigenvalues and Eigenvectors

Let $A$ be an $n \times n$ matrix. The number $\lambda$ is defined as the eigenvalue of matrix $A$ if there exists a non-zero vector $\boldsymbol{x}$ that satisfy the equation

$$A\mathbf{x} = \lambda\,\mathbf{x}. \tag{2.6}$$

Vector $\boldsymbol{x}$ is known as the eigenvector of matrix $A$ corresponding to $\lambda$. Equation (2.6) can also be rewritten as

$$(A - \lambda I)\mathbf{x} = 0, \tag{2.7}$$

whereas $I$ is the $n \times n$ identity matrix. For a non-zero vector **x** to satisfy Equation (2.7), the determinant of $A - \lambda I$ must equal to 0. The roots of $\det(A - \lambda I)$ are also the eigenvalues of matrix $A$. The set of all vectors **x** satisfying Equation (2.6) is also known as the eigenspace of matrix $A$ corresponding to $\lambda$.

### 2.1.4 Support Vector Machine

Support Vector Machine (SVM) is a classifier using the method of supervised machine learning (Chang, C. C. & Lin, 2011). The goal of SVM is to construct an optimal hyperplane that separate two or more datasets for classification as illustrated in Figure 2.2 (Shoker et al., 2005). The optimal hyperplane is constructed so as to obtain the maximal margin from the nearest samples of different datasets, known as the support vectors. The separating hyperplane is expressed by the equation

$$\mathbf{w} \cdot \mathbf{x} - \mathrm{b} = 0 \tag{2.8}$$

where vector **w** represents the weight vector and b the intercept term. The width of the margin is given as $\frac{2}{\|w\|}$ and the optimal hyperplane is obtained by maximizing the width of the margin.

When perfect separation is not possible, a regularization parameter known as the soft margin constant, c is introduced in the SVM. The soft margin constant controls the trade-off between a low error on training data and a large margin separating the training data. When c is small, the classification mistakes are given less importance and maximizing the margin becomes a higher priority. Conversely when c is large, more focus is given on avoiding misclassification at the expense of keeping the separating margin small.

In cases where the datasets are not linearly separable in the original finite dimensional space such as $x$ and $y$ in two dimensional space, the data can be re-mapped into a sufficiently higher dimensional space as shown in Figure 2.3 (Huang et al., 2006). This mapping is conducted by using a defined kernel function, $k(x, y)$, which presumably ensures an easier separation of the datasets (Phadke & Rege, 2016). The hyperplane defined in the higher dimensional space can be seen as a non-linear separating hyperplane in the original finite dimensional space. Therefore, this approach is also known as the non-linear SVM.

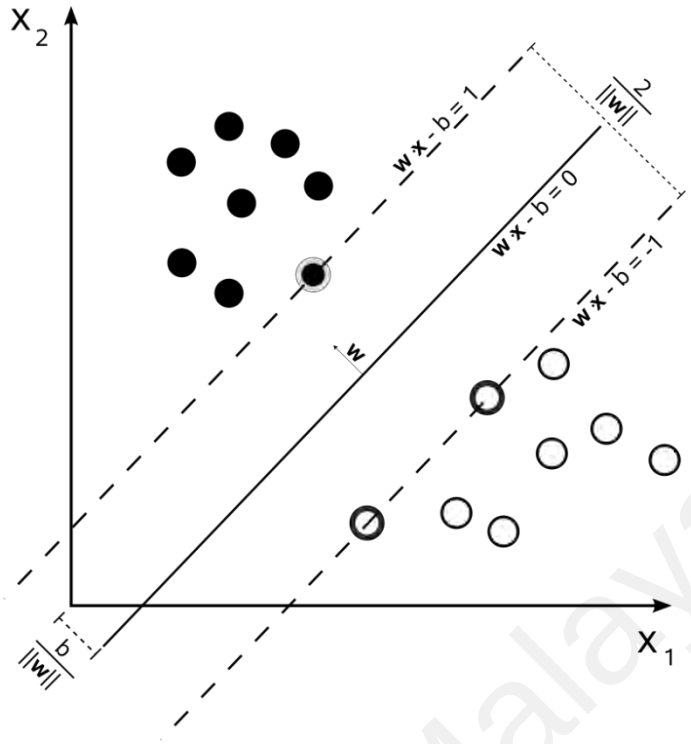


**Figure 2.2: Maximal margin hyperplane of SVM separating the sample data from two classes (Sanei & Chambers, 2007).**

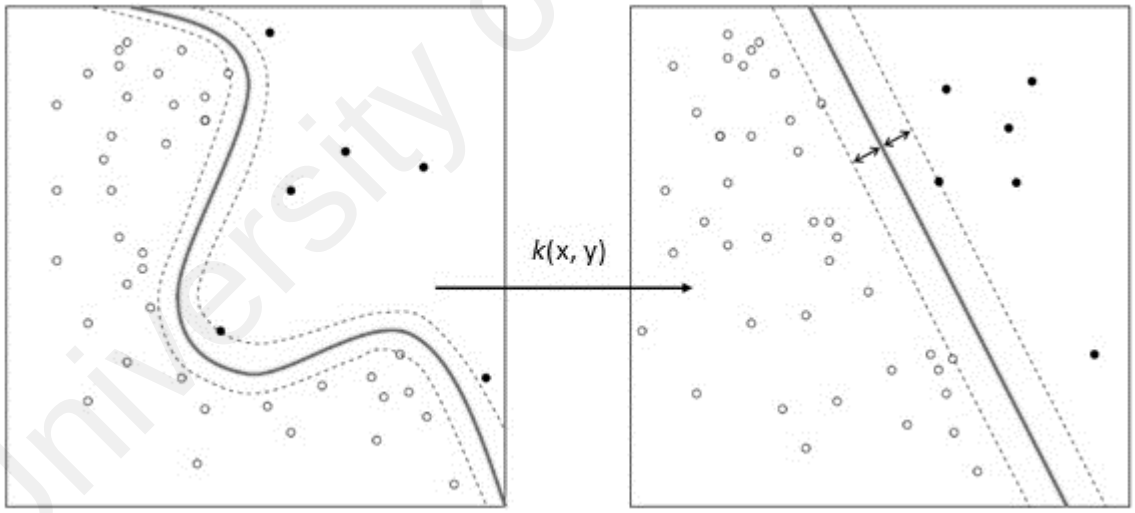


**Figure 2.3: Kernel machine transforms linearly non-separable data of two classes into linearly separable data (Sanei & Chambers, 2007).**

### 2.1.5 Density Based Spatial Clustering of Application with Noise

Density Based Spatial Clustering of Application with Noise (DBSCAN) is an unsupervised machine learning algorithm for clustering (Ester et al., 1996). DBSCAN

take advantage of the differences in density distributions of data to separate the data into different clusters. The objects are clustered based on density, i.e. the data points with similar density distribution are classified as a cluster (Agrawal et al., 1998). In other words, data points in high density regions are classified as a cluster and data points in low density region are classified as noise. The input parameters of DBSCAN are radius of circle, $\varepsilon$ and the minimum number of data points, *minPts* that fall within the radius to be classified as a cluster. A cluster consists of core and border points that satisfy the following properties:

- The core points within the cluster are mutually connected in their density.
- A border point falls within the density of any core point of the cluster is assigned as a member of the cluster.

An example of DBSCAN clustering of data points with radius of circle, $\varepsilon$ and *minPts* = 4 is presented in Figure 2.4 (Lutins, 2017). In Figure 2.4, the red colour points represent the core points that met the *minPts* criteria, yellow colour points represent the border points that does not meet the *minPts* criteria but still assigned as part of the cluster, while the blue colour point outside of radius $\varepsilon$ from any core point is considered as noise. The advantage of unsupervised machine learning algorithm is that it does not require training or training data as compared to supervised machine learning algorithm.

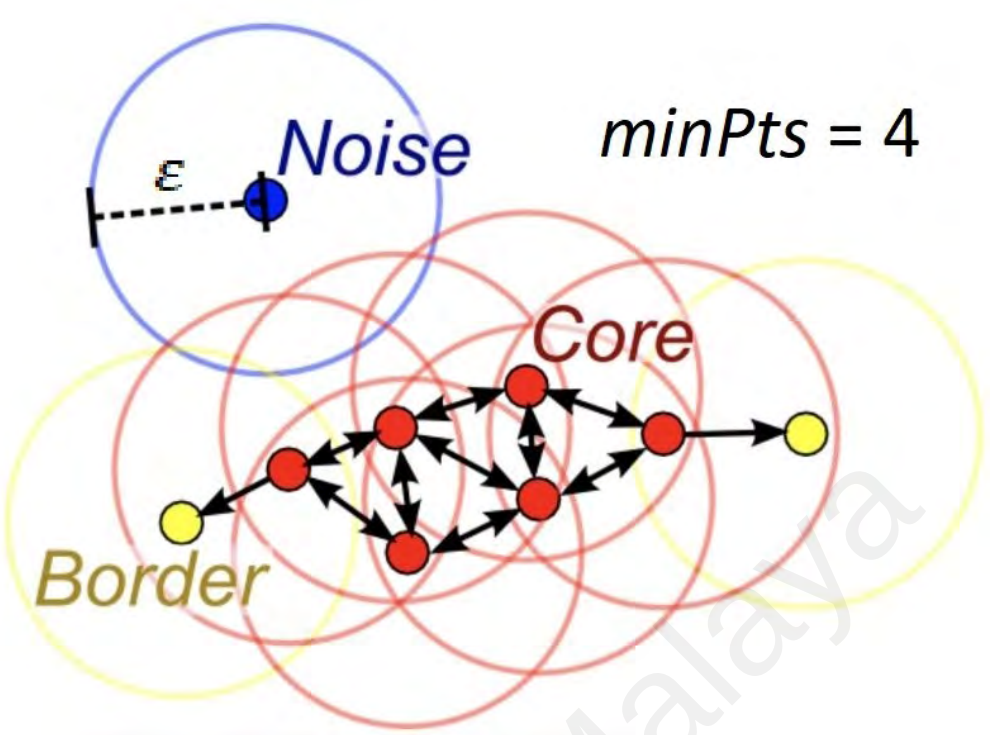


**Figure 2.4: An example of DBSCAN clustering with radius of circle, $\varepsilon$ and *minPts* = 4. (Lutins, 2017).**

## 2.2 Neurophysiology of Pain

Various efforts have been made toward developing an objective measure quantifying pain experience using brain imaging techniques such as functional magnetic resonance imaging (fMRI) (Wager et al., 2013), positron emission tomography (PET) (Kupers et al., 2011), and electroencephalography (EEG) to study the nociceptive processing of pain in human brain (Dowman, R. et al., 2008a; Huber et al., 2006; Jones, 2005). Although majority of brain-imaging studies confirmed that somatosensory cortices (SI and SII) are involved in the processing of painful stimuli, brain activation on other sites of the brain are also observed during pain (Chen et al., 2006; Haefeli et al., 2014; Kakigi et al., 2004). The brain network that involved in the perception of pain consists of primary somatosensory cortex (SI), secondary somatosensory cortex (SII), insula, anterior cingulate (ACC), prefrontal cortices (PFC) and thalamus (Th) (Apkarian et al., 2005).

Three components of pain are involved during the activation of pain network, namely sensory, affective and also the cognitive components of pain. The sensory component describes the sensory-discriminative pain experience with qualities, such as stinging, burning or arching. The sensory component of pain also describes identifiable locations and durations of the pain involved. Affective motivational experience of pain involves the emotional unpleasantness that is experienced when pain is present. The affective component of pain motivates the individual to engage in a behaviour that avoid further damage. Cognitive modulation of subjective pain perception involves cortical activities such as attention, hypnosis, expectation of pain and placebo effect when pain is experienced. The cognitive component of pain often invoked Event Related Desynchronization (ERD) of alpha activities in cortical network within pain related areas. Activation of brain network responding to the sensory, affective and cognitive components of pain and their relation with alpha rhythm are further discussed in (Peng et al., 2015).

It was observed that frequency specific neuronal activity in the brain network is associated with the pain state (Prichep, Leslie S. et al., 2011). This suggests that pain induced activation in the brain network is qualitatively and quantitatively distinguishable with neurophysiological approach. Comprehensive reviews on human brain mechanisms on pain perception are presented in (Apkarian et al., 2005) and (Bromm & Lorenz, 1998).

### 2.2.1 Labour Pain

Labour pain is characterized by regular, painful uterine contractions which increase in frequency and intensity during the first stage of labour (Labor & Maguire, 2008). With each uterine contraction, pressure is transmitted to the cervix causing stretching and

distension and causes pain through the activation of excitatory nociceptive afferents. The pain is transmitted by small unmyelinated C-fibres into the main sympathetic chain. Pain is felt in the lower abdomen, sacrum and back during this stage.

Labour pain provides an excellent model of acute pain. It is associated with obvious sensory events, namely uterine contractions and cervical dilation, which can be measured in terms of frequency, intensity, spatial extent and duration (Melzack, 1993). These characteristics make labour pain a suitable case of pain for the study of pain assessment (Abushaikha & Oweis, 2005).

## 2.3 Correlation of Pain and EEG

Given the technical difficulties and expense of fMRI and PET, EEG-based methods for pain detection would be most readily adaptable to bed-side applications. Consequently, considerable efforts have been expended in testing the potential of EEG for pain assessment in the clinic (Gram et al., 2015; Hadjileontiadis, 2015; Kumar, S. et al., 2015). It was highlighted that electrophysiological method of measurement such as EEG is capable to examine human brain activity during pain (Apkarian et al., 2005). Measurement of event related potentials (ERP) within the EEG recording can reveal the activation of specific brain regions following rapid phasic painful stimuli (Gram et al., 2013; Iannetti et al., 2008; Le Pera, D. et al., 2002). However, in this paradigm the brief stimuli may not faithfully simulate natural or clinical pain, even when considering acute pain (Gram et al., 2015; Hadjileontiadis, 2015; Nir et al., 2012). Furthermore, the recording of ERP can hardly be used as a clinical tool for monitoring of a patient's pain experience, as the short-interval ERP might bear no relation to the tonic pain being

assessed (Peng et al., 2014). Therefore, continuous EEG analysis is used instead to characterize tonic pain during more natural and prolonged stimuli (Nir et al., 2012).

Frequency domain analysis has been applied to study the changes in frequency bands activities of EEG signals associated with the experience of pain. This can be achieved by using either Fast Fourier Transform (FFT), a Regression Model (RM) or Wavelet Transform (WT) (Ocak, 2009; Subasi & Ercelebi, 2005). Changes in the relative power of individual frequency bands, in particular a decrease of alpha and increase of beta activity, have frequently been detected upon inflicting a noxious stimulus to healthy volunteers (Chang, P. F. et al., 2002b; Giehl et al., 2013; Shao et al., 2012). Table 2.1 present a summary of literature review in the changes of EEG activities observed in association with the presence of various pain conditions.

Changes of EEG in alpha frequency and amplitude measured at bilateral temporal scalp electrodes (T7 and T8) has been suggested to reflect the subjective perception of tonic pain (Nir et al., 2012; Nir et al., 2010). However, the observed changes in alpha activity are unlikely to be pain specific, but may be due to the perceptual cues such as attention being utilized in response to pain (Bromm & Lorenz, 1998). Furthermore, alpha activity also reflects attentional demands such as alertness and expectancy (Klimesch et al., 1998). It is generally held that alpha activity is not itself definitive to reflect EEG responses to pain, as alpha activity is also modulated by the cognitive and affective components of pain (Peng et al., 2015). Therefore, the suppression of alpha oscillatory activities often reported in the literature is unlikely to be pain-specific, but may in large part reflect attention modulation involved in orientation and organization of adaptive motor behaviour in response to experimentally applied painful stimuli (Bromm & Lorenz, 1998; Peng et al., 2015; Peng et al., 2014).

On the other hand, increases in beta power and in the higher frequency component of the gamma band, i.e. 30 - 100 Hz upon application of painful stimuli have also been widely reported (Chang, P. F. et al., 2002b; Giehl et al., 2013; Huber et al., 2006; Peng et al., 2014). These changes may reflect the composite of primary responses to pain stimuli, as well as artifacts arising from increased muscles activity, as attested by Electromyogram (EMG) recording during painful stimuli (Chang, P. F. et al., 2002b; Peng et al., 2014). The gamma band is particularly susceptible to high frequency noises including the power line and EMG due to clenching of teeth or other facial muscles movement corresponding to pain and is therefore not being considered in this study.

Beta frequency are known to be closely related to motor activity and highly susceptible to muscles artifacts (Veselis, 2015). Therefore, the observed beta activity during pain may also be associated with motor activity in the facial muscles or spreading of muscles activity which often accompany the pain experience (Bromm & Lorenz, 1998). Furthermore, increase in beta activity may also be related to the desynchronization of alpha being replaced by faster rhythms since that the border of these frequencies is not clearly defined (Veselis, 2015). For these reasons, apparent oscillation of beta and higher frequency band activities must be interpreted carefully in the context of pain perception (Dowman, R. et al., 2008a).

In (Gram et al., 2015), the authors have asserted that the relative theta activity responds dynamically to pain experience irrespective of the mode of stimulation. However, the results in that study were assessed from globally averaged EEG activities, and thus could not be attributed to any particular brain region by source localization. As such, findings of increased delta or slow cortical activities correlating to pain experience may be vulnerable to artifacts from oculomotor activities such as wincing or various eye blinking

activities that are often evoked by the experience of pain (Dowman, R. et al., 2008a; Hagemann & Naumann, 2001).

In general, the reported responses in EEG frequency bands activities in response to painful stimuli are inconclusive, and fail to address specifically the phenomenology of pain experience (Pinheiro et al., 2016). As pain is multidimensional, with sensory, affective and cognitive modulation components in play, it is difficult to ascertain which aspects of the pain experience actually provoked the observed EEG changes (Chang, P. F. et al., 2002b). In addition, non-specific temporal changes may also mask the specifically pain-related EEG features (Dowman, R. et al., 2008a).

Several studies have also been proposed to distinguish the state of the EEG recorded during experimental pain condition (Misra et al., 2017; Vijayakumar et al., 2017). In particular, these studies focused on experimental pain condition using tonic thermal stimuli and attempted to classify the state of pain by using SVM or Random Forest Models. These studies have achieved a rather astounding accuracy in classifying the state of pain of up to 89.5%. However, these studies are conducted in a controlled environment with stimulated pain experience and does not include natural tonic pain.

A pain index from 0 to 10 have also been attempted using fuzzy logic to predict the level of pain of the patient in post-operative condition (Kumar, S. et al., 2015). In this study, the patients' EEG were recorded in pre-operative and post-operative states and were requested to rate their level of pain during the post-operative condition. Fuzzy logic was used to predict the level of pain of the patients. The study has achieved remarkable milestone in quantifying the level of pain experienced by the patient, limited to the condition of pain experienced in a post-operative environment. The result of this study

indicates that the EEG may directly or indirectly reflect the patient's pain level and this level can be measured or predicted using an appropriate algorithm.

**Table 2.1: Literature review on studies that reported EEG changes due to various pain conditions. (↑: Increased; ↓: Decreased; δ: delta activity; θ: theta activity; α: alpha activity; β: beta activity; γ: gamma activity).**

| Authors | Pain Condition | EEG changes in response to pain | Remarks |
|---|---|---|---|
| (Prichep, L. S. et al., 2018) | Chronic Pain | ↑: θ (overall), low-α (overall) | Logistic Regression Analysis predicts severity of pain. |
| (Hansen et al., 2017) | Cold Pressor Test | ↓: α-2 (cingulate, pre- and postcentral gyri)<br>↑: δ (overall), θ (overall), β (overall) | Cingulate changes were correlated with pain intensity. |
| (Misra et al., 2017) | Tonic Thermal Stimulus | ↓: low-β (contralateral sensorimotor cortex)<br>↑: γ, θ (overall, medial prefrontal cortex) | Classification using SVM achieved cross-validation accuracy of 89.58% |
| (Vijayakumar et al., 2017) | Tonic Thermal Stimulus | Only reported training and classification using δ, θ, α, β and γ bands activities | Classification using Random Forest Models achieved accuracy of 89.45%. |
| (Gram et al., 2015) | Cold Pressor Test | ↓: θ (overall), α-1 (overall), α-2 (overall)<br>↑: δ (overall), β-3 (overall), γ (overall) | θ activities are correlated to pain ratings. |
| (Kumar, S. et al., 2015) | Post-Operative | ↓: Hjorth Activity (P3, P4)<br>↑: Spectral Entropy (P3, P4) | Estimated Pain Index of 0-10 is achieved. |
| (Hadjileontiadis, 2015) | Tonic Cold Pain | Wavelet Higher Order Spectral (WHOS) (δ, θ, α, β and γ) | Novel method of WHOS based on quadratic phase coupling (QPC). |

**Table 2.1, continued.**

| Authors | Pain Condition | EEG changes in response to pain | Remarks |
|---|---|---|---|
| (Graversen et al., 2015) | Analgesic Remifentanil | ↓: θ (overall, F1), α (overall, C6)<br>↑: δ (overall, F1) | Condition changes from pain to absent of pain. |
| (Brokjær et al., 2015) | Morphine Intake | ↓: θ (Cz) | Condition changes from pain to absent of pain. Results are not significant until 120 minutes after dosing. |
| (Peng et al., 2014) | Thermal Contact Heat | ↓: α (contralateral-central)<br>↑: γ (overall) | α activities reflect cognitive process.<br>γ activities partly reflect tonic pain processing. |
| (Giehl et al., 2013) | Thermal Contact Heat | ↓: α-1 (lower central), α-2 (lower central)<br>↑: δ (higher right parietal and right occipital) | Results are not influenced by attention manipulation. |
| (De Vries et al., 2013) | Chronic Pancreatitis | ↓: Peak alpha frequency (PAF) (parietal, occipital) | Decrease of PAF correlated with duration of pain. |
| (Jensen, M. P. et al., 2013b) | Spinal Cord Injury | ↓: α (overall)<br>↑: θ (P3, O1, O2) | α activity is correlated to higher pain intensity caused by other factors. |
| (Jensen, M. et al., 2013a) | Spinal Cord Injury | ↓: θ (overall)<br>↑: α (overall) | Condition changes from pain to absent of pain. |

**Table 2.1, continued.**

| Authors | Pain Condition | EEG changes in response to pain | Remarks |
|---|---|---|---|
| (Panavaranan & Wongsawat, 2013) | Thermal Contact Heat | ↓: α (P3)<br>↑: β (P3) | Differentiate pain and no pain condition at 96.97%. However, the achieved results are questionable. |
| (Saithong et al., 2012) | Thermal Contact Heat | ↓: α (P3, P4)<br>↑: β (P3, P4) | α activities recover after stimulation of pain. |
| (Nir et al., 2012) | Thermal Contact Heat | ↓: α-1 (T7, T8) | α-1 power (T7, T8) negatively correlated to pain intensity. |
| (Shao et al., 2012) | Cold Pressor Test | ↓: θ (frontal), α (parietal occipital)<br>↑: β (temporal), γ (temporal) | Left frontal θ, anterior cingulate (ACC) α and posterior cingulate (PCC) β activities are negatively correlated to subjective pain rating. |
| (Nir et al., 2010) | Thermal Contact Heat | ↑: Peak Alpha Frequency (PAF) (T7, T8) | PAFs at T7, T8 are correlated to pain intensity. |
| (Sitges et al., 2010) | Chronic Pain | ↓: δ (P3, P4, Cz, Fz), θ-1 (T7, T8), α-2 (P3, P4), β-1 (Pz), β-2 (Pz)<br>↑: Entropy at P4 compared to P3 | Decreased α activities due to sustained attention cause by persistent pain. |

**Table 2.1, continued.**

| Authors | Pain Condition | EEG changes in response to pain | Remarks |
|---|---|---|---|
| (Egsgaard, L. et al., 2009) | Cuff Pressure Pain | ↓: α-1 (centre) for high alpha group<br>↑: α-2 (parietal-occipital) for low alpha group | High and low alpha group individual may present different brain processing to pain. |
| (Dowman, Robert et al., 2008b) | Cold Pressor Test | ↓: α (contralateral temporal)<br>↑: α (posterior), γ (overall) | Temporal α activities are consistent with pain related activities in SI, SII. Posterior α activities due to attention being drawn toward pain. Observed changes in γ activities may be due to EMG. |
| (Rissacher et al., 2007) | Cold Pressor Test | ↓: θ (frontal), α (temporal-parietal)<br>↑: β-2 (overall) | Changes in θ activities caused by anxiety, changes in α activities due to attention or visual activity, changes in β activities due to arousal. |
| (Huber et al., 2006) | Thermal Contact Heat | ↓: θ (left frontal-temporal), α (frontal temporal)<br>↑: δ-2 (overall), β (left temporal) | Results are not specific to pain. Applying temperature below pain threshold produced similar results. |

**Table 2.1, continued.**

| Authors | Pain Condition | EEG changes in response to pain | Remarks |
|---|---|---|---|
| (Chang, P. F. et al., 2004) | Capsaicin Injection | ↓: α (posterior), θ (overall during muscle pain)<br>↑: δ (frontal), β (overall during muscle pain) | Difference between skin pain and muscle pain is addressed. |
| (Chang, P. F. et al., 2003) | Hypertonic Saline Injection | ↓: α-1 (posterior), α-2 (posterior)<br>↑: β-2 (overall) | α activities gradually resumed after hypertonic saline injection. |
| (Chang, P. F. et al., 2002b) | Cold Pressor Test | ↓: α (POz)<br>↑: δ (F8), θ (F8), β (temporal) | Changes in α and β activities are immediate, δ activities changes gradually. |
| (Chang, P. F. et al., 2002a) | Hypertonic Saline Injection | ↓: α-1 (right temporal-posterior), α-2 (Pz, POz) | Results not observed in aversive auditory arousal that induced similar arousal and unpleasantness. |
| (Le Pera, Domenica et al., 2000) | Hypertonic Saline Injection | ↑: δ (P3, P4), α-1 (P3, P4), β-2 (P3, P4) | Increase of δ and α-1 activities are not observed compared to non-painful stimuli. |

# CHAPTER 3: METHODOLOGY

The block diagram of the developed integrated system consists of four major steps, i.e. EEG recording, signal pre-processing, features selection and classification as shown in Figure 3.1. First of all, EEG recording is conducted in both laboratory and also clinical environment for application in clinical monitoring. Subsequently, signal pre-processing is applied to remove artifacts in the noisy raw EEG signals as part of the development of the complete system. Last but not least, the study extends to the process of features selection and classification of pain response in a clinical study during the first stage of labour.

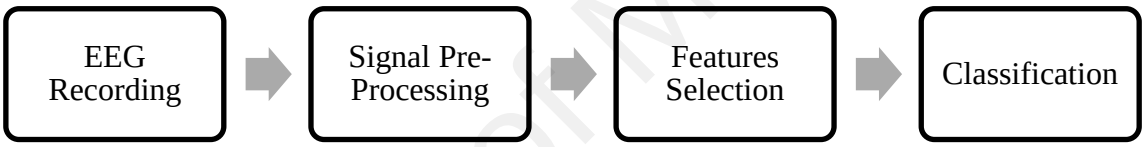


**Figure 3.1: Block diagram of the complete system for clinical monitoring and BCI application using EEG signals.**

## 3.1 EEG Recording

EEG acquisition equipment g.USBamp (g.tec, Austria) was used to acquire EEG signals from the subjects. The electrodes were placed as specified by the 10-20 system. There were 16 electrodes used in the study, corresponding to channels FP1, FP2, F3, Fz, F4, T7, C3, Cz, C4, T8, P3, Pz, P4, O1, Oz and O2. The ground electrode was set at FPz, and the reference point fixed on the left earlobe (A1). The recording scalp impedance was kept below 5 kΩ, with a sampling rate of 256 Hz. A notch filter of 50 Hz (Butterworth, order 4), corresponding to the local power mains and a band pass filter of 0.5 to 100 Hz (Butterworth, order 8) were applied during the recordings.

### 3.1.1 EEG Recording in the Laboratory

Eleven healthy volunteers, consists of 7 males and 4 females with mean age (±SD) 27.4 (6.2) years old, have given informed consent to participate in this study. The recording procedure is as describe in Section 3.1. The recording sessions are conducted in Applied Control and Robotics Laboratory (ACRLAB) in the Faculty of Engineering, University of Malaya. The subjects are instructed to maintain a natural upright sitting position with eyes open for up to 30 minutes. EEG signals with eye blink artifacts are recorded following involuntary eye blink activities. An example of a session of EEG recording conducted in the laboratory is shown in Figure 3.2.


**Figure 3.2: Example of an EEG recording session conducted in the laboratory.**

### 3.1.2 EEG Recording in Clinical Condition

In a study involving subjects in clinical condition, ten parturient women of mean age (±SD) 29.6 (4.9) years admitted in the labour ward of the University Malaya Medical Centre (UMMC) participated in this study. The subjects were in their active phase of first stage of labour, defined by cervical dilation of 2 - 10 cm. The subjects reported painful experience due to intense and frequent uterine contractions. All participating subjects were right-handed, were not receiving any medication known to affect the EEG, and had no history of neurological or psychiatric disease. Informed consent was obtained from all individual subjects included in the study. Each subject gave written consent to the experimental procedures, in a study conforming to the Declaration of Helsinki, and approved by the local research ethics committee from UMMC (Ethical Clearance: 20156-1404). Cardiotocography (CTG) was recorded simultaneously throughout the EEG recordings, which lasted for up to 30 minutes for each individual subject. Figure 3.3 shows an example of a recording session conducted in the clinical condition.

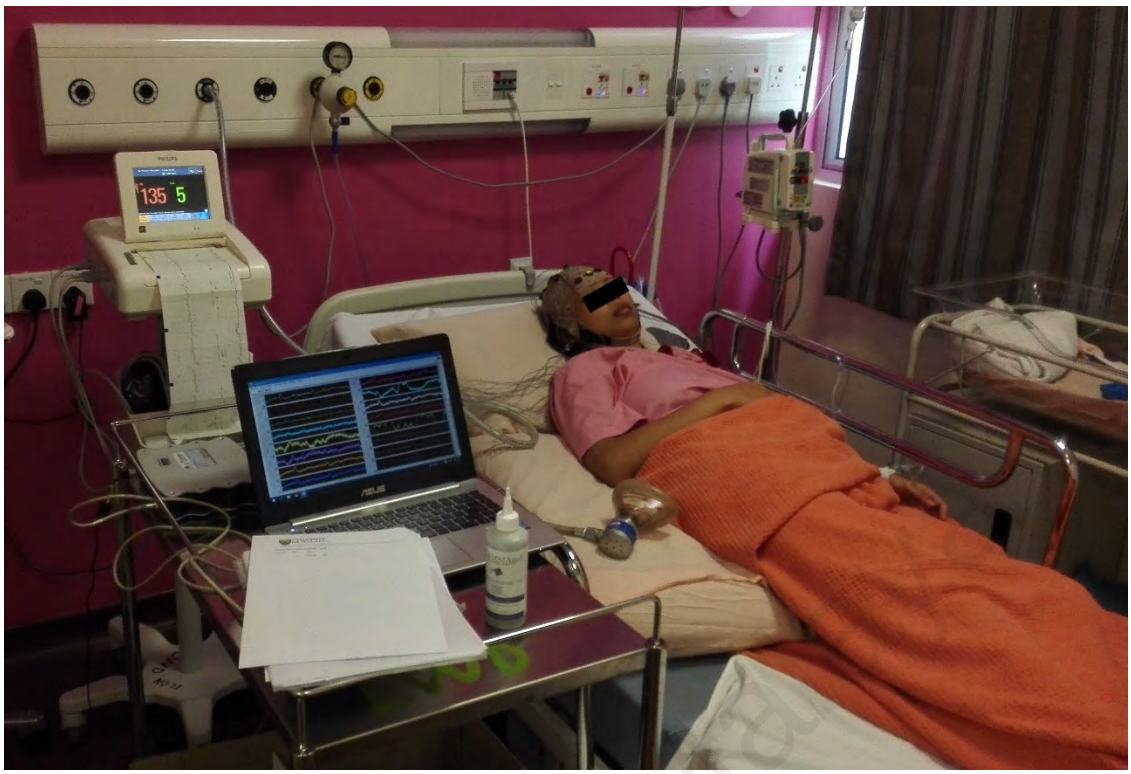

**Figure 3.3: Example of an EEG recording session conducted in the clinical condition.**

### 3.1.2.1 Labelling of EEG Signals as "Resting" or "Pain" State

In an effort to quantify objectively the pain experience independent of any subjective input from the subjects expressed through the NRS or the Wong-Baker faces, it is assumed that the pain experience is present during bouts of uterine contraction throughout the first stage of labour, as revealed by a surge in the CTG signal. The CTG is calibrated with resting state as the baseline level and any surge exceeding this baseline indicates the onset of a cycle of uterine contraction. Each epoch of the EEG signals is labelled as either "resting" or "pain" state according to the phase of uterine contraction observed in the simultaneously recorded CTG tracing. In other words, the epochs of EEG signals outside the bouts of uterine contraction episodes are labelled as "resting" state, and the epochs of recorded EEG signals with present uterine contraction are labelled as "pain" state. A representative CTG tracing corresponding to approximately 15 minutes of recording

containing several cycles of uterine contraction defining the “resting” and “pain” states is depicted in Figure 3.4.

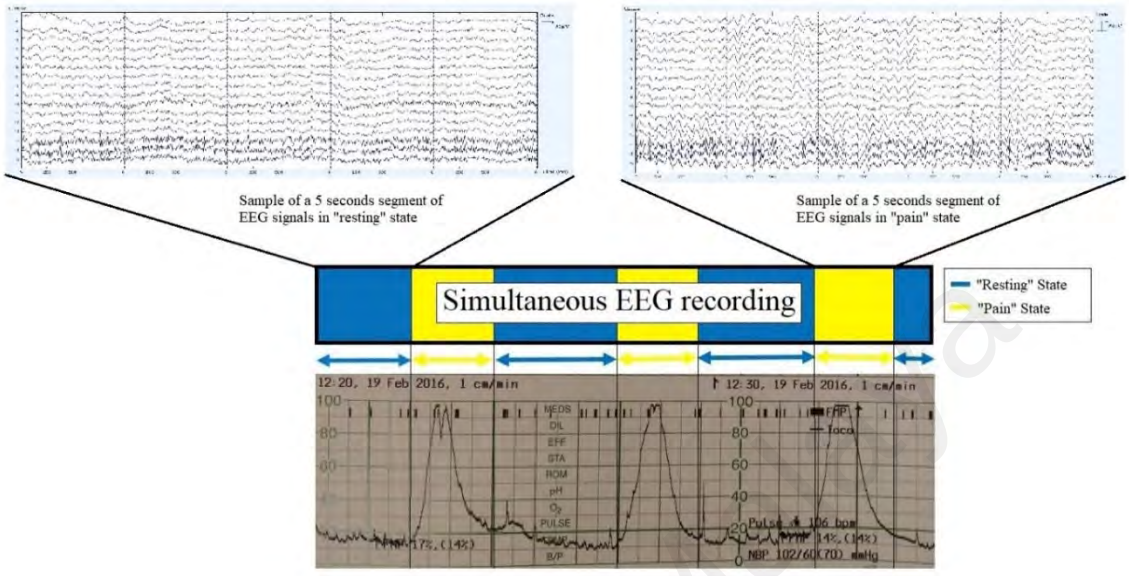


**Figure 3.4: An example of CTG recording indicating cycles of uterine contraction during the first stage of labour. Simultaneously recorded EEG signals are labelled into “resting” when CTG signals are at baseline level, or “pain” states, defined by phasic uterine contraction as indicated by the CTG trace.**

## 3.2 Signal Pre-Processing

Two methods of EEG signal pre-processing are presented in this study by using supervised and unsupervised machine learning algorithms to identify the artifactual ICs during the Wavelet-ICA process. Figure 3.5 shows an in-depth block diagram for EEG signal pre-processing utilizing Wavelet-ICA with supervised machine learning algorithm using SVM to identify and remove the artifacts in EEG signals. Meanwhile, the method of EEG signal pre-processing utilizing Wavelet-ICA with unsupervised machine learning algorithm using DBSCAN is presented in Figure 3.6. Firstly, the EEG signals are passed through Wavelet Multiresolution Analysis (WMA) to remove noise and artifacts outside of the frequency bands of interest of EEG signals. Following after, ICA algorithm is applied to decompose the EEG signals into individual ICs and the ICs containing

artifactual components are identified using the SVM or DBSCAN algorithm. Lastly, the identified ICs with artifactual components are passed through the wavelet artifacts removal model and the resulted wavelet components and ICs are recombined to form the filtered clean EEG signals. The advantage of using SVM is that it allows real time application in ongoing EEG recordings, but has the disadvantage of requiring training the model in advance with training data. On the other hand, the DBSCAN algorithm does not allow real time application as the data have to be collected beforehand to determine the clustering during the unsupervised process. However, the DBSCAN algorithm required no training in advance. Further details on the EEG signal pre-processing methods are explained in the following chapters.

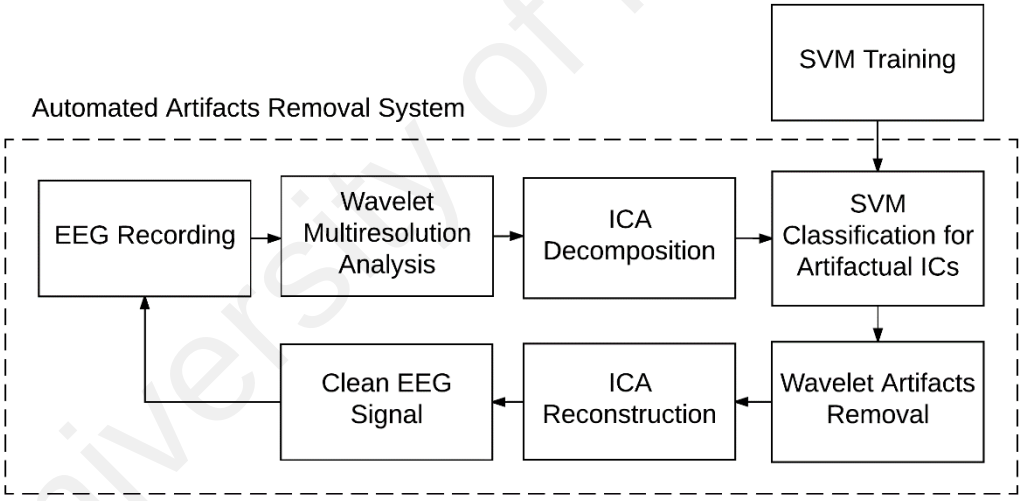


**Figure 3.5: Block diagram of the proposed artifacts removal system using Wavelet-ICA and pre-trained SVM for artifactual ICs identification.**

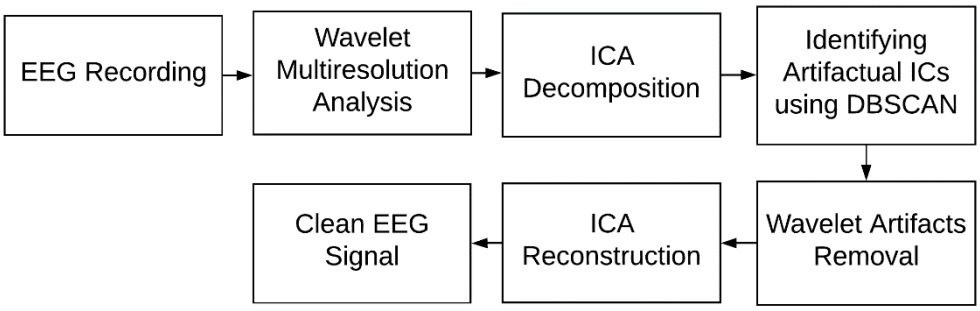


**Figure 3.6: Block diagram of the proposed artifacts removal system using Wavelet-ICA and DBSCAN for identification of artifactual ICs.**

### 3.2.1 Wavelet Multiresolution Analysis

WMA was first applied to the EEG recording in order to exclude all but the frequency bands of interest from 0.5 to 32 Hz containing the frequency bands of EEG activities. Each channel of the recorded signal is decomposed by DWT to 8 levels using a mother wavelet of Daubechies wavelet (db8) (Mamun et al., 2013). WMA deletes details at levels D1 and D2, corresponding to the frequency range of 32 to 128 Hz and also the mother wavelet A8, corresponding to the frequency range of 0 to 0.5 Hz. As such, WMA retain relevant details of D8 to D3, corresponding to the frequency range of interest for EEG signals, i.e. 0.5 to 32 Hz. The wavelet details from D8 to D3 represent the traditional frequency bands of EEG signals defined as delta (0.5 to 4 Hz), theta (4 to 8 Hz), alpha (8 to 12 Hz) and beta (12 to 32 Hz) bands respectively (Teplan, 2002). WMA filtered most of the artifacts out of the frequency range of interest, notable high frequency noise (>32 Hz), and linear trend movement at extremely low frequency (0 to 0.5 Hz).

### 3.2.2 ICA Decomposition

After preliminary filtering of the EEG signal by WMA, the processed signal is decomposed into ICs by using the Matrix-Pencil algorithm (Chunqi et al., 2000). The

number of ICs is constrained to be less than or equal to the number of channels of the EEG signal, which is 16 in this study. The matrix-pencil algorithm is selected over alternates such as fastICA or the Infomax algorithm due to its superior performance in application for non-stationary signals (Chunqi et al., 2000; Hyvarinen & Oja, 2000). Additionally, the matrix-pencil algorithm based on second-order statistics also presents less computational load than algorithms based on higher-order statistics.

### 3.2.3 SVM Training and Classification

The decomposed ICs are evaluated by a pre-trained linear SVM to determine whether the ICs contain any artifactual component. The SVM is trained using features of selected sample ICs that contain the target artifactual components, which are in the present case eye blink artifacts. Indeed, the eye blink artifact is one of the most common artifacts in EEG signals. This study also proposes the use of kurtosis, variance, Shannon's entropy and range of amplitude as the most salient descriptive features to distinguish eye blink artifacts from EEG signals. These features are selected from an extensive number of possible factors based on their discriminative properties to identify the eye blink artifact. In particular, it is found that the eye blink artifact has a significantly higher amplitude in the proposed features compared to an uncontaminated EEG signal. These features are used as the training data and also as test data for evaluation in SVM. Notice that the selection of these features is not only useful for isolation of the eye blink artifact, but can also serve for other artifactual components such as those arising from electromyogram (EMG) signals. The selection and combination of features and training data of SVM should allow the system to identify any target artifactual components present in an EEG recording. Once an IC is identified as containing artifactual component, it is sent for further processing by the wavelet artifact removal model.

A separated validation algorithm is applied to validate the ICs that are classified as constituting an artifactual component. This measure is introduced in order to support the validity of the result of SVM classification for future datasets. In the algorithm, the absolute value of each proposed features is calculated from the identified artifactual ICs, and compared with the other uncontaminated ICs. If the artifactual ICs' value exceed by a factor of at least three times the common mean value (Nolan et al., 2010), then it can properly be considered as containing a significant artifactual component, and its features can be incorporated in the training of SVM for future classification. This procedure of updating the training data ensures that the system is adaptive to future datasets.

### 3.2.4 Identifying Artifactual ICs using DBSCAN

The DBSCAN is an unsupervised machine learning algorithm used to identify the artifactual ICs during the process of Wavelet-ICA in this study. The features extracted from the ICs are similar to the supervised approach presented in Section 3.2.3, i.e. the kurtosis, variance, Shannon's Entropy and range of amplitude to determine the eye blink artifacts (Agrawal et al., 1998). The parameters of DBSCAN, namely the radius of circle, $\varepsilon$ and minimum number of points, *minPts* are calibrated by running simple experiment on the sample training data. Practically, the parameters can be freely selected in this unsupervised approach. However, in this study, the training data are utilized as sample data to optimize the selection of the parameters. Once the parameters of $\varepsilon$ and the *minPts* with reasonable performance in the training data are selected, the *minPts* is adjusted to fit with the total number of data points in application. For example, if the *minPts* is determined to be 50 in a sample training data with 2000 data points, the value of *minPts* would be adjusted to 25 if the application consist of only 1000 data points.

### 3.2.5 Wavelet Artifacts Removal

Wavelet artifact removal is applied to the ICs identified by SVM or DBSCAN as constituting artifactual components. This step is introduced to filter out the target artifactual components without completely removing the entire ICs that may yet contain cerebral activities of interest. The ICs are again decomposed by DWT and the wavelet coefficients of each wavelet component are calculated. The wavelet component with a coefficient exceeding the universal value for wavelet denoise is deemed to be purely artifactual, and is thus removed (Castellanos & Makarov, 2006; Khatun et al., 2016; Mahajan & Morshed, 2015). The universal value, *K* for wavelet denoise is calculated as

$$K = \sqrt{2 \log \mathrm{N}}\, \sigma, \tag{3.1}$$

where N is the length of the data to be processed and

$$\sigma = \frac{\mathrm{median}(|W(j,k)|)}{0.6745} \tag{3.2}$$

represents the magnitude of neuronal wide band signal. In equation (3.2), $|W(j,k)|$ represents the absolute value of the wavelet coefficient, with constant 0.6745 accounting for the Gaussian noise. The selection and calculation for the universal value is discussed in details in (Donoho & Johnstone, 1994; Mamun et al., 2013).

### 3.2.6 Wavelet and ICA Reconstruction

After the removal of artifacts, the remaining wavelet components are reconstructed into ICs by inverse DWT. Finally, inverse ICA is applied to reconstruct the filtered ICs into clean EEG signals with artifacts removed.

## 3.3 Features Selection

In an application to classify the existence of pain in clinical condition, features of interest in both time and frequency domains were extracted from each epoch of the EEG signals for use in training a further SVM to classify the state of pain. The extracted features in this study included spectral activities, statistical features and non-linear features (Sai et al., 2019). In general, the spectral activities consist of the relative and absolute frequency band activities traditionally designated as delta, theta, alpha and beta bands. Other statistical and non-linear features shown in Table 3.1 are also extracted for consequent classification. As a result of statistical analysis in this study, all the features are ranked in descending order of class separability criteria using independent evaluation criteria for binary classification (Dash & Liu, 1997). The ranking describes the capability of a particular feature in separating the two labelled groups, namely, “resting” and “pain” states. The ranking of features is conducted by using the *rankfeatures* function available in MATLAB.

**Table 3.1: List of extracted features from EEG epochs.**

| | |
|---|---|
| Spectral Activities | Relative Power of Delta (%), Theta (%), Alpha (%) and Beta (%) bands<br><br>Absolute Power of Delta, Theta, Alpha and Beta bands<br><br>Peak Frequency and Amplitude of Peak Frequency |
| Statistical Features | Mode, Median and Mean<br><br>First Quartile and Third Quartile Values<br><br>Variance, Standard Deviation, Skewness, Kurtosis and Range<br><br>Root Mean Square Value (Vrms)<br><br>Maximum and Minimum Values |
| Non-linear Features | Hjorth Mobility and Hjorth Complexity<br><br>Shannon's Entropy and Energy Entropy<br><br>Hurst Exponent<br><br>Fractal Dimension<br><br>Number of Peaks and Number of Valleys |

## 3.4 Classification of EEG Signals in Clinical Condition

Classification algorithms using supervised machine learning are applied to classify an epoch of the EEG data to either "resting" or "pain" state. Unsupervised machine learning algorithms such as the DBSCAN failed to perform meaningfully for this task due to its complexity. The Support Vector Machine (SVM) algorithm with Radial Basis Function (RBF) kernel are employed in this study. The complete procedural sequence of the study from EEG and CTG recordings to training of the SVM and obtaining a classification accuracy using test data are summarized in Figure 3.7. The recorded EEG data is first filtered using the pre-processing and filtering steps as described in Section 3.2, in this case using Wavelet-ICA with SVM and aid of visual inspection for the best performance. Then, the EEG data are labelled as either "resting" or "pain" state in accordance to the CTG tracing as described in Section 3.1.2.1. The EEG data are randomly assigned to training data (80%) and test data (20%). The classification model was constructed using only the training data. The model is optimized by iteratively training and testing the model with different parameters of gamma, g and the soft margin constant, c using five-fold cross-validation with the training data, in order to obtain the highest possible cross-validation accuracy. Once the values of the parameters g and c that yielded the highest accuracy were identified, a classification model was trained using these parameters and ran against the test data to determine the performance of the SVM.

The performance of the system is evaluated for its sensitivity as given by

$$\text{Sensitivity} = \frac{\text{TP}}{\text{TP} + \text{FN}} \times 100\%, \tag{3.3}$$

and for the specificity of the system, as determined by

$$\text{Specificity} = \frac{\text{TN}}{\text{TN} + \text{FP}} \times 100\%. \tag{3.4}$$

Whereas the overall accuracy of the SVM is thus given by

$$\text{Accuracy} = \frac{\text{TP} + \text{TN}}{\text{TP} + \text{TN} + \text{FP} + \text{FN}} \times 100\%. \tag{3.5}$$

In these formulae, TP represents the number of True Positive, TN the True Negative, FP the False Positive and FN the False Negative events.

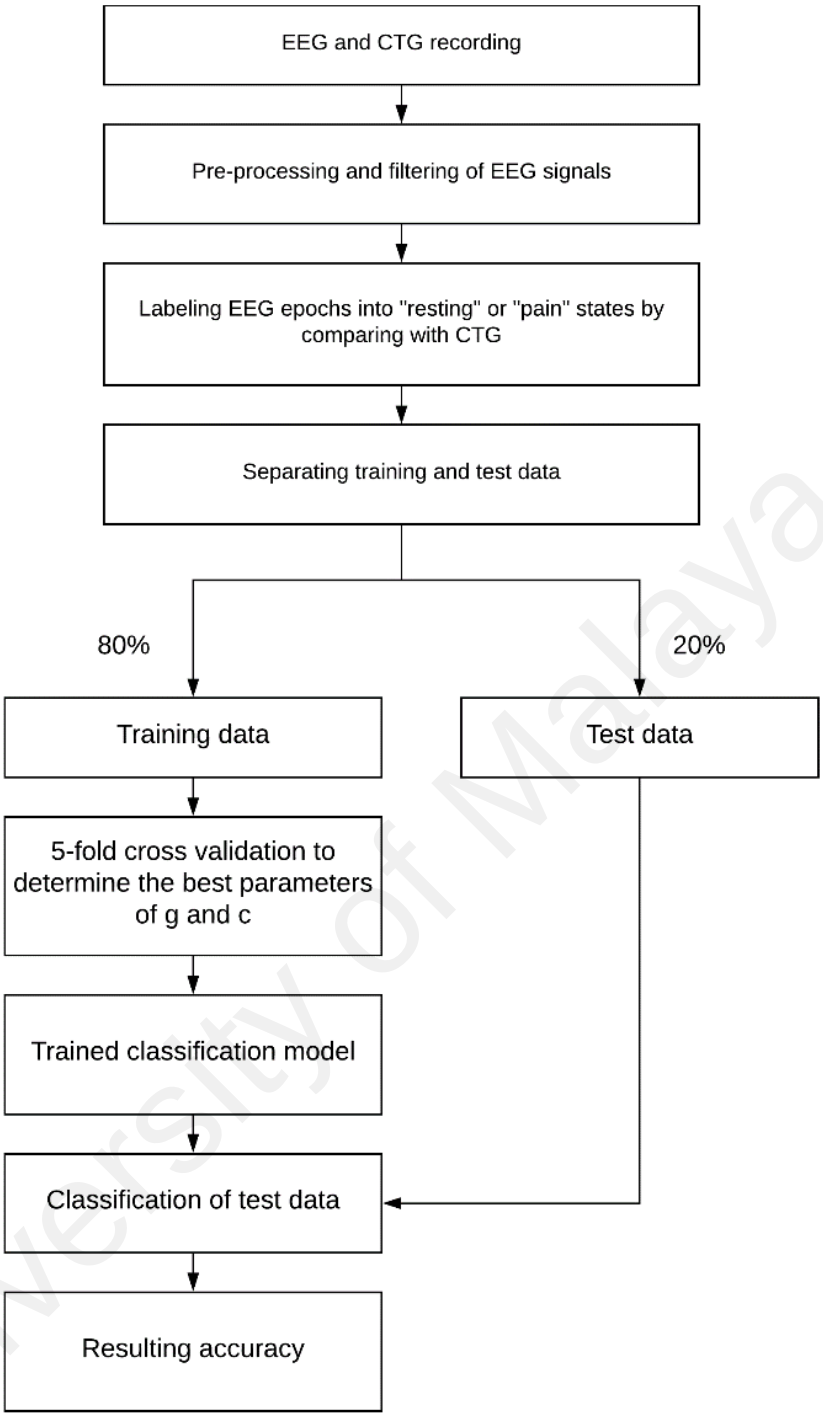




**Figure 3.7: The flowchart of the study beginning with EEG and CTG recordings and proceeding to classification of "resting" and "pain" state using the SVM algorithm with an RBF kernel. Five-fold cross-validation is used to identify the optimum parameters of gamma, g and soft margin constant, c.**

# CHAPTER 4: RESULTS

The proposed EEG pre-processing system is demonstrated on an EEG data recorded in the laboratory and tested on a publicly available EEG dataset from EEGLAB (Delorme & Makeig, 2004). The system's robustness and reproducibility are validated against the public data from EEGLAB to serve as a benchmark for future research. The proposed system achieved satisfactory results in removing artifactual components while retaining cerebral activities of interest. Finally, the complete system is tested in a clinical study of pain caused by uterine contractions during the first stage of labour. Changes in the frequency bands activities from "resting" to "pain" state are analysed and the features are ranked in descending order of separability criteria. Classification of the EEG signals are conducted using SVM with RBF kernel function and finally the optimization process is conducted using PCA.

## 4.1 Pre-Processing and Artifact Removal using EEG Signals Recorded in the Laboratory

This section presents the results of artifacts removal process using the methods of EEG signal pre-processing described in Section 3.2. The procedure for EEG signals recording is as described in Section 3.1.1. An example of a recorded five seconds segment of a 16-channels raw EEG signals are shown in Figure 4.1.

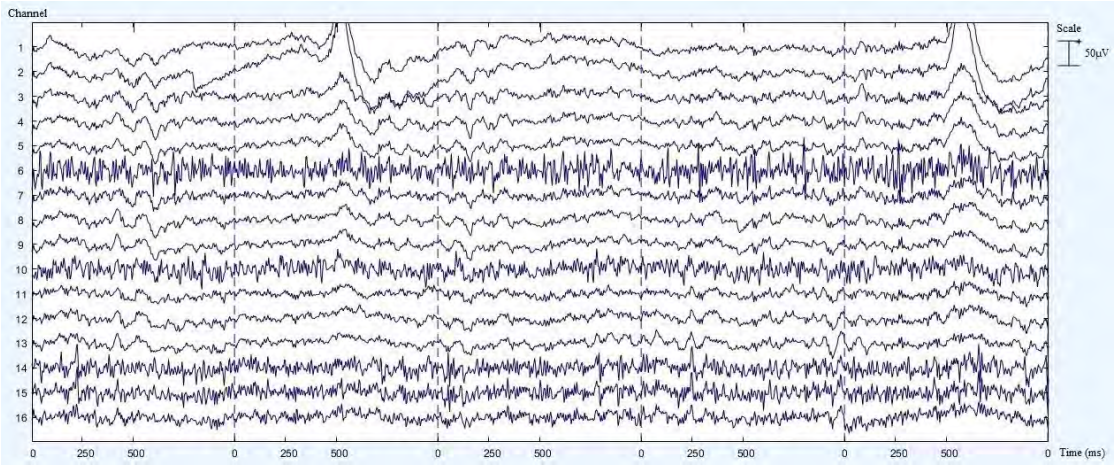


**Figure 4.1: An example of a five seconds segment of the recorded 16-channels raw EEG signals.**

### 4.1.1 Effect of Wavelet Multiresolution Analysis

The recorded signals are first passed through WMA to retain only the frequency bands of interest using 8 levels decomposition and mother wavelet of db8. The signals remaining after passage through WMA are shown in Figure 4.2. It is observed that most of the artifacts lying outside of the frequency bands of interest are efficiently removed with minimal distortion to the time and frequency resolution of the EEG signals (Sai et al., 2018). This pre-processing also eases ICA decomposition at later stages in the signal processing.

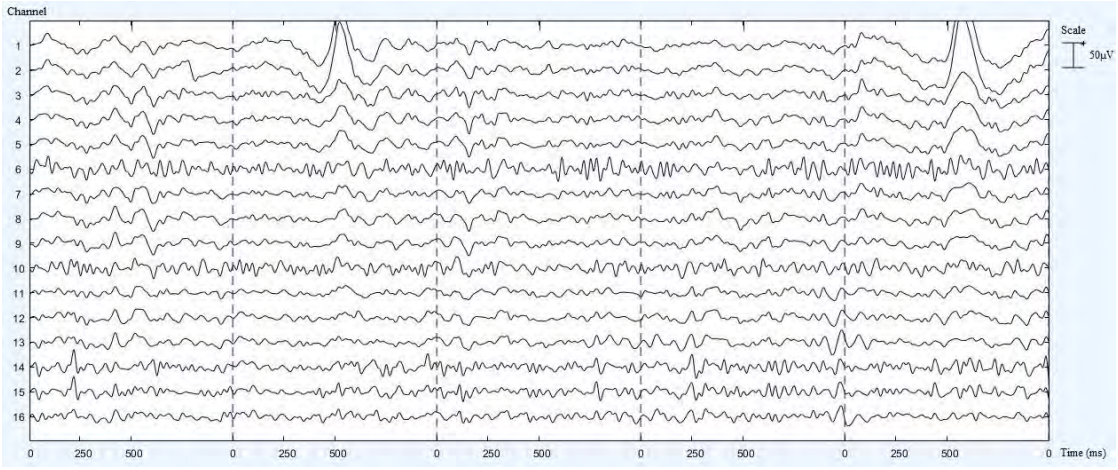


**Figure 4.2: The EEG signals after a pre-processing step using WMA. This step is conducted to retain only the frequency bands of interest (0.5 to 32 Hz).**

### 4.1.2 Separating the Artifactual Components through ICA

However, some of the artifactual components overlapping the frequency resolution of EEG signal were not removed by WMA. In particular, it is noted that the eye blink artifacts remained in the second and fifth segments of the five seconds epoch shown in Figure 4.2. ICA is applied to the 16-channels signal in Figure 4.2 and decomposed the signals into its estimated statistically independent and non-Gaussian ICs. The resulting 16 ICs decomposed by ICA using the Matrix-Pencil algorithm are shown in Figure 4.3.

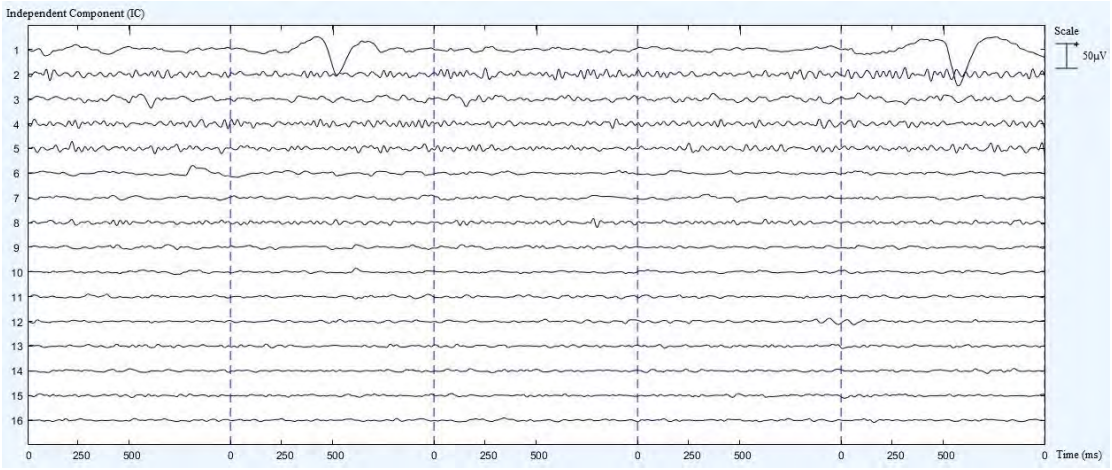


**Figure 4.3: Decomposed 16 ICs from EEG signal using ICA.**

By visual inspection, it can be observed that the first IC contains the eye blink artifacts. The values of the kurtosis, variance, Shannon's entropy and range of each IC are shown in Figure 4.4. It can be seen that IC1 has outlier value in each of the features proposed to separate eye blink artifacts from cerebral activities.

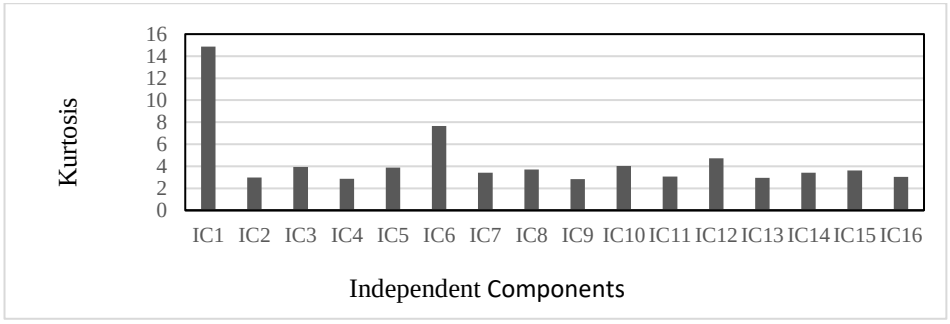


(a) Value of kurtosis of separated ICs.

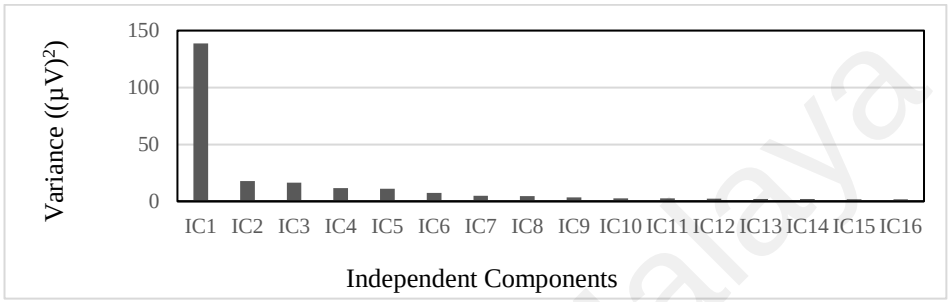


(b) Amplitude of variance of separated ICs.

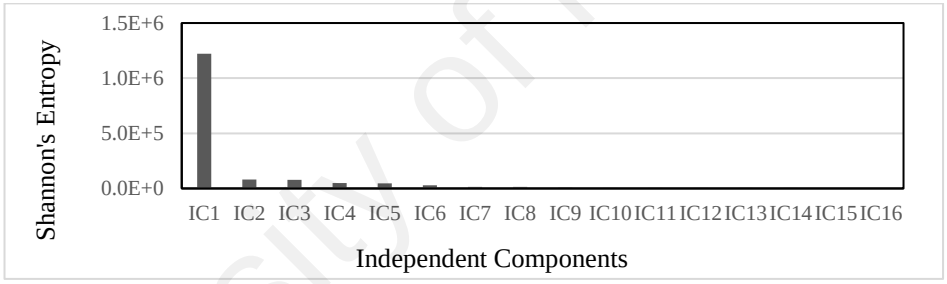


(c) Amplitude of modulated Shannon's Entropy of separated ICs.

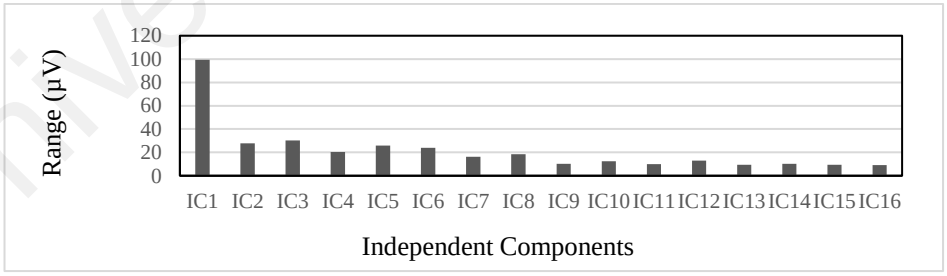


(d) Value of range of separated ICs.

**Figure 4.4: Selected features that differentiate IC1, which contain eye blink artifacts, from the other ICs. The four descriptive features presented are (a) kurtosis, (b) variance, (c) absolute value of Shannon's entropy and (d) range of amplitude.**

### 4.1.3 Classification of Artifactual ICs using SVM

Linear SVM trained with similar features from training data containing the target artifactual component classified that IC1 indeed contain an artifactual component. The SVM is trained using a total training data of 5,000 ICs containing eye blink artifacts and also randomly selected 5000 non-artifactual ICs, extracted from 10 participating subjects and labelled by visual inspection (Gabsteiger et al., 2014). Parameters of SVM are selected as linear kernel with soft margin constant, c = 10, determined by using 5-fold cross-validation with the training data. The SVM classified IC1 as artifactual IC. Then, IC1 is further validated by the criteria of having key features with absolute value at least three times the common mean. The identified features of the first IC are included in the training dataset for future classification of eye blink artifact.

### 4.1.4 Unsupervised Artifactual ICs Identification using DBSCAN

Unsupervised machine learning algorithm using DBSCAN is also presented as an alternative method to identify the artifactual ICs in this study. The training data are used as a sample to calibrate the parameters of radius of circle, $\varepsilon$ and minimum number of points, *minPts* by testing for a possible combination of the parameters. In this study, the optimized parameters are obtained as $\varepsilon = 2.6$ and *minPts* = 135 for sample training data of 5000 data points. Following after, the DBSCAN algorithm is used for unsupervised clustering of artifactual and non-artifactual ICs in the test data. In this example, the DBSCAN algorithm also classified IC1 as artifactual IC.

### 4.1.5 Filtering and Recombination

To filter the artifactual components in IC1, wavelet artifact removal is applied to isolate the wavelet components with coefficient that exceeded the universal value, as

defined in Section 3.2.5. This method effectively removed the eye blink artifact identified in IC1, while minimizing the risk of inadvertently removing the cerebral activities of interest that present in IC1. Wavelet and ICA reconstruction are performed after the removal of the artifactual components. The final reconstructed clean EEG signal of the five seconds segment example is shown in Figure 4.5.

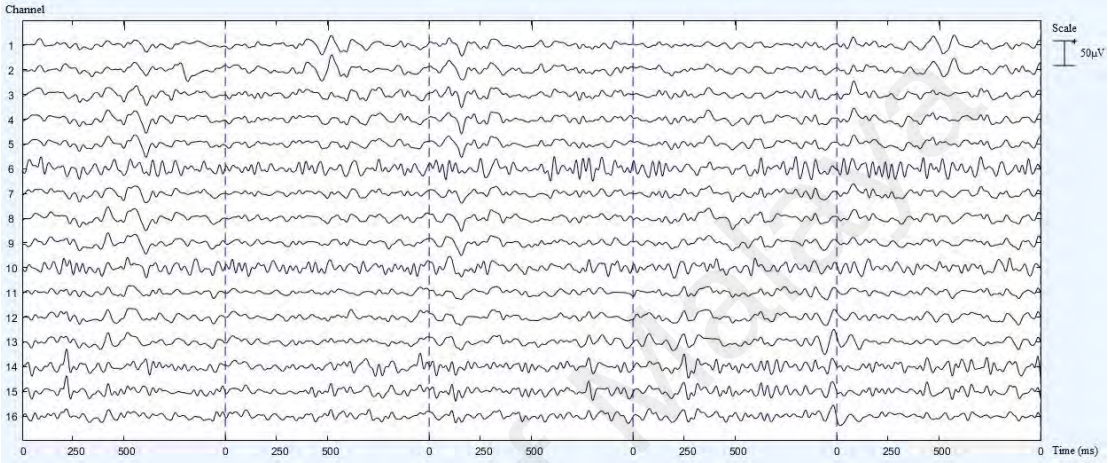


**Figure 4.5: Filtered 16-channels clean EEG signals using the proposed methods.**

## 4.2 Performance Evaluation using Public Dataset from EEGLAB

To validate further the robustness and reproducibility of the proposed system, the system is tested using a publicly available dataset from EEGLAB. This dataset is a recording of 32 channels, thus serving to investigate the extendibility of the system to an EEG recording of higher spatial resolution. The scalp locations corresponding to each of the 32 channels can be found at (Delorme & Makeig, 2004). As with data in Section 4.1, the EEG signal was resampled at 256 Hz and divided into five seconds epochs for further processing. Wavelet-ICA with SVM have the best performance in identification of artifactual and non-artifactual ICs, and also the highest correlation coefficient after filtering. An epoch of the original signal and the corresponding filtered result using Wavelet-ICA with SVM is shown in Figure 4.6(a) and (b) respectively. It is observed

that, as with the 16-channels recording, the artifactual components attributed to eye blink and lateral eye movement are effectively removed, while cerebral activities of interest within the relevant frequency bands of the EEG signal are retained.

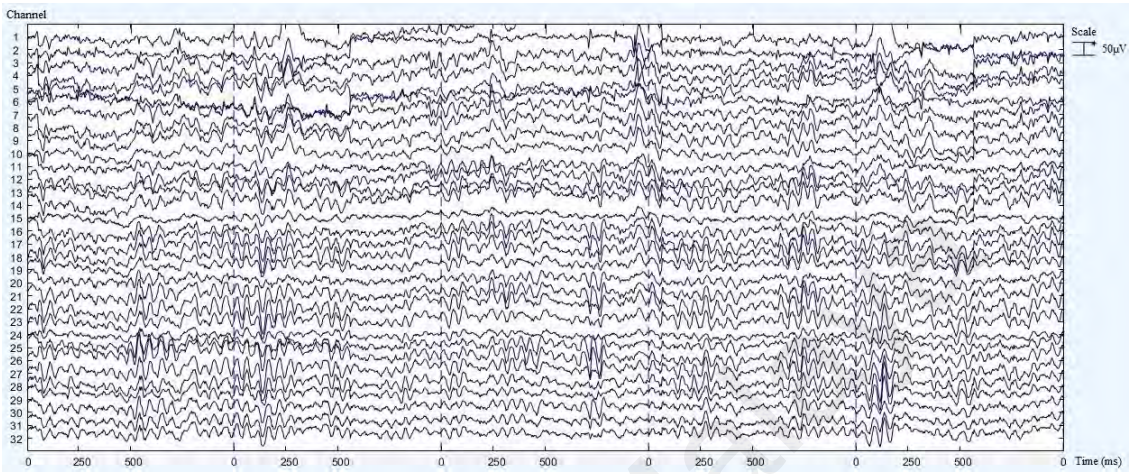


(a) An example of a five seconds segment of dataset from EEGLAB

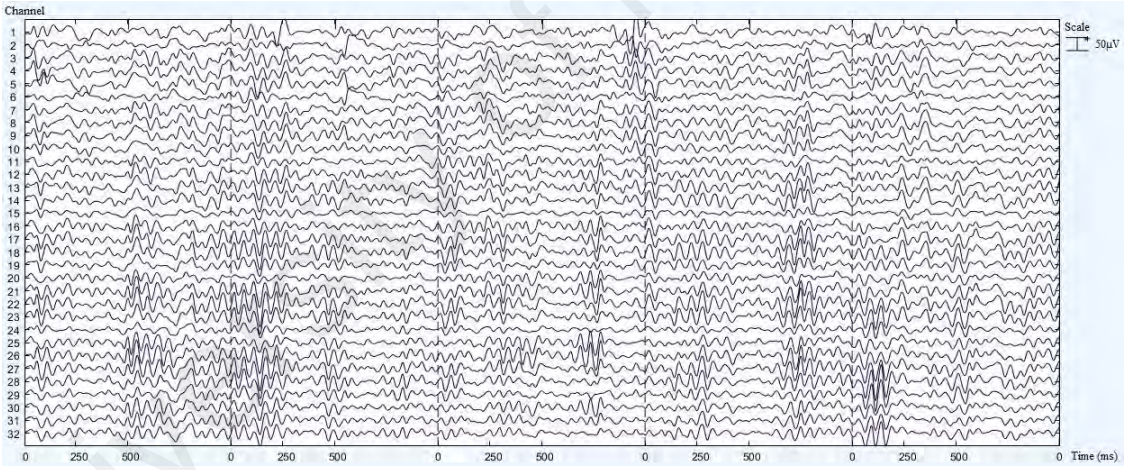


(b) Filtered EEG signals from the similar five seconds segment

**Figure 4.6: An example of (a) a segment of 32-channels EEG signals from dataset of EEGLAB and (b) the corresponding filtered signals using Wavelet-ICA with SVM.**

### 4.2.1 Accuracy in Identification of Artifactual and Non-Artifactual ICs

The labelled artifactual and non-artifactual ICs of the dataset from EEGLAB by visual inspection is shown in Figure 4.7. It can be seen that the artifactual ICs have unusually high value of kurtosis, variance, Shannon's Entropy and range of amplitude as previously

described in the example in Section 4.1.2. During the classification process, Wavelet-ICA with linear SVM using the parameter of c = 10 recorded an average accuracy of 99.1% using the dataset from EEGLAB. The performance of Wavelet-ICA with SVM is shown in the confusion matrix in Table 4.1 and the result of classification is shown in the scatter plot in Figure 4.8. On the other hand, Wavelet-ICA with DBSCAN using the parameters of $\varepsilon = 2.6$ and $minPts = 19$ recorded an average accuracy of 97.9% as shown in Table 4.2. The result of clustering using DBSCAN is shown in Figure 4.9. A comparison of the performance of SVM and DBSCAN with the standard thresholding method is shown in Table 4.3. It is observed that Wavelet-ICA with SVM have the best performance in identification of artifactual ICs as compared to Wavelet-ICA with DBSCAN or the conventional thresholding method.

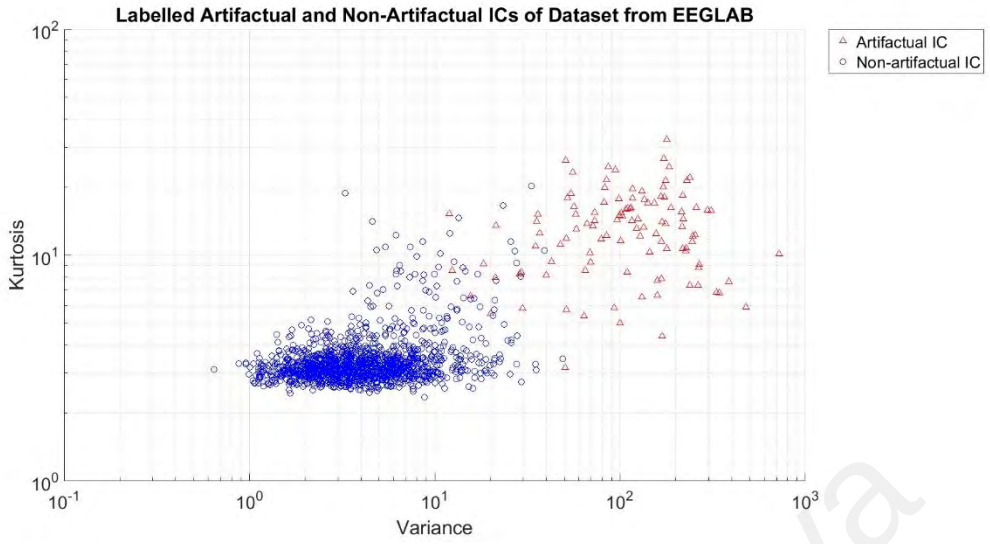


(a)

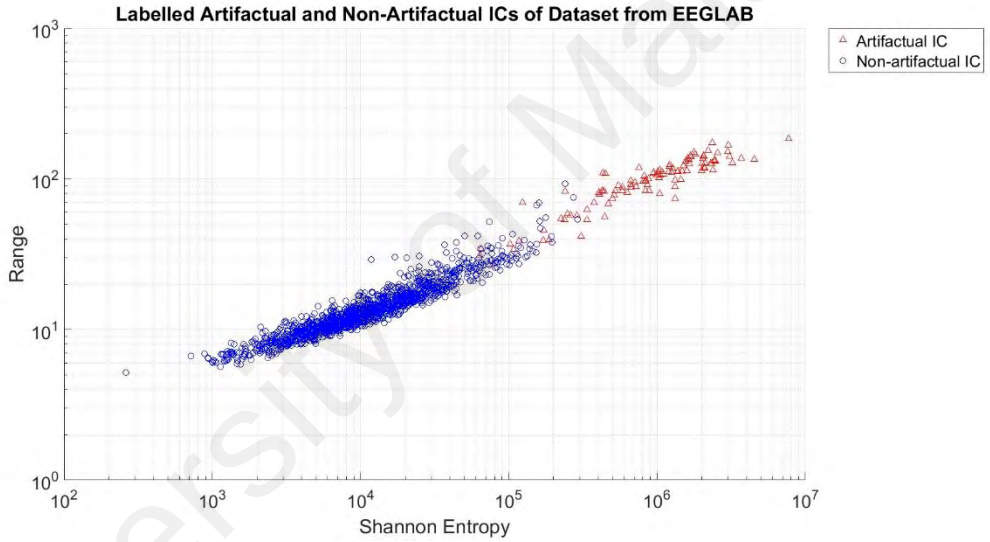


(b)

**Figure 4.7: Labelled artifactual and non-artifactual ICs of the dataset from EEGLAB by visual inspection. Figure (a) and (b) are presented to illustrate all four features, i.e. kurtosis, variance, Shannon's entropy and range used in the classification or clustering process.**

**Table 4.1: Confusion matrix for classification of ICs using SVM with dataset from EEGLAB.**

| | Predicted: Non-Artifactual | Predicted: Artifactual |
|---|---|---|
| Actual: Non-Artifactual | (TN) 665 | (FP) 5 |
| Actual: Artifactual | (FN) 1 | (TP) 33 |

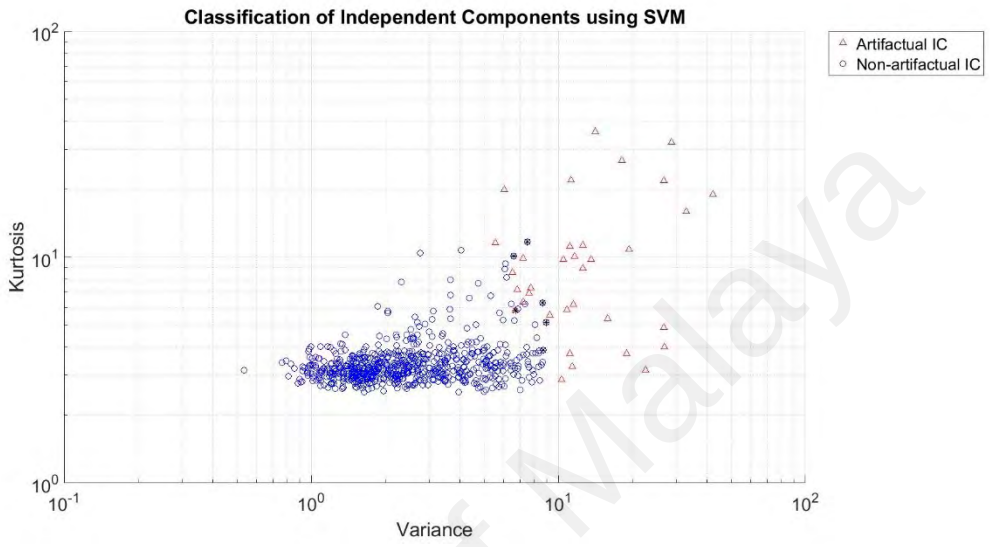


(a)

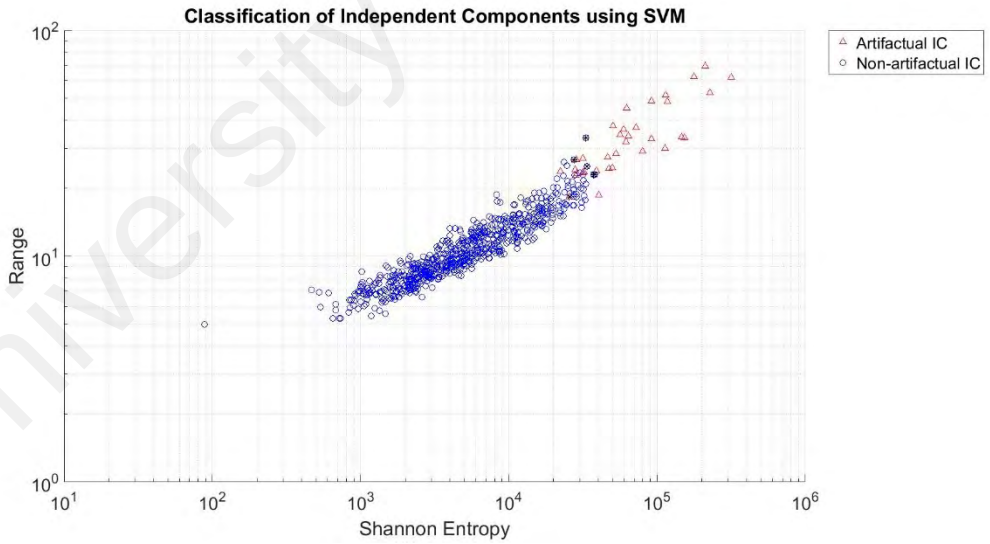


(b)

**Figure 4.8: Scatter plot present the classification of artifactual and non-artifactual ICs with pre-trained linear SVM with c = 10. * denotes the instances of misclassification as compared to labels by visual inspection.**

**Table 4.2: Confusion matrix for classification of ICs using DBSCAN with dataset from EEGLAB.**

| | Predicted: Non-Artifactual | Predicted: Artifactual |
|---|---|---|
| Actual: Non-Artifactual | (TN) 657 | (FP) 13 |
| Actual: Artifactual | (FN) 2 | (TP) 32 |

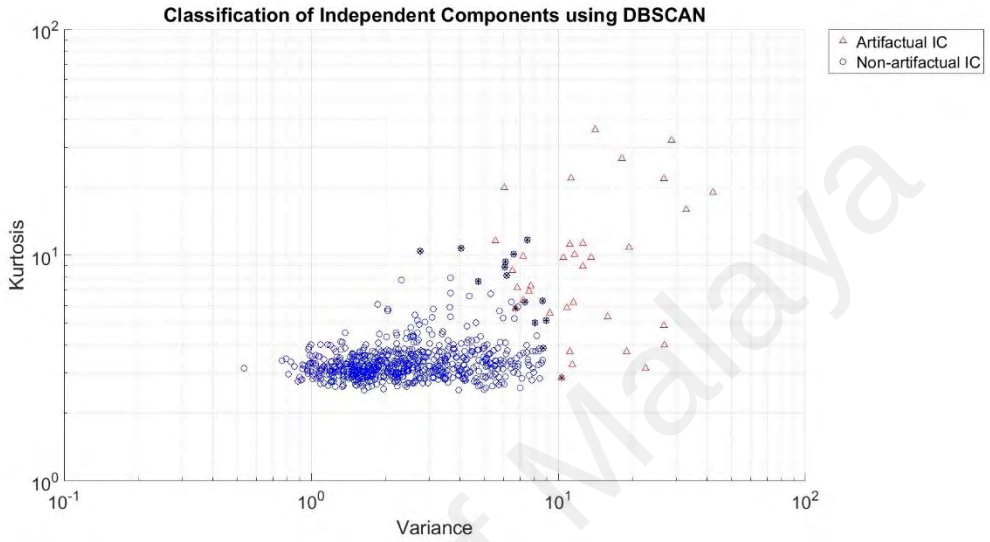


(a)

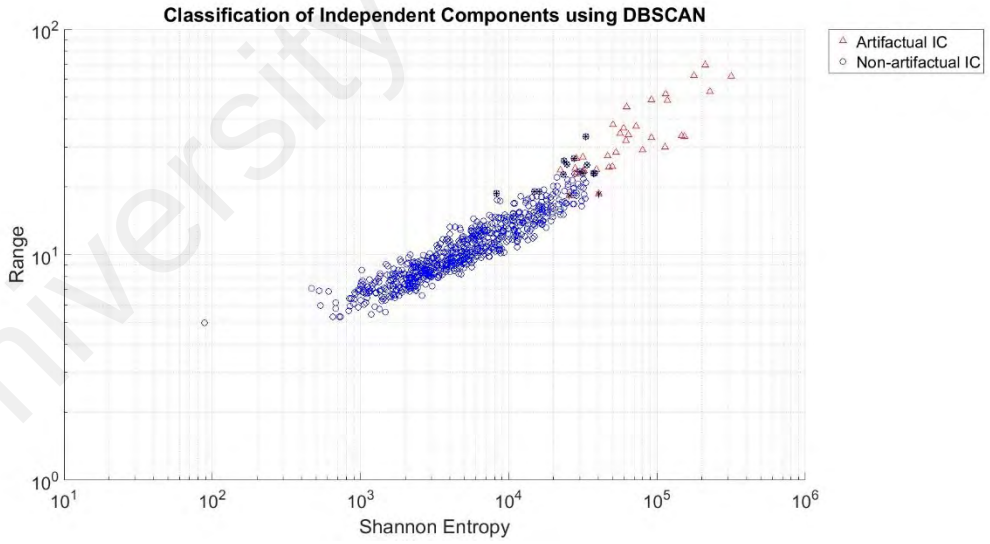


(b)

**Figure 4.9: Unsupervised clustering of artifactual and non-artifactual ICs with DBSCAN with $\varepsilon$ = 2.6 and *minPts* = 19. * denotes the instances of misclassification as compared to labels by visual inspection.**

**Table 4.3: Sensitivity, Specificity and Accuracy of different methods in the identification of artifactual ICs using dataset from EEGLAB as compared to the standard thresholding method.**

| | Artifacts Identification with pre-trained SVM (%) | Unsupervised Clustering with DBSCAN (%) | Artifacts Identification with Threshold (Mahajan & Morshed, 2015) (%) |
|---|---|---|---|
| Sensitivity | 97.1 | 94.1 | 90.0 |
| Specificity | 99.3 | 98.1 | 98.0 |
| Accuracy | 99.1 | 97.9 | 95.2 |

### 4.2.2 Performance Evaluation with Correlation Coefficient

Using the same dataset from EEGLAB, the correlation coefficient of the filtered clean EEG signals with the signals before artifacts removal is also computed. This is conducted to confirm that the artifacts removal process did not alter or introduce much distortion to the original EEG signal. The average value of the correlation coefficient achieved by the proposed method of Wavelet-ICA with SVM or DBSCAN is presented in Table 4.4, where the results for Wavelet-ICA with threshold and also zeroing-ICA (where the entire artifactual IC is deleted instead of using Wavelet Artifacts Removal) with an otherwise similar SVM are also compared.

Wavelet-ICA with SVM performed consistently better and yielded an overall average correlation coefficient of 0.955. On the other hand, the method with DBSCAN yielded an overall average correlation coefficient of 0.947. The alternate methods of Wavelet-ICA with threshold and zeroing-ICA with SVM both have an overall average correlation coefficient value of 0.946. The method of Wavelet-ICA with SVM performed better than Wavelet-ICA with DBSCAN or threshold due to the more accurate identification of artifactual components. False detection rate was lower, resulting in lesser unnecessary removal of wavelet components. Meanwhile, the method of Wavelet-ICA with SVM also performed better than zeroing-ICA with SVM, as a result of using wavelet artifact

removal instead of removing the entire IC with artifactual components, consequently resulting that the cerebral activities of interest are better retained. The only drawback with SVM is that it requires training with training data in advance, while the methods using DBSCAN or thresholding does not required training. The drawback of DBSCAN method is that it could not be applied in real time processing as the unsupervised machine learning algorithm required all the data points to be present in order to begin the clustering process. In conclusion, Wavelet-ICA with SVM have the best performance in pre-processing and filtering of EEG signals and will thus be applied as the preferred filtering method in further discussion.

**Table 4.4: Comparison of correlation coefficients for Wavelet-ICA with SVM (mean: 0.955 ± 0.03), with DBSCAN (mean: 0.947 ± 0.03), with threshold (mean: 0.946 ± 0.03) and zeroing-ICA with SVM (mean: 0.946 ± 0.04) using dataset from EEGLAB.**

| Electrode Channel | Wavelet-ICA with SVM | Wavelet-ICA with DBSCAN | Wavelet-ICA with threshold (Mahajan & Morshed, 2015) | Zeroing-ICA with SVM (Shoker et al., 2005) |
|---|---|---|---|---|
| 1 | 0.865 | 0.861 | 0.859 | 0.827 |
| 2 | 0.826 | 0.826 | 0.820 | 0.780 |
| 3 | 0.943 | 0.941 | 0.939 | 0.930 |
| 4 | 0.952 | 0.949 | 0.949 | 0.941 |
| 5 | 0.948 | 0.947 | 0.946 | 0.937 |
| 6 | 0.902 | 0.898 | 0.888 | 0.878 |
| 7 | 0.945 | 0.943 | 0.940 | 0.932 |
| 8 | 0.958 | 0.955 | 0.954 | 0.949 |
| 9 | 0.958 | 0.954 | 0.954 | 0.948 |
| 10 | 0.953 | 0.950 | 0.950 | 0.941 |
| 11 | 0.966 | 0.964 | 0.961 | 0.958 |
| 12 | 0.963 | 0.959 | 0.957 | 0.955 |
| 13 | 0.970 | 0.966 | 0.966 | 0.964 |
| 14 | 0.964 | 0.958 | 0.957 | 0.956 |
| 15 | 0.944 | 0.943 | 0.941 | 0.931 |
| 16 | 0.970 | 0.965 | 0.963 | 0.964 |
| 17 | 0.966 | 0.957 | 0.956 | 0.961 |
| 18 | 0.973 | 0.963 | 0.963 | 0.969 |
| 19 | 0.969 | 0.963 | 0.963 | 0.963 |
| 20 | 0.975 | 0.968 | 0.966 | 0.970 |
| 21 | 0.971 | 0.958 | 0.957 | 0.967 |
| 22 | 0.965 | 0.947 | 0.946 | 0.961 |
| 23 | 0.973 | 0.962 | 0.961 | 0.969 |
| 24 | 0.971 | 0.965 | 0.963 | 0.965 |
| 25 | 0.978 | 0.966 | 0.964 | 0.975 |
| 26 | 0.971 | 0.955 | 0.954 | 0.968 |
| 27 | 0.964 | 0.944 | 0.944 | 0.961 |
| 28 | 0.972 | 0.960 | 0.959 | 0.969 |
| 29 | 0.976 | 0.968 | 0.965 | 0.973 |
| 30 | 0.971 | 0.954 | 0.952 | 0.967 |
| 31 | 0.968 | 0.951 | 0.949 | 0.965 |
| 32 | 0.970 | 0.956 | 0.954 | 0.966 |
| Average ± Standard Deviation | 0.955 ± 0.03 | 0.947 ± 0.03 | 0.946 ± 0.03 | 0.946 ± 0.04 |

## 4.3 EEG Responses to Pain due to Uterine Contraction during Labour

On the experimental results with clinical pain condition, ten subjects each with 30 minutes of EEG recordings resulted in a total of 18000 one second epochs of recorded EEG signals were included for the analysis. After discarding data that had been corrupted due to technical complications such as faulty electrodes, 15030 epochs of data remained. After denoising and artifacts removal via the pre-processing and filtering steps as described in Section 3.2, unrecoverable data are discarded with aid of visual inspection and there remained 9907 epochs of EEG signals, consisting of 2661 epochs corresponding to "pain" and 7246 epochs corresponding to "resting" state. The state contributions differed amongst the 10 subjects, due to their differing contraction rates at the time of recording. The data were analysed using EEGLAB (Delorme & Makeig, 2004), and the classification of state of pain using SVM was conducted in the MATLAB environment (Chang, C. C. & Lin, 2011).

### 4.3.1 Reported NRS due to Uterine Contraction

During the 30 minutes of EEG and CTG recording, the subjects experienced from five to eleven cycles of uterine contraction. The subjects then reported the extent of pain experience using the NRS after each cycle of uterine contraction. Figure 4.10 shows the average reported NRS for each subject. It is evident that the mean intensity and relative standard deviation of pain rating caused by the uterine contractions differed between subjects. Some subjects rated a wider range of pain scores while some remained consistent throughout the whole recording session. Nonetheless, all NRS ratings of four or above given after a cycle of uterine contraction in contrast to 0 during "resting" state confirmed that the subject experienced significant pain during the cycles of uterine contraction.

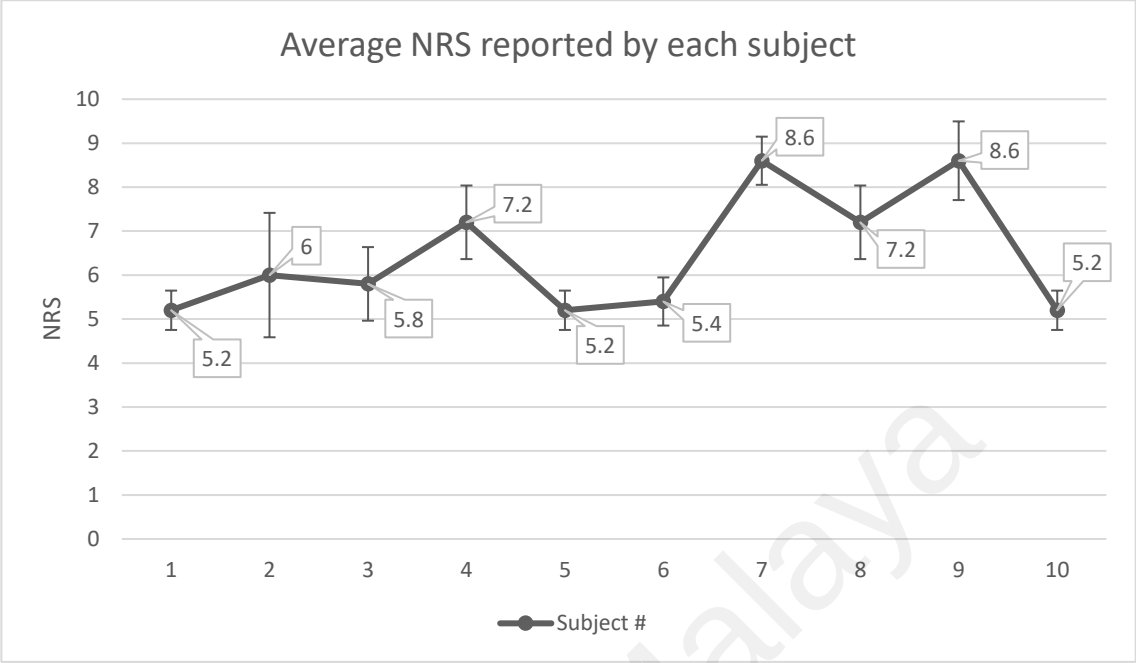


**Figure 4.10: Mean and standard deviation of NRS reported by each subject after the cycles of uterine contraction during the 30 minutes recording period.**

### 4.3.2 Analysis of Relative Power of Frequency Bands between "Resting" and "Pain" States

This section discusses the changes in relative power of frequency bands contributed by all ten subjects, contrasting the results for "resting" and "pain" states. The differences in global averaged EEG amplitudes are shown in Figure 4.11(a) whereas the differences observed in each individual EEG channel are depicted in Figure 4.11(b). The relative power was used in this study as it is more robust to inter-individual differences, and more reliable for detecting changes in frequency band activities than are contrasts of absolute power (Gram et al., 2015). The magnitudes of frequency bands power are normalized and averaged for each individual subject, and then averaged across the entire group, thus ensuring that each individual contributed with equal weighting to the depiction of the overall distributions (Kumar, A. & Anand, 2006). Paired sample t-test is conducted using

MATLAB function and Bonferroni correction is applied for multiple comparisons. The topographic distributions of frequency bands power in Figure 4.12 highlight the localized EEG changes in association with painful uterine contractions.

The differences of EEG spectral activities between “resting” and “pain” states as defined in this study are compared. Using the “resting” state as baseline and consider the transition from “resting” to “pain” state, globally increased delta and beta power, together with deceased theta and alpha power are observed. The increase in delta power are observed particularly at the frontal (possibly due to residual eye blink and wincing artifacts) and the parietal brain regions. Decreased relative theta power is observed at the bilateral central and parietal region, possibly related to the somatosensory association areas. In addition, the results shown globally decreased alpha power, notably prominent in the fronto-central and occipital regions covering the prefrontal and also the occipital cortexes, which may reflect the affective and cognitive modulations of pain. Finally, an unspecific globally increased beta power was observed over the entire brain regions upon the transition from “resting” to “pain” state, implicating the activation of the brain network involved in the processing of pain.

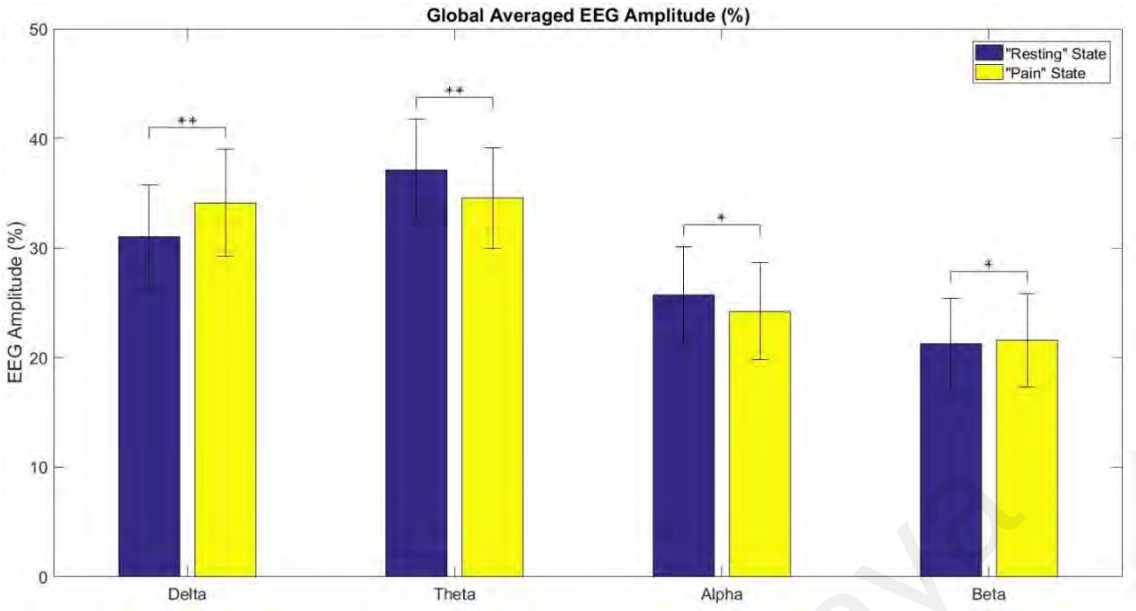


(a) Global averaged EEG amplitudes.

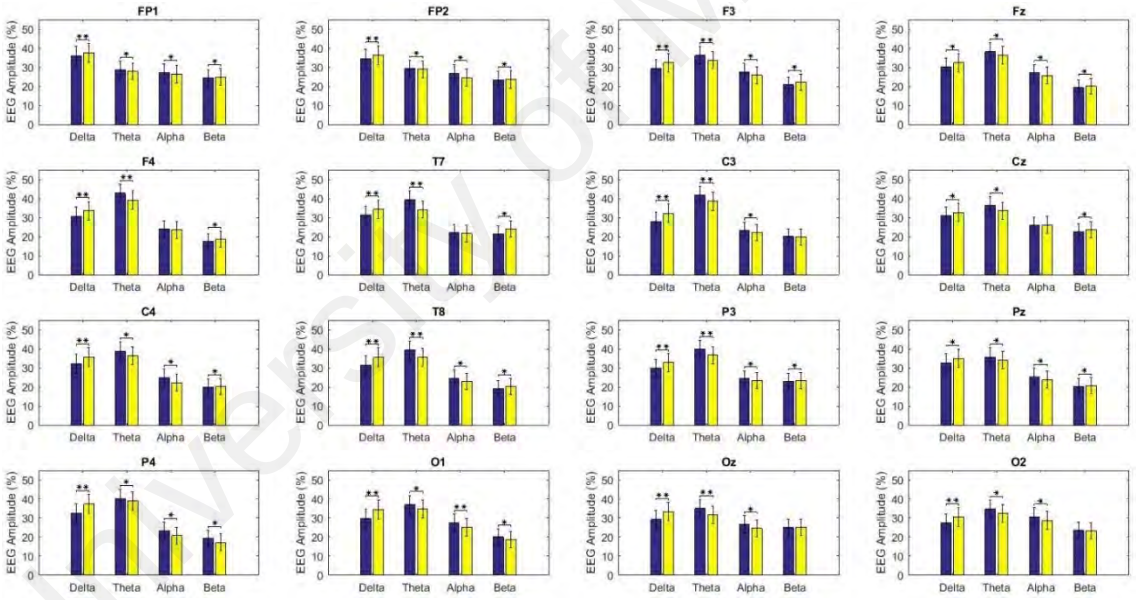


(b) Averaged EEG amplitudes for each channel.

**Figure 4.11: Distribution of relative spectral activities of EEG signals corresponding to "resting" and "pain" state defined in this study. Part (a) shows the averaged normalized global distributions and (b) shows the averaged normalized distributions corresponding to each channel. * and ** indicate statistical significance at $p < 0.05$ and $p < 0.01$ respectively (Bonferroni corrected for multiple comparisons).**

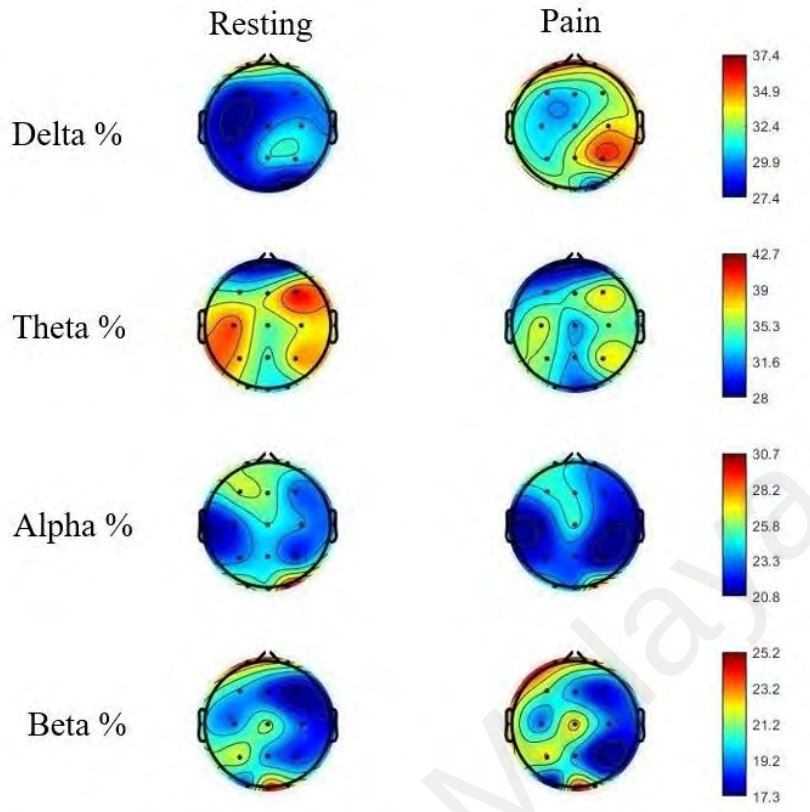


**Figure 4.12: Normalized topographic distribution of relative spectral activities corresponding to "resting" and "pain" state defined in this study.**

### 4.3.3 Ranking of Features Separating the "Resting" and "Pain" States

Table 4.5 shows the top 30 features ranked in descending order of class separability criteria. It is observed that the statistical properties with high correlation to the amplitude and volatility of the EEG signals such as variance, standard deviation and kurtosis in occipital, frontal and parietal regions showed significant changes and present as good indicator to separate the "resting" and "pain" states. Meanwhile, the frequency bands activities are also present as effective indicators to separate the two labelled groups in this study. On the other hand, features with low correlation to the amplitude and volatility of the EEG signals such as the mean, median and skewness are not present and may not be the most effective features to separate the labelled groups.

**Table 4.5: Ranking of features in descending order of class separability criteria. * and ** indicate statistical significance at p < 0.05 and p < 0.01 respectively, while n.s. indicates not significant (Bonferroni corrected for multiple comparisons).**

| Ranking | Feature | Channel | Significance |
|---|---|---|---|
| 1 | Variance | Oz | ** |
| 2 | Beta % | Pz | * |
| 3 | Theta % | P3 | ** |
| 4 | Standard Deviation | O1 | ** |
| 5 | Hjorth's Complexity | FP2 | ** |
| 6 | Number of Peak | Cz | ** |
| 7 | Kurtosis | Fz | * |
| 8 | Number of Peak | F3 | * |
| 9 | Shannon Entropy | F3 | ** |
| 10 | Energy Entropy | F3 | ** |
| 11 | Peak Frequency | O2 | * |
| 12 | Alpha Power | FP2 | * |
| 13 | Theta % | FP2 | * |
| 14 | Beta % | O2 | n.s. |
| 15 | Range | F3 | ** |
| 16 | Delta Power | F3 | ** |
| 17 | Theta Power | F3 | ** |
| 18 | Amplitude of Peak Frequency | FP2 | ** |
| 19 | Alpha % | T8 | * |
| 20 | Kurtosis | FP1 | ** |
| 21 | Variance | P3 | * |
| 22 | Energy Entropy | P4 | ** |
| 23 | Alpha Power | Cz | n.s. |

**Table 4.5, continued.**

| Ranking | Feature | Channel | Significance |
|---|---|---|---|
| 24 | Beta Power | Pz | * |
| 25 | Kurtosis | O2 | * |
| 26 | Amplitude of Peak Frequency | Pz | * |
| 27 | Beta Power | O1 | * |
| 28 | Delta % | Cz | * |
| 29 | Vrms | F3 | ** |
| 30 | Alpha % | FP1 | * |

### 4.3.4 Classification of State of Pain using SVM

As a practical application, this study aims to construct a generalized model for classification of state of pain across subjects by using a supervised machine learning algorithm. The classification model is constructed to predict the "resting" or "pain" internal state experienced by the subjects using the EEG signals as an objective marker. The generalized model was trained and tested using the normalized data across subjects to achieve a single composite model that is able to distinguish between "resting" and "pain" states for all subjects. The generalized model was trained and tested using SVM with an RBF kernel function.

The SVM was trained and tested using the 31 features listed in Table 3.1 for each of the 16-channels electrodes, resulting in a total of 496 features. The model was first trained and tested using the training data within a range of parameters extending for gamma, g (0.01 to 1 with increments of 0.01 per step) and for the soft margin constant, c (1 to 100 with increments of 1 per step). Then, the test data were used for evaluation of the trained classification model. The results of classification are shown in the confusion matrix of

Table 4.6. The classification model achieved sensitivity of 85.4% and specificity of 80.7% with an overall accuracy of 83.0%, when the optimized parameters g = 0.28 and c = 4 are applied, as determined by five-fold cross-validation. A three-dimensional plot to describe the variation of classification accuracy to the choice of parameters is depicted in Figure 4.13. Results of this generalized model lend support to the development of generalizable pain assessment during labour by using the EEG signals.

**Table 4.6: Confusion matrix of classification result achieved by the generalized model.**

| | Predicted Class: Pain | Predicted Class: Resting | Classification Accuracy (%) |
|---|---|---|---|
| Actual Class: Pain | 439 | 75 | Sensitivity: 85.4 |
| Actual Class: Resting | 106 | 444 | Specificity: 80.7 |
| Overall Accuracy | | | Overall: 83.0 |

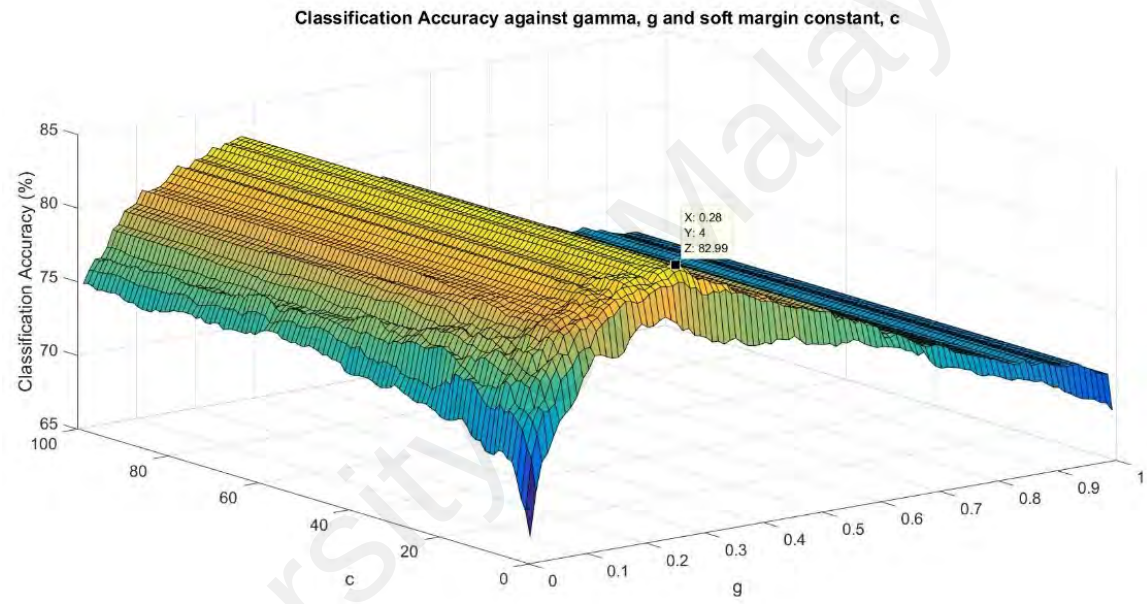


**Figure 4.13: Classification accuracy of SVM achieved by using different parameters of gamma, g and soft margin constant, c. The maximum classification achieved is highlighted in the figure together with the optimized parameters (X, Y, Z).**

### 4.3.5 Dimension Reduction using PCA

In this section, we attempt to reduce the number of features using principal component analysis (PCA) to reduce the risk of overfitting when high number of features are present in relation to the amount of data. After applying dimension reduction using PCA, the resulting principal components are ranked in descending order of class separability criteria based on their component variance. Figure 4.14 shows the classification accuracy as a function of the number of features with and without PCA under similar classification criteria. A classification accuracy above 80% can be obtained using only the top 30 features when PCA is applied. Maximum classification accuracy is achieved at 84% using 68 features in total. PCA provided features with better separability criteria compared to the set of raw features, which are less able to describe the relevant changes in the EEG characteristics in relation to the transition from "resting" to "pain" state. The drawback of using PCA is that the resulted PCs are presented as a combination of multiple features and could not be easily retrieved. Table 4.7 and Figure 4.15 describe the confusion matrix and the classification accuracy, which is maximal ($g = 0.4$, $c = 5$, Acc = 84.0%) when using 68 features. The classification model after feature reduction is less likely to overfit as it eliminated a large number of redundant features not contributing positively to the classification model. Better classification results can also be seen in comparing Figure 4.15 with Figure 4.13 when different parameters are applied, indicating that the risk of overfitting is indeed reduced. The classification result supports the possibility of using EEG signals for objective identification of pain experience due to uterine contraction during the first stage of labour.

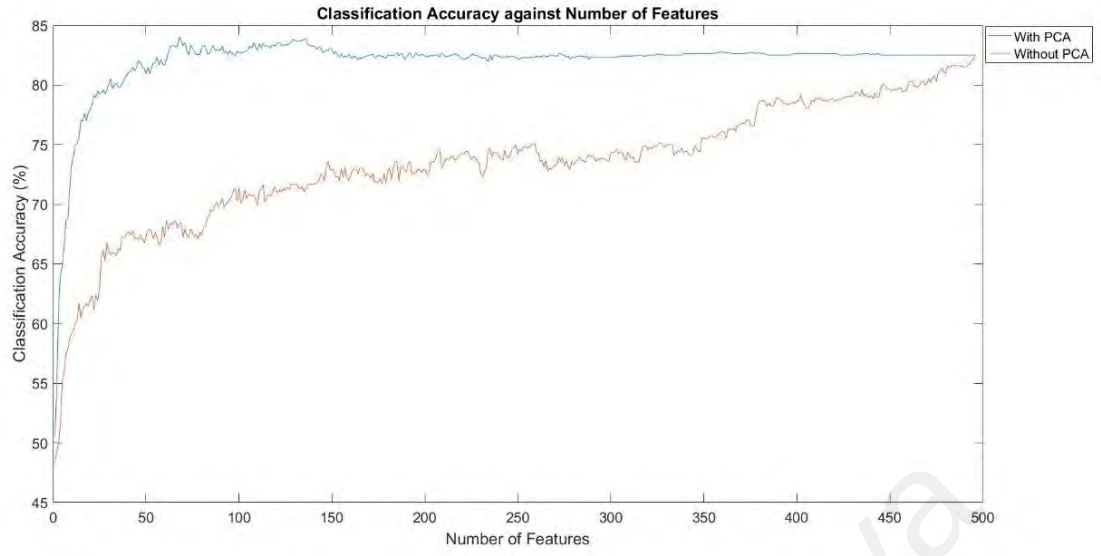


**Figure 4.14: Classification accuracy against number of features ranked in descending order of class separability criteria, with and without PCA.**

**Table 4.7: Confusion matrix of classification result achieved by the generalized model with number of features reduced to 68 using PCA.**

| | Predicted Class: Pain | Predicted Class: Resting | Classification Accuracy (%) |
|---|---|---|---|
| Actual Class: Pain | 448 | 66 | Sensitivity: 87.2 |
| Actual Class: Resting | 104 | 446 | Specificity: 81.1 |
| Overall Accuracy | | | Overall: 84.0 |

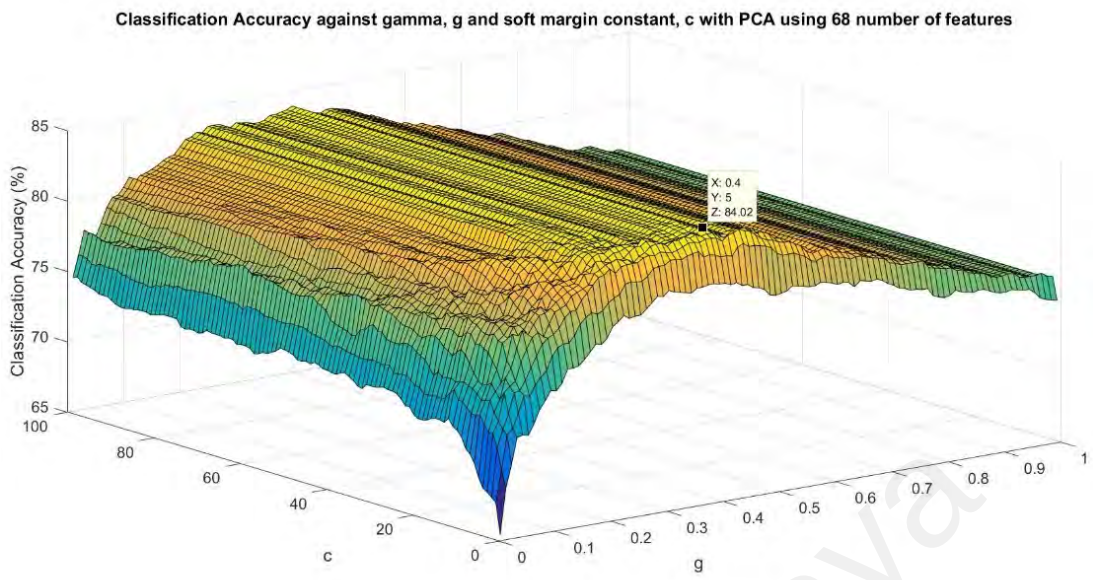


**Figure 4.15: Classification accuracy of SVM achieved by using different parameters of gamma, g and soft margin constant, c with number of features reduced to 68 using PCA. The maximum classification achieved is highlighted in the figure together with the optimized parameters (X, Y, Z).**

# CHAPTER 5: DISCUSSION

Section 5.1 presents the discussion for the methods of EEG signal pre-processing and artifacts removal presented in this study. Different methods of artifacts removal are compared and their advantages or disadvantages discussed in relation to the pre-processing method with the best performance, in this case the Wavelet-ICA with SVM. Further modification on the method of Wavelet-ICA with SVM to include all kinds of artifactual components are also presented. Following after, the application of EEG signals for clinical monitoring in the classification of state of pain due to uterine contractions during the first stage of labour are discussed in Section 5.2. The neurophysiological responses observed in EEG signals due to pain and implications of this study are further discussed.

## 5.1 EEG Pre-Processing and Artifacts Removal with Wavelet-ICA and SVM

The advantage of the proposed system for multichannel EEG artifacts removal is that the pre-trained SVM are fitted to estimate an optimum hyperplane separating the artifactual ICs from those indicative of cerebral activity. Notice that it is also possible to automatically identify artifactual IC by arbitrarily setting a thresholding value anywhere between the amplitude of the artifactual ICs and other ICs. However, this variant approach is often rigid and unsuitable to be applied for sporadic and non-stationary signal such as the case of EEG. The arbitrarily defined threshold may fail to detect the artifactual component or inadvertently introduced false detection near the boundary of the thresholding value. On the other hand, method of unsupervised machine learning using DBSCAN requires all data points to be ready in order to begin the clustering. This approach may present a hindrance to the possibility of real time processing of the EEG signals. In contrast, the SVM-based approach to separate artifactual ICs is shown to be

more reliable than DBSCAN or the existing methods using thresholding, as in (Mahajan & Morshed, 2015; Mammone et al., 2012; Nolan et al., 2010). Linear SVM is used in this study based on its ability to identify artifactual components that possess features with outlier values extending far across the hyperplane. Additionally, linear SVM also required less computational load than reiterative thresholding methods (Nolan et al., 2010). The only disadvantage of Wavelet-ICA with SVM is that it requires training and the availability of training data in advance. Parameters of the SVM can be further optimized, but this at the risk of overfitting.

The steps of training the SVM in the Wavelet-ICA approach is summarized as follow. First, the features that best describe the target artifactual components that may present in the desired application are selected. Then, the ICs containing the target artifactual components are assigned as training data to the SVM. After a series of testing the trained SVM model with the test data, the features of validated artifactual ICs are sent to update the training dataset for future classification. The proposed system has the potential to be extended to accommodate and exclude diverse kinds of artifacts present in future EEG recording. This generalizability can be achieved by selecting statistical features that best represent the target artifactual component, and retraining the SVM using an updated collection of training data.

The selection of features and training data of SVM is thus crucial for the accuracy and effectiveness of the overall system. The training data are first selected by identifying the artifactual components using both visual inspection and assessment of its most salient descriptive features. For the purpose of this study, only the low frequency eye blink artifacts is by far considered, as this is the most common and troublesome artifactual component encountered in EEG signals. The most salient features of eye blink artifacts included the variance, kurtosis, Shannon's entropy and range of amplitude. These features

were identified and selected based on their magnitudes being significantly higher in conjunction with an eye blink than in its absence. In general, the features selected for training and testing of SVM must be adequate to describe the artifactual component, which condition is met by the present findings.

This study also presented a possible combination of integrating SVM into Wavelet-ICA for removal of multiple artifacts present in the EEG signal, not just for eye blinks. In other words, integration of SVM suggests a potential possibility to accommodate all kinds of artifacts that exist in the EEG signals such as the ECG and EMG artifacts. This adaptability can be achieved by selecting the appropriate features and training data used in the training of the SVM. Nonetheless, the list of potential artifactual components and their corresponding descriptive features is beyond the scope of current study, which aim only to enable the use of EEG in clinical monitoring and BCI application. It is anticipated that future research should serve to identify the most descriptive features of other artifactual components such as cardiac and muscles artifacts, and remove without substantial loss of specific cerebral signals.

## 5.2 EEG Reponses to Pain due to Uterine Contraction

This is the first research study that targets the complex problem of objective identification of pain experience during the first stage of labour by using the EEG approach. It was shown that the pain experience caused by uterine contraction during the first stage of labour was associated with notable changes in the relative spectral activities of EEG signals. In general, globally increased relative delta and beta activities and decreased relative theta and alpha activities are observed following pain caused by uterine contractions. The results are consistent with generally reported observations in

experimental pain study (Chang, P. F. et al., 2004; Gram et al., 2015; Huber et al., 2006; Peng et al., 2014; Sai et al., 2019; Shao et al., 2012).

It is suggested that the decrease of relative alpha band activity observed in this study is unlikely to be pain-specific, as opposed to speculations in some other EEG pain studies (Gram et al., 2015; Nir et al., 2012; Peng et al., 2014). In general, the alpha band is primarily effected by changes in attention and alertness (Klimesch et al., 1998; Peng et al., 2015), and is known to be negatively correlated with the focus of attention during task performance (Ray & Cole, 1985). As such, the suppression of alpha band activity commonly reported in the literature is likely a marker for attentional shift in response to pain, rather than pain *per se* (Giehl et al., 2013; Gram et al., 2015; Peng et al., 2014). It is argued that the observed alpha ERD in these earlier studies was more likely a reflection of specific attentional and memory processes that were task-related (Peng et al., 2015). Experimental evocation of pain by application of either dermal heating or the cold pressor test arouses the subject's attention, thus inducing suppression of alpha oscillatory activity in the sensorimotor cortex, regardless of the particulars of attentional modulation applied in the particular study (Peng et al., 2014). However, the present study did not manipulate directly the subject's attention. As the pain due to uterine contraction is tonic and natural, alpha band activities are less likely to be modulated. As the result, the observed suppression of alpha oscillations over frontal regions likely reflects the activation of ACC as a consequence of underlying attentional or affective-emotional processing due to the pain experience (Peng et al., 2015). On the other hand, the decrease of alpha activities at the occipital region observed in this study is likely a reflection of cognitive engagement occurring when the pain experience due to uterine contraction is present.

The pain-evoked increase of delta activity observed in frontal cortical regions is likely attributable to artifacts from residual eye blinks or other ocular activities that often

accompany the pain experience (Dowman, R. et al., 2008a). However, in the present study increased delta activity was also observed on the right parietal region of the scalp, which is not so readily attributed to ocular activities. In general, low frequency activation is principally related to motivational regulation, which can be linked to negative effect and the activation of an avoidance-withdrawal system (Chang, P. F. et al., 2002b). Therefore, the present finding of reduced delta activity may reflect in part the functional synchronization of brain activity in the parietal lobe upon pain experience, in relation to atavistic defensive or withdrawal mechanisms (Hadjileontiadis, 2015).

On the other hand, the results shown during uterine contractions decreased theta activity in bilateral central and parietal regions comprising the somatosensory cortices, as also reported previously in an experimental pain study (Dowman, R. et al., 2008a). The decrease of low frequency oscillatory activities in this region could be related to activation of primary and secondary somatosensory cortices (SI and SII), in relation to the sensory modulation of painful experience. However, due to inherent limitations of the scalp EEG technique, which include low spatial resolution cortical mapping, the study could not unambiguously attribute the pain-related decrease in theta oscillatory activities to a particular source in the somatosensory association areas.

The observed widespread (frontal, central and posterior) increase in beta activity is a strong indicator of hyperarousal in response to painful experience. A shift from lower frequency to higher frequency activity indicated the activation and synchronization between cortical areas of the well-described brain network responding to pain, comprising SI, SII, ACC, insula, prefrontal cortex and thalamus (Apkarian et al., 2005; Bromm & Lorenz, 1998; Peng et al., 2014; Shao et al., 2012). SI and SII activities induced by pain have been associated with the sensory-discriminative component of pain, while ACC activation reflects the affective-emotional component due to pain (Bromm & Lorenz,

1998; Peng et al., 2015). The finding of broadly distributed enhancement of beta activities suggests that pain experience modulates the cortical excitability not only of the pain and sensorimotor system, but involves a more widespread cortical system. This finding also supports the network model of pain perception, implicating involvement of multiple brain regions rather than processing within a "singular centre" (Apkarian et al., 2005; Chang, P. F. et al., 2002b; Pinheiro et al., 2016). This network is confirmed in a cross-modal imaging study using PET (Kupers et al., 2011). However, the observed widespread increase in beta activity in the present study may also be contaminated by EMG sources due to cranial muscles contraction or clenching of teeth that certainly accompany the pain of uterine contractions. Anticipating this possibility, a comprehensive filtering method is applied to isolate and remove high frequency noise and artifactual components including the EMG signals. Therefore, the EMG signals have had little disruption to the observed increase of beta band activity, which may properly be attributed to the presence of pain experience evoked by uterine contractions.

Other than the conventional spectral activities, certain statistical and non-linear EEG features corresponding to pain experience that have not hitherto been well-studied are also considered. Generally, the analyses showed that the EEG signals had increased amplitude and volatility during painful uterine contraction events. Thus, a number of significant changes are observed in the statistical properties related to the EEG amplitude. In particular, statistical features such as variance, range of amplitude, Vrms and non-linear features such as Hjorth activities and Energy Entropy all of which positively correlated with the amplitude of the EEG signals showed statistically significant changes at certain electrode locations during the pain experience. Nonetheless, this study could not identify any single statistical or non-linear features that can be used to accurately describe the occurrence of pain experience. On the other hand, statistical features

unaffected by the amplitude or volatility such as mean, median and skewness showed no such significant changes with pain.

Although no single analysed feature is sufficient to describe the overall occurrence of pain, the combined features may serve for a classification model with supervised machine learning algorithm (Sankar et al., 2013). Therefore, in addition to the analysis of changes in EEG activities, this study also attempted to classify the "resting" or "pain" state of the subjects using the SVM. The SVM classifier is chosen in this study for its outstanding ability in classifying two classes and the ease of training the SVM classifier using limited training data. The classification algorithms using SVM with an RBF kernel function achieved satisfactory results, classifying the presence of pain experience associated with uterine contraction at 83% accuracy, as benchmarked by an accuracy of 75% achieved in an earlier study with an experimental pain condition (Vatankhah et al., 2013). Moreover, by reducing the number of features using PCA and considering only the 68 top ranked features with highest class separability criteria, a maximum classification accuracy of 84% is achieved. Applying PCA reduced the risk of overfitting without sacrificing the overall performance of the SVM. However, the PCs are made up by mixture of orthogonal transformation of the original features and therefore it is difficult to ascertain the individual contribution of the original features to the classification results.

It is also interesting to note that by considering each subject individually yields a better overall classification result as compared to a generalized model. This finding most likely reflects the inter-individual differences between participants, which might include scalp thickness and the scalp impedances of the electrodes during the recording. Also, it is reasonable to suppose that individual differences exist in the pain-specific brain network, manifesting in distinct activation patterns during pain processing. As this study involved only participants during labour, there are necessarily certain limitations in the

generalizability of present findings to other pain conditions, and across gender. Nonetheless, the generalized classification model at least serves as a benchmark to assess the presence of pain experience during uterine contraction by using the EEG signals. The classification of state of pain are able to complement physician's decision to administrate epidural anaesthesia during labour, additional to the interpretation of the subjective perception of pain experience by the patient.

# CHAPTER 6: CONCLUSION AND RECOMMENDATION

This chapter presents the conclusion of the study and recommendation for relevant future works to further enhance the versatility of the application.

## 6.1 Conclusion

This study explored a new hybrid procedure for automatic identification and removal of EEG artifacts by applying machine learning algorithms using pre-trained linear SVM and DBSCAN to identify the artifactual components in Wavelet-ICA. The method of Wavelet-ICA with SVM substantially improves identification of artifactual components and is found more reliable as compared to DBSCAN or standard thresholding method. Moreover, it promises to be generalizable for diverse kinds of artifacts, upon selecting proper features and training data. The system is able to function automatically and isolate a distinctly cleaned EEG signal directly from a raw EEG recording, thus potentially lending itself for applications such as clinical diagnosis or BCI. It was found that the system delivers satisfactory artifact removal without much degrading to the time and frequency resolution of the EEG signals.

As an application for clinical monitoring, this study explored the changes in EEG activities during the present of pain experience associated with uterine contraction during the first stage of labour, as monitored by CTG tracing. In particular, globally increased delta and beta activities together with decreased theta and alpha activities are observed subject to the presence of pain with acute uterine contractions. However, it is generally held that changes in alpha activities may not directly reflect the pain experience, but rather the affective modulation altered by the pain. In an effort to classify the presence of pain using supervised machine learning algorithm, a classification accuracy of 83% is achieved by using SVM classifier with an RBF kernel function. Furthermore, the

classification model using a reduced pool of features via PCA achieved a higher accuracy of 84%, using only 68 PCs made out of a total of 496 features. Our findings lend support to the utility of EEG signals as a clinical tool to achieve an objective method of pain assessment during the first stage of labour, which could inform a decision to administer epidural anaesthesia. This approach may prove generalizable to a number of conditions in which the patients are unable to convey their internal state.

## 6.2 Recommendation for Future Works

Further work should serve to identify features best describe other artifactual components to tackle the problem of noise and artifacts in EEG signals. Additionally, more work should also serve to develop a monitoring system to objectively classify the presence of pain, not only during labour, but generalized for a range of acute or chronic pain conditions. Ultimately, it may be possible to develop an objective method that is able to qualitatively and quantitatively assess the level of pain experience by tracking the changes in human brain in foreseeable future.

## REFERENCES


Abdi, H., & Williams, L. J. (2010). Principal component analysis. *Wiley Interdisciplinary Reviews: Computational Statistics, 2*(4), 433-459. doi:10.1002/wics.101

Abushaikha, L., & Oweis, A. (2005). Labour pain experience and intensity: a Jordanian perspective. *International Journal of nursing practice, 11*(1), 33-38.

Agrawal, R., Gehrke, J., Gunopulos, D., & Raghavan, P. (1998). *Automatic subspace clustering of high dimensional data for data mining applications* (Vol. 27): ACM.

Alfirevic, Z., Devane, D., & Gyte, G. M. (2006). Continuous cardiotocography (CTG) as a form of electronic fetal monitoring (EFM) for fetal assessment during labour. *Cochrane Database Syst Rev*(3), Cd006066. doi:10.1002/14651858.cd006066

André-Obadia, N., Lamblin, M. D., & Sauleau, P. (2015). French recommendations on electroencephalography. *Neurophysiologie Clinique/Clinical Neurophysiology, 45*(1), 1-17. doi:http://dx.doi.org/10.1016/j.neucli.2014.11.002

Ang, K. K., Chua, K. S. G., Phua, K. S., Wang, C., Chin, Z. Y., Kuah, C. W. K., . . . Guan, C. (2015). A randomized controlled trial of EEG-based motor imagery brain-computer interface robotic rehabilitation for stroke. *Clinical EEG and Neuroscience, 46*(4), 310-320.

Apkarian, A. V., Bushnell, M. C., Treede, R.-D., & Zubieta, J.-K. (2005). Human brain mechanisms of pain perception and regulation in health and disease. *European Journal of Pain, 9*(4), 463-484. doi:10.1016/j.ejpain.2004.11.001

Arns, M., Conners, C. K., & Kraemer, H. C. (2013). A decade of EEG theta/beta ratio research in ADHD: a meta-analysis. *Journal of attention disorders, 17*(5), 374-383.

Bijur, P. E., Latimer, C. T., & Gallagher, E. J. (2003). Validation of a verbally administered numerical rating scale of acute pain for use in the emergency department. *Acad Emerg Med, 10*(4), 390-392.

Brokjær, A., Olesen, A. E., Kreilgaard, M., Graversen, C., Gram, M., Christrup, L. L., . . . Drewes, A. M. (2015). Objective markers of the analgesic response to morphine in experimental pain research. *Journal of Pharmacological and Toxicological Methods, 73*, 7-14. doi:http://dx.doi.org/10.1016/j.vascn.2015.01.005

Bromm, B., & Lorenz, J. (1998). Neurophysiological evaluation of pain. *Electroencephalography and Clinical Neurophysiology, 107*(4), 227-253. doi:http://dx.doi.org/10.1016/S0013-4694(98)00075-3

Castellanos, N. P., & Makarov, V. A. (2006). Recovering EEG brain signals: Artifact suppression with wavelet enhanced independent component analysis. *Journal of Neuroscience Methods, 158*(2), 300-312. doi:http://dx.doi.org/10.1016/j.jneumeth.2006.05.033

Chang, C. C., & Lin, C. J. (2011). LIBSVM: A Library for Support Vector Machines. *Acm Transactions on Intelligent Systems and Technology, 2*(3), 27. doi:10.1145/1961189.1961199

Chang, P. F., Arendt-Nielsen, L., & Chen, A. (2002a). Differential cerebral responses to aversive auditory arousal versus muscle pain: specific EEG patterns are associated with human pain processing. *Experimental Brain Research, 147*(3), 387-393. doi:10.1007/s00221-002-1272-9

Chang, P. F., Arendt-Nielsen, L., & Chen, A. C. N. (2002b). Dynamic changes and spatial correlation of EEG activities during cold pressor test in man. *Brain Research Bulletin, 57*(5), 667-675. doi:http://dx.doi.org/10.1016/S0361-9230(01)00763-8

Chang, P. F., Arendt-Nielsen, L., Graven-Nielsen, T., & Chen, A. C. N. (2003). Psychophysical and EEG responses to repeated experimental muscle pain in humans: Pain intensity encodes EEG activity. *Brain Research Bulletin, 59*(6), 533-543. doi:http://dx.doi.org/10.1016/S0361-9230(02)00950-4

Chang, P. F., Arendt-Nielsen, L., Graven-Nielsen, T., Svensson, P., & Chen, A. C. N. (2004). Comparative EEG activation to skin pain and muscle pain induced by capsaicin injection. *International Journal of Psychophysiology, 51*(2), 117-126. doi:http://dx.doi.org/10.1016/j.ijpsycho.2003.01.001

Chavez, M., Grosselin, F., Bussalb, A., Fallani, F. D. V., & Navarro-Sune, X. (2018). Surrogate-based artifact removal from single-channel EEG. *IEEE Transactions on Neural Systems and Rehabilitation Engineering, 26*(3), 540-550.

Chen, W.-T., Yuan, R.-Y., Shih, Y.-H., Yeh, T.-C., Hung, D. L., Wu, Z.-A., . . . Lin, Y.-Y. (2006). Neuromagnetic SII responses do not fully reflect pain scale. *NeuroImage, 31*(2), 670-676. doi:http://dx.doi.org/10.1016/j.neuroimage.2005.12.015

Chunqi, C., Zhi, D., Sze Fong, Y., & Chan, F. H. Y. (2000). A matrix-pencil approach to blind separation of colored nonstationary signals. *IEEE Transactions on Signal Processing, 48*(3), 900-907. doi:10.1109/78.824690

Dash, M., & Liu, H. (1997). Feature selection for classification. *Intelligent Data Analysis, 1*(1), 131-156. doi:https://doi.org/10.1016/S1088-467X(97)00008-5

de Beer, N. A., van de Velde, M., & Cluitmans, P. J. (1995). Clinical evaluation of a method for automatic detection and removal of artifacts in auditory evoked potential monitoring. *J Clin Monit, 11*(6), 381-391.

de Vries, M., Wilder-Smith, O. H. G., Jongsma, M. L. A., van den Broeke, E. N., Arns, M., van Goor, H., & van Rijn, C. M. (2013). Altered resting state EEG in chronic pancreatitis patients: toward a marker for chronic pain. *Journal of Pain Research, 6*, 815-824. doi:10.2147/JPR.S50919

Delorme, A., & Makeig, S. (2004). EEGLAB: an open source toolbox for analysis of single-trial EEG dynamics including independent component analysis. *Journal of Neuroscience Methods, 134*(1), 9-21. doi:http://dx.doi.org/10.1016/j.jneumeth.2003.10.009

Donoho, D. L., & Johnstone, J. M. (1994). Ideal spatial adaptation by wavelet shrinkage. *Biometrika, 81*(3), 425-455. doi:10.1093/biomet/81.3.425

Dowman, R., Rissacher, D., & Schuckers, S. (2008a). EEG indices of tonic pain-related activity in the somatosensory cortices. *Clin Neurophysiol, 119*(5), 1201-1212. doi:10.1016/j.clinph.2008.01.019

Dowman, R., Rissacher, D., & Schuckers, S. (2008b). EEG indices of tonic pain-related activity in the somatosensory cortices. *Clinical Neurophysiology, 119*(5), 1201-1212. doi:10.1016/j.clinph.2008.01.019

Egsgaard, L., Wang, L., & Arendt-Nielsen, L. (2009). Volunteers with high versus low alpha EEG have different pain–EEG relationship: a human experimental study. *Experimental Brain Research, 193*(3), 361-369. doi:10.1007/s00221-008-1632-1

Egsgaard, L. L. (2009). *Cerebral processing and cortical plasticity during tonic and phasic painful stimulation.* Aalbord University.

Ester, M., Kriegel, H.-P., Sander, J., & Xu, X. (1996). *A density-based algorithm for discovering clusters in large spatial databases with noise.* Paper presented at the Kdd.

Gabsteiger, F., Leutheuser, H., Reis, P., Lochmann, M., & Eskofier, B. M. (2014). SVM for Semi-automatic Selection of ICA Components of Electromyogenic Artifacts in EEG Data. In J. Goh (Ed.), *The 15th International Conference on Biomedical Engineering: ICBME 2013, 4th to 7th December 2013, Singapore*. Cham: Springer International Publishing.

Giehl, J., Meyer-Brandis, G., Kunz, M., & Lautenbacher, S. (2013). Responses to tonic heat pain in the ongoing EEG under conditions of controlled attention. *Somatosensory & Motor Research, 31*(1), 40-48. doi:10.3109/08990220.2013.837045

Gotman, J., Skuce, D. R., Thompson, C. J., Gloor, P., Ives, J. R., & Ray, W. F. (1973). Clinical applications of spectral analysis and extraction of features from electroencephalograms with slow waves in adult patients. *Electroencephalography and Clinical Neurophysiology, 35*(3), 225-235. doi:http://dx.doi.org/10.1016/0013-4694(73)90233-2

Gram, M., Graversen, C., Nielsen, A. K., Arendt-Nielsen, T., Morch, C. D., Andresen, T., & Drewes, A. M. (2013). A novel approach to pharmaco-EEG for investigating analgesics: assessment of spectral indices in single-sweep evoked brain potentials. *Br J Clin Pharmacol, 76*(6), 951-963. doi:10.1111/bcp.12120

Gram, M., Graversen, C., Olesen, S. S., & Drewes, A. M. (2015). Dynamic spectral indices of the electroencephalogram provide new insights into tonic pain. *Clinical Neurophysiology, 126*(4), 763-771. doi:http://dx.doi.org/10.1016/j.clinph.2014.07.027

Graversen, C., Malver, L. P., Kurita, G. P., Staahl, C., Christrup, L. L., Sjøgren, P., & Drewes, A. M. (2015). Altered Frequency Distribution in the Electroencephalogram is Correlated to the Analgesic Effect of Remifentanil. *Basic & Clinical Pharmacology & Toxicology, 116*(5), 414-422. doi:10.1111/bcpt.12330

Gu, Y., Farina, D., Murguialday, A. R., Dremstrup, K., Montoya, P., & Birbaumer, N. (2009). Offline identification of imagined speed of wrist movements in paralyzed ALS patients from single-trial EEG. *Frontiers in neuroscience, 3*, 3.

Guarnieri, R., Marino, M., Barban, F., Ganzetti, M., & Mantini, D. (2018). Online EEG artifact removal for BCI applications by adaptive spatial filtering. *Journal of Neural Engineering, 15*(5), 056009.

Haas, L. F. (2003). Hans Berger (1873-1941), Richard Caton (1842-1926), and electroencephalography. *Journal of neurology, neurosurgery, and psychiatry, 74*(1), 9-9. doi:10.1136/jnnp.74.1.9

Hadjileontiadis, L. J. (2015). EEG-Based Tonic Cold Pain Characterization Using Wavelet Higher Order Spectral Features. *Biomedical Engineering, IEEE Transactions on, 62*(8), 1981-1991. doi:10.1109/TBME.2015.2409133

Haefeli, J., Freund, P., Kramer, J. L. K., Blum, J., Luechinger, R., & Curt, A. (2014). Differences in cortical coding of heat evoked pain beyond the perceived intensity: An fMRI and EEG study. *Human Brain Mapping, 35*(4), 1379-1389. doi:10.1002/hbm.22260

Hagemann, D., & Naumann, E. (2001). The effects of ocular artifacts on (lateralized) broadband power in the EEG. *Clin Neurophysiol, 112*(2), 215-231.

Hamaneh, M. B., Chitravas, N., Kaiboriboon, K., Lhatoo, S. D., & Loparo, K. A. (2014). Automated Removal of EKG Artifact From EEG Data Using Independent Component Analysis and Continuous Wavelet Transformation. *IEEE Transactions on Biomedical Engineering, 61*(6), 1634-1641. doi:10.1109/TBME.2013.2295173

Hansen, T. M., Mark, E. B., Olesen, S. S., Gram, M., Frokjaer, J. B., & Drewes, A. M. (2017). Characterization of cortical source generators based on electroencephalography during tonic pain. *J Pain Res, 10*, 1401-1409. doi:10.2147/jpr.s132909

Hong, K. S., & Khan, M. J. (2017). Hybrid Brain–Computer Interface Techniques for Improved Classification Accuracy and Increased Number of Commands: A Review. *Frontiers in Neurorobotics, 11*(35). doi:10.3389/fnbot.2017.00035

Hong, K. S., Khan, M. J., & Hong, M. J. (2018). Feature Extraction and Classification Methods for Hybrid fNIRS-EEG Brain-Computer Interfaces. *Front Hum Neurosci, 12*, 246. doi:10.3389/fnhum.2018.00246

Huang, T.-M., Kecman, V., & Kopriva, I. (2006). *Kernel based algorithms for mining huge data sets* (Vol. 1): Springer.

Huber, M. T., Bartling, J., Pachur, D., Woikowsky-Biedau, S. v., & Lautenbacher, S. (2006). EEG responses to tonic heat pain. *Experimental Brain Research, 173*(1), 14-24. doi:10.1007/s00221-006-0366-1

Hyvarinen, A. (1999). Fast and robust fixed-point algorithms for independent component analysis. *IEEE Transactions on Neural Networks, 10*(3), 626-634. doi:10.1109/72.761722

Hyvarinen, A., & Oja, E. (2000). Independent component analysis: algorithms and applications. *Neural Netw, 13*(4-5), 411-430.

Iannetti, G. D., Hughes, N. P., Lee, M. C., & Mouraux, A. (2008). Determinants of Laser-Evoked EEG Responses: Pain Perception or Stimulus Saliency? *Journal of Neurophysiology, 100*(2), 815-828. doi:10.1152/jn.00097.2008

Islam, M. K., Rastegarnia, A., & Yang, Z. (2016). Methods for artifact detection and removal from scalp EEG: A review. *Neurophysiologie Clinique/Clinical Neurophysiology, 46*(4), 287-305. doi:https://doi.org/10.1016/j.neucli.2016.07.002

Jensen, M., Gertz, K., Kupper, A., Braden, A., Howe, J., Hakimian, S., & Sherlin, L. (2013a). Steps Toward Developing an EEG Biofeedback Treatment for Chronic Pain. *Applied Psychophysiology and Biofeedback, 38*(2), 101-108. doi:10.1007/s10484-013-9214-9

Jensen, M. P., Sherlin, L. H., Gertz, K. J., Braden, A. L., Kupper, A. E., Gianas, A., . . . Hakimian, S. (2013b). Brain EEG activity correlates of chronic pain in persons with spinal cord injury: clinical implications. *Spinal Cord, 51*(1), 55-58.

Jones, A. K. P. (2005). The Role of the Cerebral Cortex in Pain Perception. In D. M. Justins (Ed.), *Pain 2005 - An updated review* (pp. 59-68): IASP Press.

Jung, T. P., Makeig, S., Humphries, C., Lee, T. W., McKeown, M. J., Iragui, V., & Sejnowski, T. J. (2000). Removing electroencephalographic artifacts by blind source separation. *Psychophysiology, 37*(2), 163-178.

Kakigi, R., Inui, K., Tran, D. T., Qiu, Y., Wang, X., Watanabe, S., & Hoshiyama, M. (2004). Human brain processing and central mechanisms of pain as observed by electro- and magneto-encephalography. *J Chin Med Assoc, 67*(8), 377-386.

Kannathal, N., Choo, M. L., Acharya, U. R., & Sadasivan, P. (2005). Entropies for detection of epilepsy in EEG. *Computer methods and programs in biomedicine, 80*(3), 187-194.

Khatun, S., Mahajan, R., & Morshed, B. I. (2016). Comparative Study of Wavelet-Based Unsupervised Ocular Artifact Removal Techniques for Single-Channel EEG Data. *IEEE Journal of Translational Engineering in Health and Medicine, 4*, 1-8. doi:10.1109/JTEHM.2016.2544298

Klimesch, W., Doppelmayr, M., Russegger, H., Pachinger, T., & Schwaiger, J. (1998). Induced alpha band power changes in the human EEG and attention. *Neuroscience letters, 244*(2), 73-76.

Kumar, A., & Anand, S. (2006). A Depth of Anaesthesia Index from Linear Regression of Eeg Parameters. *Journal of Clinical Monitoring and Computing, 20*(2), 67-73. doi:10.1007/s10877-005-9004-x

Kumar, S., Kumar, A., Trikha, A., & Anand, S. (2015). Electroencephalogram based quantitative estimation of pain for balanced anaesthesia. *Measurement, 59*, 296-301. doi:http://dx.doi.org/10.1016/j.measurement.2014.09.021

Kupers, R., Lonsdale, M. N., Aasvang, E., & Kehlet, H. (2011). A positron emission tomography study of wind-up pain in chronic postherniotomy pain. *Eur J Pain, 15*(7), 698.e691-616. doi:10.1016/j.ejpain.2011.01.003

La Vaque, T. J. (1999). The History of EEG Hans Berger. *Journal of Neurotherapy, 3*(2), 1-9. doi:10.1300/J184v03n02_01

Labor, S., & Maguire, S. (2008). The Pain of Labour. *Reviews in pain, 2*(2), 15-19. doi:10.1177/204946370800200205

Le Pera, D., Svensson, P., Valeriani, M., Watanabe, I., Arendt-Nielsen, L., & Chen, A. C. N. (2000). Long-lasting effect evoked by tonic muscle pain on parietal EEG activity in humans. *Clinical Neurophysiology, 111*(12), 2130-2137. doi:http://dx.doi.org/10.1016/S1388-2457(00)00474-0

Le Pera, D., Valeriani, M., Niddam, D., Chen, A. C., & Arendt-Nielsen, L. (2002). Contact heat evoked potentials to painful and non-painful stimuli: effect of attention towards stimulus properties. *Brain Topogr, 15*(2), 115-123.

Lee, T. W., Girolami, M., & Sejnowski, T. J. (1999). Independent component analysis using an extended infomax algorithm for mixed subgaussian and supergaussian sources. *Neural Comput, 11*(2), 417-441.

Lever, J., Krzywinski, M., & Altman, N. (2017). Principal component analysis. *Nature Methods, 14*, 641. doi:10.1038/nmeth.4346

Li, X., Guan, C., Zhang, H., & Ang, K. K. (2017). Discriminative Ocular Artifact Correction for Feature Learning in EEG Analysis. *IEEE Transactions on Biomedical Engineering, 64*(8), 1906-1913. doi:10.1109/TBME.2016.2628958

Loo, S. K., & Smalley, S. L. (2008). Preliminary report of familial clustering of EEG measures in ADHD. *American Journal of Medical Genetics Part B: Neuropsychiatric Genetics, 147*(1), 107-109.

Lutins, E. (2017). DBSCAN: What is it? When to Use it? How to use it. *Medium.* Retrieved from https://medium.com/@elutins/dbscan-what-is-it-when-to-use-it-how-to-use-it-8bd506293818

Maddirala, A. K., & Shaik, R. A. (2016). Removal of EOG Artifacts From Single Channel EEG Signals Using Combined Singular Spectrum Analysis and Adaptive Noise Canceler. *IEEE Sensors Journal, 16*(23), 8279-8287. doi:10.1109/JSEN.2016.2560219

Mahajan, R., & Morshed, B. I. (2015). Unsupervised Eye Blink Artifact Denoising of EEG Data with Modified Multiscale Sample Entropy, Kurtosis, and Wavelet-ICA. *IEEE Journal of Biomedical and Health Informatics, 19*(1), 158-165. doi:10.1109/JBHI.2014.2333010

Mammone, N., Foresta, F. L., & Morabito, F. C. (2012). Automatic Artifact Rejection From Multichannel Scalp EEG by Wavelet ICA. *IEEE Sensors Journal, 12*(3), 533-542. doi:10.1109/JSEN.2011.2115236

Mamun, M., Al-Kadi, M., & Marufuzzaman, M. (2013). Effectiveness of Wavelet Denoising on Electroencephalogram Signals. *Journal of Applied Research and Technology, 11*(1), 156-160. doi:http://dx.doi.org/10.1016/S1665-6423(13)71524-4

Marella, S. (2015). EEG artifacts. *Slide Share.* Retrieved from http://www.slideshare.net/SudhakarMarella/eeg-artifacts-15175461

Melzack, R. (1993). Labour pain as a model of acute pain. *PAIN, 53*(2), 117-120. doi:10.1016/0304-3959(93)90071-v

Misra, G., Wang, W. E., Archer, D. B., Roy, A., & Coombes, S. A. (2017). Automated classification of pain perception using high-density electroencephalography data. *J Neurophysiol, 117*(2), 786-795. doi:10.1152/jn.00650.2016

Nir, R.-R., Sinai, A., Moont, R., Harari, E., & Yarnitsky, D. (2012). Tonic pain and continuous EEG: Prediction of subjective pain perception by alpha-1 power during stimulation and at rest. *Clinical Neurophysiology, 123*(3), 605-612. doi:http://dx.doi.org/10.1016/j.clinph.2011.08.006

Nir, R.-R., Sinai, A., Raz, E., Sprecher, E., & Yarnitsky, D. (2010). Pain assessment by continuous EEG: Association between subjective perception of tonic pain and peak frequency of alpha oscillations during stimulation and at rest. *Brain Research, 1344*, 77-86. doi:http://dx.doi.org/10.1016/j.brainres.2010.05.004

Nolan, H., Whelan, R., & Reilly, R. B. (2010). FASTER: Fully Automated Statistical Thresholding for EEG artifact Rejection. *Journal of Neuroscience Methods, 192*(1), 152-162. doi:http://dx.doi.org/10.1016/j.jneumeth.2010.07.015

Ocak, H. (2009). Automatic detection of epileptic seizures in EEG using discrete wavelet transform and approximate entropy. *Expert Systems with Applications, 36*(2), 2027-2036.

Oostenveld, R., & Praamstra, P. (2001). The five percent electrode system for high-resolution EEG and ERP measurements. *Clinical Neurophysiology, 112*(4), 713-719. doi:http://dx.doi.org/10.1016/S1388-2457(00)00527-7

Panavaranan, P., & Wongsawat, Y. (2013). EEG-based pain estimation via fuzzy logic and polynomial kernel support vector machine. *Biomedical Engineering International Conference (BMEiCON), 2013 6th*, 1-4. Retrieved from doi:10.1109/BMEiCon.2013.6687668

Peng, W., Babiloni, C., Mao, Y., & Hu, Y. (2015). Subjective pain perception mediated by alpha rhythms. *Biological Psychology, 109*, 141-150. doi:http://dx.doi.org/10.1016/j.biopsycho.2015.05.004

Peng, W., Hu, L., Zhang, Z., & Hu, Y. (2014). Changes of Spontaneous Oscillatory Activity to Tonic Heat Pain. *PLoS ONE, 9*(3), e91052. doi:10.1371/journal.pone.0091052

Phadke, A. C., & Rege, P. P. (2016). Fusion of local and global features for classification of abnormality in mammograms. *Sādhanā, 41*(4), 385-395.

Pinheiro, E. S. d. S., Queirós, F. C. d., Montoya, P., Santos, C. L., Nascimento, M. A. d., Ito, C. H., . . . Baptista, A. F. (2016). Electroencephalographic Patterns in Chronic Pain: A Systematic Review of the Literature. *PLoS ONE, 11*(2), e0149085. doi:10.1371/journal.pone.0149085

Prichep, L. S., John, E. R., Howard, B., Merkin, H., & Hiesiger, E. M. (2011). Evaluation of the Pain Matrix Using EEG Source Localization: A Feasibility Study. *Pain Medicine, 12*(8), 1241-1248. doi:10.1111/j.1526-4637.2011.01191.x

Prichep, L. S., Shah, J., Merkin, H., & Hiesiger, E. M. (2018). Exploration of the Pathophysiology of Chronic Pain Using Quantitative EEG Source Localization. *Clin EEG Neurosci, 49*(2), 103-113. doi:10.1177/1550059417736444

Quazi, M. H., & Kahalekar, S. G. (2017). Artifacts removal from EEG signal: FLM optimization-based learning algorithm for neural network-enhanced adaptive filtering. *Biocybernetics and Biomedical Engineering, 37*(3), 401-411. doi:https://doi.org/10.1016/j.bbe.2017.04.003

Ray, W. J., & Cole, H. W. (1985). EEG alpha activity reflects attentional demands, and beta activity reflects emotional and cognitive processes. *Science, 228*(4700), 750-752.

Rissacher, D., Dowman, R., & Schuckers, S. A. C. (2007, 10-11 March 2007). *Identifying frequency-domain features for an EEG-based pain measurement system.* Paper presented at the Bioengineering Conference, 2007. NEBC '07. IEEE 33rd Annual Northeast.

Sai, C. Y., Mokhtar, N., Arof, H., Cumming, P., & Iwahashi, M. (2018). Automated Classification and Removal of EEG Artifacts With SVM and Wavelet-ICA. *IEEE Journal of Biomedical and Health Informatics, 22*(3), 664-670. doi:10.1109/JBHI.2017.2723420

Sai, C. Y., Mokhtar, N., Yip, H. W., Bak, L. L. M., Hasan, M. S., Arof, H., . . . Mat Adenan, N. A. (2019). Objective identification of pain due to uterine contraction during the first stage of labour using continuous EEG signals and SVM. *Sādhanā, 44*(4), 87. doi:10.1007/s12046-019-1058-4

Saithong, N., Poolpoem, W., Panavaranan, P., Saetang, J., & Wongsawat, Y. (2012). EEG-Based Acute Pain Control System. In T. Dohi & H. Liao (Eds.), *Computer Aided Surgery* (Vol. 3, pp. 101-112): Springer Japan.

Sanei, S., & Chambers, J. A. (2007). *EEG Signal Processing*: John Wiley & Sons, Ltd.

Sankar, D. A. B., Selvi, J., Durairaj, K., & Seetha Lakshmi, K. (2013). *Effective enhancement of classification of respiratory states using feed forward back propagation neural networks* (Vol. 38).

Shao, S., Shen, K., Yu, K., Wilder-Smith, E. P. V., & Li, X. (2012). Frequency-domain EEG source analysis for acute tonic cold pain perception. *Clinical Neurophysiology, 123*(10), 2042-2049. doi:http://dx.doi.org/10.1016/j.clinph.2012.02.084

Shoker, L., Sanei, S., & Chambers, J. (2005). Artifact removal from electroencephalograms using a hybrid BSS-SVM algorithm. *IEEE Signal Processing Letters, 12*(10), 721-724. doi:10.1109/LSP.2005.855539

Sitges, C., Bornas, X., Llabrés, J., Noguera, M., & Montoya, P. (2010). Linear and nonlinear analyses of EEG dynamics during non-painful somatosensory processing in chronic pain patients. *International Journal of Psychophysiology, 77*(2), 176-183. doi:http://dx.doi.org/10.1016/j.ijpsycho.2010.05.010

Sreeja, S. R., Sahay, R. R., Samanta, D., & Mitra, P. (2018). Removal of Eye Blink Artifacts From EEG Signals Using Sparsity. *IEEE Journal of Biomedical and Health Informatics, 22*(5), 1362-1372. doi:10.1109/JBHI.2017.2771783

Srinivasan, V., Eswaran, C., & Sriraam, N. (2007). Approximate entropy-based epileptic EEG detection using artificial neural networks. *IEEE Transactions on information Technology in Biomedicine, 11*(3), 288-295.

Subasi, A., & Ercelebi, E. (2005). Classification of EEG signals using neural network and logistic regression. *Computer methods and programs in biomedicine, 78*(2), 87-99.

Teplan, M. (2002). Fundamentals of EEG measurement. *Measurement science review, 2*(2), 1-11.

Vatankhah, M., Asadpour, V., & Fazel-Rezai, R. (2013). Perceptual pain classification using ANFIS adapted RBF kernel support vector machine for therapeutic usage. *Applied Soft Computing, 13*(5), 2537-2546. doi:http://dx.doi.org/10.1016/j.asoc.2012.11.032

Veselis, R. A. (2015). What about β? Relationship between pain and EEG spindles during anaesthesia. *British Journal of Anaesthesia, 115*(suppl 1), i3-i5. doi:10.1093/bja/aev223

Vijayakumar, V., Case, M., Shirinpour, S., & He, B. (2017). Quantifying and Characterizing Tonic Thermal Pain Across Subjects From EEG Data Using Random Forest Models. *IEEE Trans Biomed Eng, 64*(12), 2988-2996. doi:10.1109/TBME.2017.2756870

Wager , T. D., Atlas , L. Y., Lindquist , M. A., Roy , M., Woo , C.-W., & Kross , E. (2013). An fMRI-Based Neurologic Signature of Physical Pain. *New England Journal of Medicine, 368*(15), 1388-1397. doi:doi:10.1056/NEJMoa1204471

Wang, G., Teng, C., Li, K., Zhang, Z., & Yan, X. (2016). The Removal of EOG Artifacts From EEG Signals Using Independent Component Analysis and Multivariate Empirical Mode Decomposition. *IEEE Journal of Biomedical and Health Informatics, 20*(5), 1301-1308. doi:10.1109/JBHI.2015.2450196

Winkler, I., Haufe, S., & Tangermann, M. (2011). Automatic Classification of Artifactual ICA-Components for Artifact Removal in EEG Signals. *Behavioral and Brain Functions, 7*(1), 30. doi:10.1186/1744-9081-7-30

Woestenburg, J. C., Verbaten, M. N., & Slangen, J. L. (1983). The removal of the eye-movement artifact from the EEG by regression analysis in the frequency domain. *Biological Psychology, 16*(1–2), 127-147. doi:http://dx.doi.org/10.1016/0301-0511(83)90059-5

Wolpaw, J. R., Birbaumer, N., Heetderks, W. J., McFarland, D. J., Peckham, P. H., Schalk, G., . . . Vaughan, T. M. (2000). Brain-computer interface technology: a review of the first international meeting. *IEEE transactions on rehabilitation engineering, 8*(2), 164-173.

Wong, D. L., & Baker, C. M. (1988). Pain in children: comparison of assessment scales. *Pediatr Nurs, 14*(1), 9-17.

Yagneswaran, S., Baker, M., & Petrosian, A. (2002). *Power frequency and wavelet characteristics in differentiating between normal and Alzheimer EEG.* Paper presented at the Engineering in Medicine and Biology, 2002. 24th Annual Conference and the Annual Fall Meeting of the Biomedical Engineering Society EMBS/BMES Conference, 2002. Proceedings of the Second Joint.

Yang, B., Duan, K., Fan, C., Hu, C., & Wang, J. (2018). Automatic ocular artifacts removal in EEG using deep learning. *Biomedical Signal Processing and Control, 43*, 148-158. doi:https://doi.org/10.1016/j.bspc.2018.02.021

Zhang, J. H., Janschek, K., Bohme, J. F., & Zeng, Y. J. (2004). Multi-resolution dyadic wavelet denoising approach for extraction of visual evoked potentials in the brain. *IEE Proceedings - Vision, Image and Signal Processing, 151*(3), 180-186. doi:10.1049/ip-vis:20040315

## LIST OF PUBLICATIONS AND PAPERS PRESENTED

Sai, C. Y., Mokhtar, N., Iwahashi, M., Cumming, P., & Arof, H. (2020). Fully Automated Unsupervised Artifacts Removal in Multichannel EEG using Wavelet-ICA with DBSCAN. (Under review)

Sai, C. Y., Mokhtar, N., Yip, H. W., Bak, L. L. M., Hasan, M. S., Arof, H., Cumming, P., & Adenan N. A. M. (2019). Objective Identification of Pain due to Uterine Contraction during the First Stage of Labour using Continuous EEG Signals and SVM. *Sadhana*. 44(4), 87. doi:10.1007/s12046-019-1058-4

Sai, C. Y., Mokhtar, N., Arof, H., Cumming, P., & Iwahashi, M. (2018). Automated Classification and Removal of EEG Artifacts With SVM and Wavelet-ICA. *IEEE Journal of Biomedical and Health Informatics*, 22(3), 664-670. doi:10.1109/JBHI.2017.2723420

Sai, C. Y., Mokhtar, N., Arof, H., & Iwahashi, M. (2017). Design of Automated Real-Time BCI Application Using EEG Signals. *International Conference on Artificial Life and Robotics (ICAROB) 2017*, pp 703-706.